Sheffield Hallam University

Centrifugal ironmaking.

ROBSON, Alan Lawson.

Available from Sheffield Hallam University Research Archive (SHURA) at:

http://shura.shu.ac.uk/20285/

Published version

ROBSON, Alan Lawson. (1982). Centrifugal ironmaking. Doctoral, Sheffield Hallam University (United Kingdom)..

Copyright and re-use policy

ProQuest Number: 10700930

uest

ProQuest 10700930

CENTRIFUGAL   IRONMAKING

A THESIS

Submitted to the Council of National Academic Awards for the Degree of
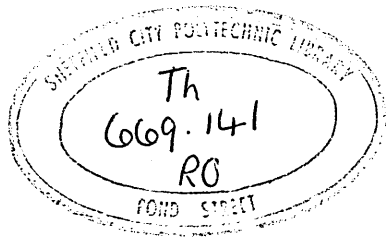
DOCTOR OF PHILOSOPHY

by

ALAN LAWSON ROBSON

For Work Carried Out at

Teesside Laboratories
British Steel Corporation

Department of Metallurgy
Sheffield City Polytechnic

May 1982

CONTENTS   Page No.

CONTENTS   cont'd   Page No.

ABSTRACT

A process for producing liquid iron from iron ore is being developed
on the pilot plant scale that avoids the use of high grade metallurgical
coal and the agglomeration of iron ore concentrates. The use of a
centrifuge furnace provides the maximum surface area for reaction between
layers of molten iron oxide and solid carbon. The iron product is
centrifuged to the walls of the reactor where it provides a protective
barrier between the highly corrosive liquid slag and the refractory
walls. Carbon monoxide, released from the reduction reaction, combusts
with oxygen in the central gas core and the heat produced is radiated
back to the reacting species.

To help understand the interaction of the various physical and chemical
reactions occurring inside the reactor, a mathematical model had been
written describing the process. Laboratory scale studies were carried
out to examine and test the validity of some of the assumptions used
in the model, and where necessary modify these assumptions. Two such
investigations were the reaction between solid carbon and liquid iron
bearing slags at temperatures up to 2 135 K, and the determination of
heat and mass transfer coefficients from the central gas core to the
rotating bed using a naphthalene sublimation technique.

To widen the basis on which the predictions from the model could be
compared with actual pilot plant operating data, a series of experiments
were carried out on the plant covering a broad range of input conditions.
These experiments were carried out in the batch mode i.e. the raw
materials were charged into the furnace until its capacity was reached,
after which the entire contents were discharged, analysed, and compared
with the predictions from the mathematical model. A systematic empirical

campaign was then carried out to determine more realistic values for the parameters used in the model. Sufficient information was obtained from this study to provide the optimum conditions for attempting continuous ironmaking operations on the pilot plant.

Three continuous ironmaking experiments were carried out, with the maximum length of continuous operation in any one experiment being of ten hours duration. Improvements in operation and measurement techniques enabled process data to be collected at regular intervals which allowed the process efficiency to be determined on a continuous basis. The iron ore input rate was held constant at 340 kg/h and high conversion efficiencies of iron from iron ore of up to 80% were obtained.

NATURE OF THE INVESTIGATION

The principal purpose of the investigation reported in this thesis was to gain sufficient understanding of the phenomena occurring in the Centrifugal Ironmaking Process to allow the process to be operated consistently with high efficiency. To do this, a pilot plant reactor was operated and modified under the direct direction of the author. In addition, experience and observation of this reactor was augmented by the predictions of a complex mathematical model of the process. The author did not develop this model, although he was involved in a number of modifications to the formalisms used and he contributed to the programme of laboratory experiments which provided values for some of the critical parameters used in the model.

Once the model had been developed and validated in a programme of comparisons, directed by the author, with the performance of the pilot plant, it was used, together with the pilot plant, to explore various operating conditions and hence to show those operating conditions which would result in the most efficient operation. This work, both for the model and the pilot plant, was planned and directed by the author.

The pilot plant had been built prior to the start of the investigations that are the subject of the thesis, and some initial experience of its operation had been obtained. The initial sections of the thesis thus describe the plant, and this initial experience, together with the mathematical model, and the output that it could provide.

The results and the theories developed are, to the best of the author's knowledge, original except where reference has been made to other investigations. No part of this thesis has been submitted for a Degree at any other University or College.

SYMBOLS USED IN THE TEXT

A	Area
A_n	Area of nozzle
a	Weight of iron oxide at zero time
a_1, a_2	Constants
C	Molar concentration
C_o	Initial molar concentration
C_{sl}	Molar concentration in the slag
C_p	Specific heat
D_i	Diffusion coefficient of species i
D_{AB}	Diffusion coefficient of species A in a mixture of A and B
d	Diameter
E	Activation energy
f	Shape factor
G	Burner thrust
h	Heat transfer coefficient
h_D	Mass transfer coefficient
J_H	Dimensionless factor for heat transfer
J_D	Dimensionless factor for mass transfer
K_p	Equilibrium reaction constant
K_s	Surface reaction rate coefficient
k, k^1	Rate constants
k_o	Rate constant at initial concentration
k_i	Mass transfer coefficient of species i
$\bar{k}$	Absorption coefficient
k_{metal}	Mass transfer coefficient in the metal phase
k_{slag}	Mass transfer coefficient in the slag phase

l	Characteristic length
M_N	Molecular weight of air
M_n	Mass flow rate through the nozzle
m	Mass concentration
m_o	Initial mass concentration
N	Number of mols
$\dot{n}_i^{11}$	Molar flux of a species i
n	Exponent
P_i	Partial pressure of species i in the bulk gas
P_e	Partial pressure at the exit
$q_{p.f.}$	Rate of carbon removal per unit external geometric surface area
$\dot{q}_r^{11}$	Heat transferred by radiation
R	Gas constant
r	Radius of particle
r_o	Base reaction rate
r_T	Reaction rate at temperature T
T	Temperature
T_i	Temperature at inlet
T_B	Temperature of bed
T_g	Temperature of gas
t	Time
U	Mass velocity
u	Velocity
V	Volume
W	Weight loss
X_i	Partial pressure of species i at the interface
$X_{CO_2}^C$	Partial pressure of CO_2 in equilibrium at the carbon surface

$x_{CO_2}^{S}$ Partial pressure of CO_2 in equilibrium at the slag surface

$\left[x_{FeO} \right]_b$ Concentration of FeO in the slag bulk

x Amount reacted after time t

y Distance from centre of particle

α Mass transfer coefficient dependent on stirring intensity

δ Thickness of gas film

Δ_p Pressure differential

ε_B Emissivity of bed

ε_g Emissivity of gas

θ Temperature

ρ Density

σ Stefan-Boltzmann constant

μ Viscosity

ω Angular velocity

ϕ, ϕ^1 Pseudo-equilibrium constants

Nu   Nusselt number

Pr   Prandtl number

Re_p Reynolds number for pipe flow

Re_r Rotational Reynolds number

Sc   Schmidt number

Sh   Sherwood number

1 INTRODUCTION

Centrifugal Ironmaking is the name given to a technique in which
liquid iron ore and coal are reacted together at high temperatures,
resulting in a liquid iron product. The reaction takes place in a
cylindrical vessel rotating at a speed high enough to hold the dense
liquid iron against the refractory walls, thus protecting them from
attack by the molten iron bearing slag and coal which float on top
of the iron.

The principal reasons favouring the Centrifugal Ironmaking process
are that low grade coals can be used as the reductant and there is no
need for charge preparation. Thus, unlike the blast furnace, this
process is independent of coking coal supply and it does not require
sinter plants, high temperature stoves, high pressure equipment and
coke ovens, so that considerable capital cost savings are possible.
Further, the centrifuge technique allows very high temperatures to be
generated within the furnace without damage to the refractories, which
are protected by the layers of liquid held against the walls. The
basic concepts of the Centrifugal Ironmaking process are given in more
detail in section 3.1.1.

To allow a thorough investigation of ironmaking using this technique,
a pilot plant was built at the Teesside Laboratories of the British
Steel Corporation. A description of this pilot plant is given in
section 6.1. Some initial operating experience of this pilot plant had
been obtained before the start of the work described in this thesis.
The majority of the earlier experiments investigated the problems of
containing liquid metal and slag within a centrifuge, and the engineer-
ing problems associated with high speed rotation. This commissioning

1

period was protracted by a hot metal breakout which delayed the experimental programme for nearly a year. During this early period it was found that strongly oxidising conditions in the gas core (5 : 1, CO_2 to CO ratio) would lead to oxidation of the metal bed and very high bed temperatures. This factor was considered to be the main cause of the "break out" referred to above. Following this commissioning period a series of batch experiments were carried out, i.e. charging the furnace with ore, coal and limestone to less than its capacity, then completely discharging the furnace contents by reducing the drum speed to zero. These experiments usually lasted about two hours. The average iron ore feed rate being 200 kg/h, with coal input rates equivalent to up to 3 x the stoichiometric carbon requirement for iron and carbon monoxide production. It was also found necessary to spread the iron ore, coal mixture over a large proportion of the furnace area to prevent local freezing at the feed end of the furnace. The injection of fine coal into the gas stream to enhance heat transfer to the reacting bed was found necessary, also the oxygen input rate was adjusted to generate a CO_2 : CO ratio of around 2 : 1 inside the furnace. Conversion efficiencies of iron ore to iron of greater than 90% were obtained from a number of experiments. Encouraged by the success of these early batch experiments, the experimental programme was then directed towards a reduction of the coal rate to around 2 x the carbon stoichiometric requirements, increasing the iron ore input rate to around 350 kg/h, and attempting continuous tapping from the furnace for a period of up to six hours. A number of different cast end dam arrangements were also examined.

A large proportion of time, $1\frac{1}{2}$ years, was spent on this programme of work, with only limited success. Continuous tapping was never achieved and the conversion efficiencies of iron ore to iron were low, usually between 0 and 50%. The problem of chemical attack of the refractories in the cast end dam became acute during the longer, continuous operation experiments and resulted in several premature terminations of experiments. The concept of mixing the reacting species by mechanical means, i.e. cycling the drum speed between an upper and lower set speed, was introduced during this operating period. Another major problem encountered when moving from the batch to the continuous experiments was that during the course of the experiment it was difficult to maintain steady input rates of the ingoing materials. Observations showed that, on occasions, even small changes in input conditions had serious repercussions on process performance and could result in a fully oxidised bed, or severe freezing of the bed. Thus a relatively narrow operating band had to be followed in order to achieve successful operation. Thus the operating flexibility of the process was not known at this time, and it was the result of this comparative lack of success that encouraged the development of the mathematical model of the process and the work described in this thesis.

2 LITERATURE SURVEY

2.1 Reduction of Iron Oxide Bearing Slags by Solid Carbon

The difficulties in carrying out laboratory scale experiments with molten slags at elevated temperatures has meant that surprisingly few investigations have been reported. The problems of containing the liquid slags and conducting these experiments under closely controlled conditions to make the results meaningful have all added to the experimental problems, plus the difficulty in interpreting experimental data from a reaction zone involving the interaction of four phases, i.e. liquid iron oxide, solid carbon, liquid iron and product gas. However, a number of investigations have been reported at lower temperatures.

Philbrook and Kirkbride[1] studied the reduction of molten slags containing up to 5% FeO from a ternary lime-alumina-silica mixture with carbon saturated iron in a graphite crucible, and with the graphite crucible only, at temperatures between 1 430 $^{\circ}$C and 1 570 $^{\circ}$C. The overall reaction was found to be 2nd order, with the slag-carbon saturated iron reaction being faster than the slag-carbon reaction. The value of the reaction rate constant between slag and graphite was determined as 1.2 x 10^{-4} g FeO/min cm^2 . (% FeO)^2.

It was not possible to deduce a reaction mechanism to interpret the results alone, however several alternative reaction mechanisms were postulated. These were in terms of intermediate reaction products, dissociation of FeO within the slag, nucleation of gas or metal, and surface phenomena leading to reaction through iron films on rising bubbles of carbon monoxide in the slag. Tarby and Philbrook[2] also studied the reduction of up to 5% FeO from both a ternary lime-alumina-silica slag and a binary lime-alumina slag in graphite crucibles, and

by carbon saturated iron in graphite crucibles, at temperatures between 1 550 ^{o}C and 1 575 ^{o}C. The reaction rate constants and orders of reaction were derived by an integration and a differential method. Using the latter method two distinct periods of reaction were identified. The first period, which was the more rapid, was stated to be caused by vigorous evolution of carbon monoxide gas resulting in forced convection within the slag. The second, and slower rate of reduction, takes over as the boiling action subsides within the system and the flow conditions within the slag become those defined by natural convection. For the slag-graphite system, they found that for the initial period an order of reaction between 1.1 and 2.0 was derived, and for the following stage a first order of reaction. The measured rate constants varied with slag composition and their differences might result from the activity of 'FeO' in the various slags.

Krainer, Beer and Brandl[3] using graphite and coke crucibles with a thermogravimetric balance studied the reduction of slags containing up to 70% iron oxide in the temperature range 1 300 to 1 500 ^{o}C. They found that reduction of iron oxide in $CaO-SiO_2$ slags occurred several times more quickly than in binary $FeO-SiO_2$ slags, but no difference in reaction rates was detected between the coke or graphite crucibles. The activation energy for the reaction was found to vary between 20 and 40 kcal/mol for the range of slags studied. They concluded that the reduction reaction proceeds via two consecutive steps:-

$$FeO + CO = Fe + CO_2 \quad \ldots\ldots\ldots\ldots\ldots \quad (2.1)$$

$$CO_2 + C = 2CO \quad \ldots\ldots\ldots\ldots\ldots \quad (2.2)$$

with the overall reaction rate being determined by reaction 2.1.

Kondakov, Rhzhonkov and Golenko[4] reduced liquid iron oxide in a graphite crucible in the temperature range 1 450 $^{\circ}$C to 1 650 $^{\circ}$C. From their observations, the gasification of carbon, reaction 2.2, was found to be the rate limiting step.

Yershov and Popova[5] studied the reaction between a spinning carbon disc and molten FeO - CaO - SiO$_2$ slags held in a zirconia crucible at 1 600 $^{\circ}$C in which the disc was immersed. The rate of reaction was determined by measuring the loss in weight of the carbon disc over a specified time with a given contact surface area between the carbon and the slag. At high FeO levels, between 40 and 60%, the rate of reaction was found to be independant of the rate of rotation of the carbon disc and the rate determining step was deduced to be by interfacial chemical kinetics. At lower FeO levels of 10 - 20%, the rate of reaction increased with increasing rotational speed of the carbon disc, and the rate limiting step was said to be the diffusion of oxygen in the slag. An increase in CaO content in the slag for a given FeO level resulted in an increase in reaction rate.

Sugata, Sugiyama and Kondo[6] used rotating carbon or coke rods reacting in a range of slag compositions with FeO levels between 5 and 90%. The reaction was carried out in pure iron crucibles which limited the temperature range studied to between 1 350 $^{\circ}$C and 1 450 $^{\circ}$C. At high rotation speeds the rate of reaction was determined by the interfacial chemical reaction FeO + C = Fe + CO. At lower rotation speeds the reaction rate was considered to be controlled by both diffusion within the slag melt and chemical reaction because the rate of reaction increased with an increase in rotation of the carbon rod.

The importance of the gas evolution step was underlined by the work of Shavrin et al[7] who used an X-ray technique to observe the evolution of gas bubbles from a graphite sphere immersed in an iron oxide-lime-boric oxide slag. They found that the shape and size of the gas bubble depended upon the properties of the melt and the surface of the carbon. They also found two regimes for the detachment of bubbles from the carbon surface, namely single bubble and multi bubble boiling, and which regime they operated in depended on the iron oxide concentration of the melt and the temperature of reaction.

X-ray studies of the interaction between liquid iron-carbon droplets and iron oxide bearing slags have been reported by Davies et al[8], which underlined the importance of surface properties on the nucleation and growth mechanism of CO bubbles. In the same paper, experiments involving the reaction of $FeO - CaO - SiO_2$ slags in graphite and coal crucibles between 1 400 and 1 500 $^{\circ}C$ were reported. No difference in the reaction rate was found when using either a graphite or a coal crucible. They concluded that the most likely mechanism controlling the reaction in their particular experimental arrangement was mass transfer in the slag phase.

2.2   Mass Transfer Model Studies

The use of isothermal scale models to study flow patterns and mass transfer coefficients in complex industrial plant has been widely used for some time now. Gray et al[9] described some of the equipment and methods employed in the solution of industrial fluid flow problems by model techniques, using air as the operating medium. Several typical examples of the problems investigated were given, including the design

of the models used, and the flow distribution in pipes and furnaces.

Bacon[10] also describes techniques in which water, as well as air, has been used as the flow medium. Techniques were described, using water as the flow medium, in which good flow visualisation was achieved inside furnace models, however for quantitative work, air should be used as the flow medium. Equality of Reynolds Number in the model and furnace was taken as the main criterion of similarity, as well as geometric similarity. Bacon described a technique for scaling down the burner nozzle used in oil-fired furnaces. This was necessary because the momentum of the fuel entering the furnace was the greatest single factor affecting the flow pattern in the furnace chamber. Thring and Newby[11] developed a criterion to account for the non-isothermal mixing of the burner flame. Their criterion essentially depended on the measure of two parameters to ensure mixing similarity, i.e. a recirculation parameter θ_r which relates the input flows and the furnace dimensions to the degree of recirculation, and an equivalent burner size to account for the temperature effects of the flame. The Thring-Newby criterion is strictly only applicable to systems with a small nozzle diameter in a large mixing chamber and to overcome these difficulties a modification to the Thring-Newby criteria was proposed by Robertson[12] in which the equivalent burner diameter was replaced by an equivalent mixing length.

Several different techniques have been used for measuring mass transfer coefficients under different geometric arrangements. Davies et al[13] and Galsworthy[14], describe a solid sublimation technique using naphthalene in their study of furnaces for the rapid heating of

8

cylindrical billets. Mass transfer coefficients were derived from the weight lost by sublimation of naphthalene when air was blown through the models, in which the naphthalene coatings represented the heat transfer surfaces of the furnaces. Heat transfer coefficients were derived from mass transfer measurements using the Chilton-Colburn analogy[15] between heat and mass transfer. Lucas et al[16] describe an electrolytic mass transfer technique using the reduction of the ferro-cyanide ion at a nickel electrode in an alkaline potassium ferri-ferrocyanide solution. The application of this method to a furnace model involves operating the model as an electrolytic cell.

Harvey et al[17] carried out experiments to determine the pressure drops and flow patterns for fluids flowing through a tube rotating about its own axis. They found that the effect of increasing the rotation of the tube was to increase the friction factor at Reynolds Number less than 3 000 and for Reynolds Number greater than 3 000 to decrease the friction factor with increasing tube rotation. At a Reynolds Number of 3 000 the friction factor had a single value irrespective of the rotational speed of the tube. However, with a Reynolds Number of 8 000 and a rotational speed of 3 000 rpm the friction factor was reduced by 50%. Rotational speeds in excess of 750 rpm also tended to suppress turbulence and extended the laminar flow region to high Reynolds Number.

2.3   Smelting Reduction

The production of iron from liquid iron ore in smelting reduction processes is usually carried out with solid carbon, charged as either coke or as coal, but the use of oil or hydrocarbons is also possible. The major problems to overcome in any smelting reduction process is to supply sufficient heat to sustain the highly endothermic reduction

reaction. This usually means the use of oxygen to obtain high gas temperatures, without reoxidising the iron produced, and the prevention of severe refractory attack by the highly aggressive iron oxide bearing slags inherent in any smelting reduction process.

The majority of smelting reduction processes have only been developed as far as the pilot plant stage and each process has attempted different variations in design or practice to overcome the problems of heat transfer and slag attack. For instance, the Eketorp-Vallak process[18] used a refractory lined container to hold the iron, slag and coke layers. Oxygen was injected into the gas phase to produce high temperatures for heat transfer to the molten bath. The iron ore was charged into the bath in the form of a curtain around the sides of the vessel, thus protecting the refractory from the high gas temperatures. The problem of slag attack of the refractory still remained.

The use of rotating furnaces in the iron and steel industry is well established, for example the S.L.R.N.[19] and Kaldo processes[20]. The DORED process[21] was similar to the Kaldo process in that an inclined cylindrical vessel was rotated to promote mixing of the reactants. Oxygen was added through the open mouth of the vessel into the central gas core. Iron ore, coke breeze and limestone were charged into the furnace to produce layers of iron, iron oxide bearing slag and coke. The combustion of the carbon monoxide to carbon dioxide inside the rotating furnace heated the refractory walls of the vessel. The rotation of the furnace was such that it carried the liquid bed up the sides of the vessel, after which, the liquid bed would rain down through the hot gas core and mix with the coke layer floating on the liquid bed at the base of the furnace. In this way heat was transferred to the

liquid bed and intimate mixing of the coke and iron oxide slag would occur. This process worked with a high degree of chemical efficiency but the continual exposure of the refractory surface to slag rich in iron ore meant that refractory consumption was excessive and the process was uneconomic to operate on a commercial basis.

A rotary furnace was again used in the Rotovert Smelting Reduction process[22] developed on the pilot plant scale at M.R.P., Lulea in Sweden. A 6 tonne converter was used with an inner diameter of 1 m, which rotated around its vertical axis, giving a liquid metal parabola 1 m high at a rotational velocity of 85 rpm. The refractory used was tar bonded dolomite, although magnesite and chrome magnesite were also used. The liquid metal parabola formed inside the converter was to protect the refractory from slag attack. The raw materials of iron ore, coke and limestone were fed onto the metal parabola. Two types of material feeding systems were tried. A stationary, continuous feeding probe, axially mounted was first used but the distribution of the charge on the parabola was poor. A movable, continuous feeding system was developed which distributed the charge over the main part of the parabolic surface. A combustion system was also developed from a simple 6 holed oxygen nozzle, axially mounted, to one with a central oxy-oil burner, plus a 17 hole oxygen lance as a secondary combustion system. Iron ore (magnetite) feed rates of up to 1000 kg/h have been tried with a maximum input of 750 kg during an experiment. The coke input was of the order of 1 tonne/tonne metal produced, which gave a coke layer thickness of up to 10 cm at the beginning of the experiment. Problems of poor heat transfer to the bed from the central gas core

were encountered and measurements indicated that only 20% of the total

heat available was transferred to the liquid bed, which was insufficient

to compensate for the heat requirements within the bed and heat losses

from the plant. Refractory wear in the upper part of the converter was

also a problem and this produced an increase in the slag basicity which

made the slag viscous and unmanageable.

A development from the Rotovert process was carried out at C.S.M., Rome,

Italy, called Rotored[23], again on the pilot plant scale. The Rotored

process, like Rotovert, spins in the vertical axis, however the base of

the converter was open, compared with the closed bottom of the Rotovert

process. On the pilot plant scale the Rotored furnace had an internal

surface area available for reaction of 1.52 m^2 and spun at 85 rpm.

The concept of the process was to feed solid coke to form a layer on the

inner walls of the furnace of sufficient depth to prevent any contact

between the walls and the iron ore. The raw materials charged were an

iron ore mix (mainly Venezuelan ores), coal and limestone with Liquid

Petroleum Gas and oxygen added in the centre of the rotating furnace.

The raw materials could be fed either as separate layers or as a mixture

through a feeder probe which traversed up and down the length of the

furnace. The proposed feeding technique, when feeding separate materials,

was to provide alternate and separate layers of a non-uniform thickness

along the reactor wall. The thickness of the ore layer was to decrease

uniformly from a maximum, corresponding to the mouth of the reactor, to

.zero at the lower part of the cylinder. The thickness of the coke layer

would be the reverse of the ore layer. It was proposed therefore to use

the upper part of the cylinder for preheating and fusing the iron ore and

the lower part for reduction as the liquid melt percolates down the coke

layer. The process has only operated in the batch mode and the standard operating procedure was to have a feeding and heating period ($\sim$70 min duration) followed by a heating and solid state reduction period ($\sim$80 min duration), followed by a further feeding and heating period, and so on. The final period (of $\sim$35 min duration) was for liquid state reduction only. Attempts to operate this process on a continuous basis have proved unsuccessful.

3   CENTRIFUGAL IRONMAKING PROCESS (C.I.P.)

3.1   Smelting Reduction

The principal chemical reaction (overall) which accounts for the reduction of iron ore (assumed to be Fe_2O_3) in smelting reduction processes is:-

$$Fe_2O_3 + 3\ C = 2\ Fe + 3\ CO \qquad \ldots\ldots\ldots\ldots (3.1)$$
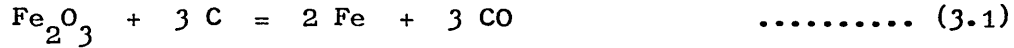
For each tonne of iron produced, 1.430 tonnes of Fe_2O_3 and 0.323 tonnes of carbon are required. In addition to the iron produced the reaction also yields 602 m^3_N of carbon monoxide gas. The reaction is highly endothermic and heat is required to sustain the reaction in addition to the heating requirements of the reactants.

The heating requirements[24] to enable the reaction to proceed, at say 1600 ^oC, are as follows:-

Heating and fusion of the ore	=	2.77 GJ/tonne Fe
Heating of the carbon (coal)	=	0.89 GJ/tonne Fe
Heat required for the reduction reaction	=	3.87 GJ/tonne Fe
		7.73 GJ/tonne Fe

It is possible to provide this heat by burning the carbon monoxide gas released from the reduction reaction:-

$$CO + \tfrac{1}{2} O_2 = CO_2 \qquad \ldots\ldots\ldots\ldots (3.2)$$

This reaction required 300 m^3_N O_2/tonne Fe to burn the carbon monoxide completely to carbon dioxide, when 6.74 GJ are released. However, it is not possible to transfer all this heat to the reaction zone and when

other thermal demands of the process are taken into account, e.g.
heat losses through furnace walls, through water cooled probes and
the dissociation of the limestone etc., it becomes obvious that the
thermal demands of the process can only be met by burning additional
fuel, say oil or coal.

The product gas from these combustion reactions is carbon dioxide
which is oxidising towards iron. Moreover, it is necessary to maintain
strongly oxidising conditions in the gas core to burn the CO and other
fuels sufficiently rapidly to liberate enough heat to sustain the
reduction reaction. It is also necessary, of course, to maintain
reducing conditions at the iron ore - carbon reaction interface. It
is clear that an understanding of the competing oxidation and reduction
reactions occurring within the furnace and the net transfer of heat and
the gaseous species from the central gas core to the reacting bed
requires a description of the processes occurring inside the furnace to
be developed. For this purpose a mathematical model describing the
key areas in the Centrifugal Ironmaking process was developed.

3.1.1 Concept

A cylindrical furnace is rotated about its horizontal axis at a
rotational speed such that the constituents of the furnace, (liquid
iron, liquid slag, solid carbon), are spread around the inner surface
of the furnace in a uniform film. The relative densities of the
constituents ensures that the constituents segregate into discrete
layers. The heaviest constituent, iron, is maintained as the outer
layer against the refractory surface and, as such, protects the refrac-
tory from attack by the iron oxide. The reaction between iron oxide

and carbon can then take place in the inner, higher temperature layer. Carbon monoxide gas is evolved from this reaction which enters the gas phase in the central region of the furnace. Oxygen is then added to the furnace which combusts the carbon monoxide to carbon dioxide, thus supplying the heat necessary to sustain the endothermic reduction reaction of the iron oxide by carbon. Whilst the furnace is spinning iron ore and coal are charged. Limestone is also added to flux the slag resulting from the coal ash and the gangue in the iron ore. When the holding capacity of the furnace is exceeded, the iron spins out into a casting chamber where it discharges through a tap hole for collection.

The feeding arrangements for the iron ore, coal and limestone are positioned at one end of the furnace, together with an oxy-oil burner, a fluidised feeder for pulverised fuel and an inlet for oxygen. The burner and pulverised fuel supply additional heat which is necessary to compensate for heat losses inherent in a small pilot plant. The casting chamber is positioned at the other end of the furnace and the exhaust gases pass through this section to atmosphere.

Two factors make the process unique, both arising from the choice of a centrifuge technique. The first is that essentially 'thin' liquid films are used. On the pilot plant a total liquid layer greater than 70 mm would be difficult to control due to instabilities which can only be overcome by raising the rotational speed of the furnace. The total volume of material held inside the furnace during ironmaking is therefore relatively small. The second factor is that high 'g' forces on solids and liquids of differing densities enhance segregation of the components. This separation could prevent the desired rapid chemical reaction rate between the coal and liquid iron oxide. However, it is

considered that self-induced stirring by the carbon monoxide gas evolved from the reduction reaction may be sufficient, if not, then the layers could be stirred by varying the rotational speed of the furnace in a cyclic manner[25].

The requirement for maintaining relatively thin layers of liquids and solids in the furnace, and the segregating effect of high 'g' forces, accent other problems in the process. There is a need to operate at very high gas core temperatures to achieve the necessary high conversion rate of iron oxide to iron. The concept of the process is to combust, with oxygen, the carbon monoxide produced from the reduction reaction. The heat released in the gas core must then be transferred back into the bed to enable the strongly endothermic reduction reaction to continue. This concept required an oxidising gas core adjacent to a highly efficient reducing bed, and is only possible if some kind of barrier exists between the gas core and the liquid bed. Coal, being the lightest constituent in the bed, floats on the slag surface and, therefore, acts as a physical barrier between the gas core and the liquid bed. However, the thickness of this coal layer is of paramount importance to the continuity of the process. Too thick a layer of coal will reduce the transfer of heat from the gas core to the coal/slag interface where reduction is occurring, since the resultant coke/coal bed is a poor conductor of heat. On the other hand, if there is too little coal floating on the top surface of the bed, then the oxidising components of the gas core can readily diffuse into the liquid slag layer and, because of the relatively thin layers, to the underlying iron layer. Very quickly this oxidising reaction can more than balance the reduction reaction giving a net result which is strongly oxidising. The process

must be operated under a balanced state so that reduction can be achieved to a high degree of efficiency even with a highly oxidising gas core. The balance state is achieved by having sufficient coal floating on the top surface of the bed such that an adequate coal coverage is obtained, yet partial sinking of the coal, because of induced stirring, or by mechanical means, can also be obtained. Areas of the slag layer will, therefore, be uncovered to such an extent that heat will be transferred into the slag layer, but giving only limited access for the oxidising components of the gas core. The increased reaction may also produce a foamy slag which will assist the partial sinking of the coal.

A further problem also exists when the coal layer is allowed to build up inside the furnace. The carbon can react with the highly oxidising gas core and if this becomes significant then the total fuel efficiency of the process is diminished. Also the reaction between carbon and carbon dioxide is endothermic and this will have the effect of chilling the coal layer, hence acting as a positive deterrent to heat transfer.

Thus the essence of the process lies in the history of the individual coal particles as they lie on or near to the liquid slag. The coal particle separates the high temperature gas core from the reduction reaction taking place around the base of the particle. The reduction reaction is strongly endothermic and if the heat supply is insufficient at any time then the carbon - slag interface temperature will cool rapidly leading eventually to local freezing in the affected area. The heat flow to this heat sink is by conduction either through the coal particle itself or through the slag. The heat conductance through the slag

is, therefore, important and partial uncovering of the slag becomes

necessary in order to transfer sufficient heat to the reaction zone.

Unfortunately, opening up the carbon layer exposes the slag layer to

the oxidising species of the gas core. Diffusion of these species

into the slag layer and ultimately into the iron layer causes reoxid-

ation of the iron and increases the concentration of ferrous ions in

the slag layer. The mechanism controlling reduction at the carbon -

slag layer are not yet fully understood in this process, but it is

considered that droplets of iron form at the interface and then are

transported under the action of centrifugal force to the iron layer.

The iron particle, containing a certain concentration of carbon, is

assumed to pick up oxygen during its movement through the slag layer.

The relative concentration of carbon and oxygen have not been estab-

lished but it is unlikely that equilibrium conditions will exist during

the movement of the iron droplets. This overall concept can be modified

by the use of rotational stirring which should enhance heat transfer and

reduction rate by the following mechanisms:-

    (i)   Rotating the coal so that effectively its conductivity
          increases.

   (ii)   Mixing the coal and slag layer together thereby enhancing
          the reaction rate by 'slippage' between the solid and
          liquid layers.

The rotating of the coal particles is an interesting concept since this

has the effect of plunging the heated surface of the coal into the slag

layer, thus the heat is directly at the carbon - slag interface where

reduction occurs. As the coal particle cools down because of the

endothermic nature of the reaction, it revolves further to bring the
cooled surface back into the gas phase for reheating. The opposite,
heated, side of the particle being plunged back into the slag layer.
It is not yet established how necessary artificially produced stirring
is to the ultimate success of the process, and it may be that sufficient
agitation is produced by the gas from the reduction reaction to enable
high yields to be obtained. This is to be hoped for, since the need
for artificial stirring adds to the mechanical complexity and expense
of the plant.

If an axial slice of the furnace is considered then it is possible to
have operating conditions where oxidation and reduction are both occurr-
ing in the slag at the same time. It is not certain which is the rate
controlling step in the series of reactions taking place, but it is
considered that the mass transfer coefficient defining the rate of
movement of oxidising gas species from the bulk gas to the slag surface
is important. This mass transfer coefficient is a function of gas
velocity in the bulk gas, but its estimation is complicated by the
furnace environment which is rotating at high speed.

To ensure that the reduction reaction is not diminished due to lack of
heat it is essential that the maximum rate of heat transfer from the
gas core is achieved. The rate of heat release is a function of four
factors: pulverised fuel and oil injection rate, carbon monoxide release
from the reduction reaction taking place in the slag and from direct
carbon burn-off, and oxygen injection rate at the feed end of the furnace.
The most important of these factors is oxygen injection since in general
there would be excess fuel available in the furnace for combustion. The

necessary rate of heat release within the bulk gas can be obtained

relatively easily, the difficulty is in ensuring efficient heat trans-

fer back to the reducing bed of the furnace. For any given heat input,

if the heat transfer mechanisms to the bed are inefficient then the

exhaust gas temperature will be unacceptably high, giving rise to a

high energy loss from the furnace. The principal mode of heat transfer

should be by radiation, since a large convective heat transfer would

also mean a large mass transfer of oxidising species from the gas core

to the bed surface. The radiative heat transfer is a function of gas

temperature and gas emissivity. The gas temperature can be increased

by increased fuel and oxygen injection but, with non-luminous flames,

higher temperatures mean high degrees of dissociation, which in turn

limits the molar concentration of H_2O and CO_2 in the gas and hence the

gas emissivity. However, the luminosity can be independantly controlled

by increasing the amount of partially burnt carbon in the gas core.

This is achieved by injecting normal power station pulverised fuel into

the gas core.

4   MATHEMATICAL MODEL

4.1   Description of the Model

The mathematical model provides a description of the process operating under steady state conditions. The reactor is divided into 180 vertical slices, and the model is constructed by writing separate heat and elemental balances on the five material streams in each slice as they move through the reactor. The five material streams are the gas, the pulverised fuel, the carbon, the ore (slag) and the iron; heat balances being carried out on each stream, but elemental balances only on the separate streams as indicated in Table 4.1.

Table 4.1   Elemental Balances on the Separate Streams

Stream / Element	Gas	Pulverised Fuel	Carbon	Slag	Iron
C	✓	✓	✓		✓
O	✓			✓	
H	✓	✓			
S	✓		✓	✓	✓
Fe				✓	✓
Si			✓	✓	
Ca			✓	✓	

Each material stream is described in terms of the separate elemental flows contained within it, the elemental flow of nitrogen in the gas phase being considered constant throughout the reactor. All the other elemental flows are allowed to vary throughout the reactor, the separate elemental balances on each slice involving the mass flows of the relevant

elements carried into and out of the slice in the separate streams.

The model assumes that material enters the reactor as oxygen, nitrogen, fuel oil, pulverised fuel, ore, coal and limestone. The oxygen and nitrogen, not in the standard air ratio but in a variable ratio to simulate varying operating ratios of oxygen to air, are assumed to enter the gas stream at slice zero, but all other material inputs can be distributed along the length of the reactor. This allows the model to simulate different operating practice. For example, the combustion mixing produced by the burner is simulated by assuming that the fuel oil enters the gas phase uniformly over the first 60 slices burning immediately and liberating its heat of combustion directly into the gas phase. The pulverised fuel is assumed to enter its own stream uniformly over the first 90 slices, this distance being chosen to simulate the way in which the fuel injector mixes the pulverised fuel into the bulk gas stream. The combustion of the pulverised fuel is subsequently analysed as described later. The inputs of coal to the carbon phase and ore and limestone to the slag phase can be distributed uniformly along the length of the reactor or given a triangular distribution with the maximum input rate placed at any point within the reactor, depending on the actual feed mechanism being simulated by the model.

In writing the heat and elemental balances on each stream in each slice, it is assumed that the interchange between adjacent slices is only brought about by the material flows from one slice to the adjacent slice, conduction and diffusion axially along the reactor being ignored. Interchange between the different streams is thus described in each heat or elemental balance in terms of processes occurring entirely within each separate slice.

The iron stream is assumed to lie against the wall of the reactor, maintained in place by the centripetal force of the rotating reactor. The slag layer lies against the iron layer and the solid carbon bed (of coal) floats on the slag layer. The centre of the reactor is occupied by the gas stream, with the pulverised fuel stream incorporated into it.

The different interchange processes considered in the model are listed below.

4.1.1   Heat Transfer

(a) From gas to carbon

This interchange is assumed to occur by convection and radiation. Calculation of the radiation transfer rate is described in Appendix 1. The convective heat transfer coefficient was calculated using standard pipe flow correlations; e.g. the Dittus-Boelter equation:-

$$Nu = 0.023 \ Re^{0.8} \ Pr^{0.3} \qquad \ldots\ldots\ldots (4.1)$$

augmented in the light of the mass transfer studies carried out in this work. However, even the augmented convective heat transfer was too small to produce heat flows that were significant in the presence of the calculated radiation fluxes.

(b) From carbon to slag

The transfer of heat from the carbon to the slag layer is brought about by conduction through the solid coal, and was analysed in terms of a coke conductivity[26] and the thickness of the coal bed. Thus the model would vary the thermal resistance of the coal bed as the bed was consumed or built up. Under certain operating conditions the coal particles

would rotate or partially sink, enhancing the flow of heat from the hot gas above them to the somewhat cooler slag. This enhancement was arbitrarily modelled by augmenting the thermal conductivity of the coal particles in the model.

(c) From slag to iron and iron to the water cooled shell

Both these heat transfer processes took place by conduction, composite thermal resistances being calculated for the transfer from the bulk slag to the bulk iron, and from the bulk iron through the lining to the water cooled shell of the reactor which was assumed to be at 100 ^{o}C. The resistances of the slag and iron layers involve the layer thicknesses. Values were chosen from plant observation and were never altered.

(d) Heat transfer with mass interchanges

Each mass exchange from one stream in any one slice to another stream in the same slice was always assumed to carry with it the sensible heat content corresponding to the stream from which it originated.

4.1.2   Carbon Transfer

(a)   From pulverised fuel to the gas stream

This interchange was involved in the combustion of the pulverised coal, assumed to be a diffusion limiting process, and detailed in Appendix 2.

(b)   From the carbon bed to gas stream

The transfer of carbon from the carbon bed to the gas stream is brought about, in part, by the combustion of the coal. This is a function of the surface reaction rate constant K_s (see Appendix 2), and the rate at which the oxidising gases reach the coal surface from the gas core. In this case the mass transport is by forced convection, such that:-

$$Sh = \frac{k_i R_\cdot \Theta_\cdot d}{D_i} \qquad \qquad \cdots \cdots \cdots (4.2)$$

where the Sherwood number, Sh, has been obtained from the standard

pipe flow relationship, e.g.

$$Sh = 0.023 \ Re^{0.8} \ Sc^{0.4} \qquad \qquad \cdots \cdots \cdots (4.3)$$

augmented in the light of the experiments to be described later.

The flux of any species, i, to the carbon surface is given as:-

$$k_i \left(P_i - X_i \right)$$

where P_i and X_i are, respectively, the partial pressures of i in the

bulk gas and at the reaction surface.

Now the nett flux of hydrogen and oxygen containing species per atom

of hydrogen and oxygen is zero, therefore the rate of carbon oxidation

is equal to the nett flux of carbon containing species.

Thus,

$$K_s \cdot X_{O_2} = k_{CO} \left(X_{CO} - P_{CO} \right) + k_{CO_2} \left(X_{CO_2} - P_{CO_2} \right) \ \cdots (4.4)$$

If the gases are in equilibrium at the interface, then,

$$X_{CO_2} = K_p \cdot X_{CO} \sqrt{X_{O_2}} \qquad \qquad \cdots \cdots \cdots (4.5)$$

Solution of these equations for the interface temperature gives the

rate of coal combustion.

In addition, carbon is transported from the coal bed into the gas phase

as a product of the reduction of the iron oxide in the slag. The

kinetic model assumed for this reaction will be described later.

(c) From the carbon bed to the iron stream

As described subsequently, iron drops are formed by the reaction between the iron bearing slag and the coal particles in the carbon bed. It is assumed that these droplets contain a fixed proportion of carbon when they form and thus their passage through the slag into the iron layer carries the corresponding flux of carbon. The actual proportion of carbon allotted by the mathematical model was set in the light of plant experience.

(d) From the iron to the gas stream

Under certain operating conditions, the iron layer can become directly exposed to the gas phase whence carbon can be burnt out of the iron stream. The mechanism of this decarburisation process possibly involves a carbon boil and is described in the model in terms of a first order equation, values of the constant in this equation being chosen so that the carbon levels predicted by the model are in line with those achieved in plant operation.

4.1.3   Oxygen Transfer

(a) From the slag stream to the gas stream

Oxygen is transferred from the slag stream to the gas stream as a result of the reduction of the iron oxide in the slag. The kinetics of this reaction formed a specific facet of this investigation, and are therefore described in section 5.

(b) From the gas stream to the slag stream

Under certain operating conditions the gas stream could be highly oxidising and, with the cover provided by the carbon bed removed, the

gas stream could reoxidise the slag stream. The kinetic equations
used in the model are specified in Appendix 3.

4.1.4   Iron Transfer

(a) From the slag stream to the iron stream

Droplets of iron form as the coal particles reduce the iron oxide in
the slag stream. The rate at which they form is described, as stated
above, in section 5. Once they are formed, the centripetal force in
the rotating reactor causes the iron droplets to be thrown into the
iron layer against the refractory wall.

(b) From the iron stream to the slag stream

Once again, highly oxidising conditions could be built up in the reactor
under certain operating conditions, and could produce highly oxidising
slags. These could reoxidise the iron layer, the equations used in the
model to describe this process being described in Appendix 4.

4.1.5   Coal and Limestone Decomposition

The coal contains volatiles and moisture, silica and lime. An arbitrary
model is assumed for its decomposition: once the coal has been heated to
625 ^{o}C, after entering the carbon stream, the volatiles and moisture it
contains are driven off into the gas stream, and the lime and silica of
its ash content enter the slag stream.

Limestone, added with the coal, is assumed to enter the slag stream
directly where it decomposes; carbon dioxide entering the gas stream
and the lime produced dissolving in the slag. This decomposition
reaction constitutes a major thermal load on the process.

4.2   Mode of Operation of Model

In principal, the parameters involved in the mathematical model could
be divided into two categories:- parameters fixed as a result of
literature survey or prior laboratory or pilot plant experiment, and
parameters that were varied in order to simulate different plant operat-
ing conditions. In this latter category were the input rates of fuel
oil, pulverised fuel, coal, limestone, oxygen, air and ore, and the
spread of the input materials.

For any given 'run' of the model, single values of all these parameters
were set and the model operated. The output from the model provided
values, in each slice, for the following variables:- the temperatures
of the gas, carbon, slag and iron streams; the amounts of iron oxide
reduced and iron oxidised in the slice; the amount of carbon burnt; the
depth of the carbon bed; the gas composition and heat losses. Table 4.2
presents a condensed illustration of the output from the model.

As will be described later, comparisons between inferences drawn from
the variables provided by the model and from observations of the per-
formance of the pilot plant were used to test and modify the model, and
then to understand, and thereby subsequently improve, the performance
of the pilot plant.

Divisions of Furnace Length	Temperature °C									Oil	P.F.	Iron			Coal (Carbon)				Gas Core % Vol.		
	T_G	T_{G-C}	T_C	T_{C-S}	T_{G-S}	T_S	T_{S-Fe}	T_{Fe}	T_{Fe-R}			Added	Reduced	Oxidised	Added	Burnt	Cover %	Depth cm	CO_2	CO	O_2
20	1263	788	770	763	848	666	638	634	631	477	0.30	124			259		42	0.63	9	0	58
30	2108	1802	1525	1524	1909	1520	1451	1441	1432	716	0.44	186	5	1	428	18	62	0.63	17	0	45
40	2478	1802	1712	1712	2302	1736	1661	1651	1640	955	0.59	248	81	40	597	18	43	0.65	20	5	34
50	2605	1804	1760	1760	2420	1786	1707	1696	1685	1198	0.74	310	241	62	767	18	38	0.62	21	10	26
60	2666	1806	1841	1841	2501	1864	1770	1757	1745	1432	0.89	372	415	85	936	18	40	0.54	22	15	19
70	2653	1808	1976	1976	2517	1991	1891	1878	1865		1.04	434	520	110	1105	18	62	0.61	23	16	16
80	2640	1808	1995	1995	2509	2009	1917	1904	1892		1.19	496	600	128	1274	18	71	0.75	24	18	13
90	2617	1810	1985	1985	2486	1999	1911	1898	1886		1.26	557	675	144	1444	18	76	0.91	25	18	11
100	2587	1810	1961	1961	2454	1974	1890	1878	1866			619	749	158	1613	18	84	1.08	26	18	9
110	2556	1810	1934	1934	2420	1947	1865	1853	1841			681	821	172	1728	18	92	1.25	27	19	8
120	2501	2318	2286	2286	2263	2263	2134	2116	2102			743	894	184	1951	89	100	1.30	29	19	6
130	2451	2276	2246	2246	2228	2228	2135	2122	2108			805	964	194	2120	175	100	1.30	30	19	4
140	2389	2210	2182	2182	2165	2165	2083	2072	2058			867	1033	202	2294	249	100	1.34	30	20	2
150	2304	2123	2095	2095	2080	2080	2010	2000	1987			929	1100	210	2459	306	100	1.41	31	21	1
160	2186	2005	1978	1978	1965	1965	1911	1904	1891			991	1167	218	2628	342	100	1.52	30	22	0
170	2052	1867	1840	1840	1828	1828	1790	1784	1773			1053	1243	226	2797	357	100	1.74	29	24	0
180	1929	1758	1733	1733	1720	1720	1671	1664	1653			1115	1292	233	2950	359	100	1.92	28	25	0

TABLE 4.2

CONDENSED MATHEMATICAL MODEL OUTPUT

KEY TO TABLE 4.2

The colums shown in Table 4.2 are as follows:-

T_G —   Temperature of Gas (^{O}C)

T_{G-C} —   Temperature of Gas - Carbon Interface (^{O}C)

T_C —   Temperature of Carbon (^{O}C)

T_{C-S} —   Temperature of Carbon - Slag Interface (^{O}C)

T_{G-S} —   Temperature of Gas - Slag Interface (^{O}C)

T_S —   Temperature of Slag (^{O}C)

T_{S-Fe} —   Temperature of Slag - Iron Interface (^{O}C)

T_{Fe} —   Temperature of Iron (^{O}C)

T_{Fe-R} —   Temperature of Iron - Refractory Interface (^{O}C)

Oil   —   g atoms of carbon in oil per s x 10^3

P.F.   —   g atoms of carbon in pulverised fuel per s

Iron Added   —   g atoms of iron added in iron ore per s x 10^3

Iron Reduced   —   g atoms of iron reduced from slag per s x 10^3

Iron Oxidised   —   g atoms of iron oxidised from iron layer per s x 10^3

Coal Added   —   g atoms of carbon added in coal per s x 10^3

Coal Burnt   —   g atoms of carbon combusted from coal layer per s x 10^3

Cover %   —   percentage of slag layer covered by coal layer

Depth   —   thickness of coal layer floating on slag layer (cm)

5   LABORATORY EXPERIMENTS

5.1   Kinetics of the Reduction of Molten Iron Containing

Slags by Solid Carbon

5.1.1   Reaction Kinetics

The reduction of iron oxide from a molten slag using solid carbon is a heterogeneous reaction, whose rate can be expressed by the equation:-

$$\frac{dN}{dt} = -A^1 . k^1 . C^n \qquad \dots\dots\dots\ (5.1)$$

where $\frac{dN}{dt}$ is the rate of the reaction, A^1 is the actual area of the reaction interface, C is the molar concentration of the iron containing species, FeO, in the slag, n is an exponent representing the order of the reaction and k^1 is a rate constant. If the reaction is taking place in a given volume of slag, V, a mass balance on the iron that it contains shows that:-

$$V \frac{dC}{dt} = \frac{dN}{dt} \qquad \dots\dots\dots\ (5.2)$$

so that equation (5.1) becomes:-

$$\frac{dC}{dt} = - \frac{A^1 k^1}{V} C^n \qquad \dots\dots\dots\ (5.3)$$

However, it is seldom possible to measure the actual reaction area, A^1, so that the reaction rate is related to some suitable nominal area, A, and to a corresponding nominal rate constant, k. Thus equation (5.3) becomes:-

$$\frac{dC}{dt} = - \frac{Ak}{V} C^n \qquad \dots\dots\dots\ (5.4)$$

When the rate of reaction is independent of the concentration of iron in the slag - the reaction is of zeroth order - the value of n is zero and equation (5.4) becomes:-

$$\frac{dC}{dt} = -\frac{Ak}{V}$$ .... (5.5)

or $$C = C_o - \frac{Ak}{V} t$$ .... (5.6)

where C_o is the concentration of iron in the slag at the start of the experiment. Under these conditions, the mole concentration, or with small error the mass concentration, will vary linearly with time.

When the rate of the reaction is proportional to the concentration of iron in the slag - the reaction is of first order - the value of n = 1, and equation (5.4) becomes:-

$$\frac{dC}{dt} = -\frac{Ak}{V} C$$ .... (5.7)

or $$Log \frac{C}{C_o} = -\frac{Akt}{V}$$

Thus a plot of $\frac{C}{C_o}$, or approximately of $\frac{m}{m_o}$ where m is the mass concentration, will give a straight line against t.

Previous work[27] had shown the reaction between iron containing slags and solid carbon to be of zeroth order at high FeO (>60%) contents, but suggested that it could be of first order at lower FeO contents. It had also shown the rate constant to follow an Arrhenius type relationship:-

$$k = k_o \exp\left(-\frac{E}{RT}\right)$$ .... (5.8)

where k_o is a constant and E is known as the activation energy.

However, the experiments had not been conducted at temperatures above 1 450 °C (1 723 K), although slag temperatures are normally above 1 450 °C in the Centrifugal Ironmaking Process. Moreover, FeO contents in the slag in the process vary in the range 15 to 55 mass %, a range that had only been covered cursorily in the previous experiments.

Thus the work carried out by the author was concerned with establishing a technique for studying the kinetics of the reaction at temperatures above 1 450 °C and at concentrations closer to those found in the C.I.P. process.

5.1.2   High Temperature Reduction Apparatus

The reduction apparatus is shown diagrammatically in Figure 1, and consisted of a 450 KHz, 12 kW high frequency heater with a graphite crucible acting as susceptor placed inside a gas tight silica tube.

The water cooled head unit was designed to allow the slag to be charged directly into the hot carbon crucible, and to allow any number of slag samples to be taken during an experimental run using 3 mm mild steel dip sampling rods. The temperature throughout an experimental run was to have been monitored using an optical pyrometer sighted on the base of the crucible, close to the slag/graphite interface. However, practical difficulties were encountered in sighting the pyrometer and this technique was abandoned. The temperature was recorded by a thermocouple dipping into the melt. For slag temperatures up to 1 973 K, platinum - platinum 13% rhodium thermocouples were used, and for higher slag temperatures tungsten - tungsten 26% rhenium thermocouples were used. The thermocouples were sheathed in a closed ended

34

FIGURE 1   THE HIGH TEMPERATURE REDUCTION
APPARATUS

FIGURE 1   THE HIGH TEMPERATURE REDUCTION APPARATUS
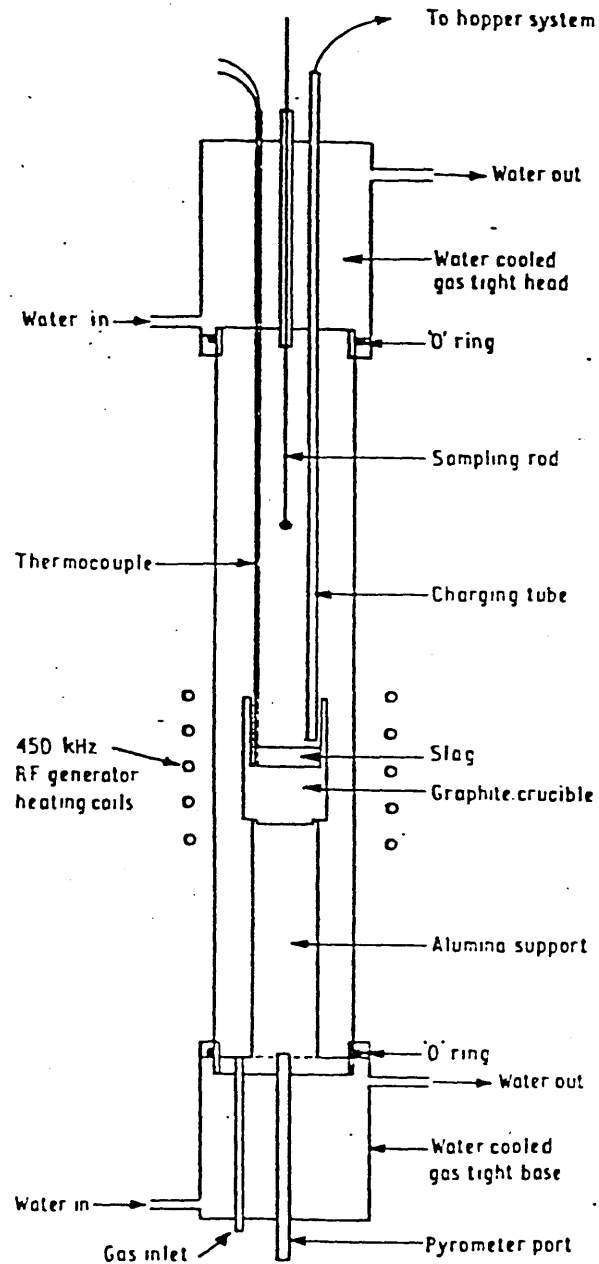
alumina tube. At slag temperatures greater than 1 923 K, slag attack on the alumina was appreciable and to reduce the amount taken into solution by the slag, the alumina tube was sheathed by a graphite sleeve.

5.1.2.1 Crucible Material and Construction

There were several development stages in the design of the graphite crucible before an optimum shape was achieved. The material used throughout was electrode graphite.

One major difficulty in carrying out reduction rate experiments at temperatures greater than 1 773 K is being able to maintain a uniform reaction temperature between the crucible and the slag, and the accurate measurement of the reaction temperature. The graphite crucibles used in earlier work for reaction temperatures up to 1 723 K were of a thin walled, thin base design, Figure 2a. However, these were found to be unsuitable for the higher temperature work because of the fluctuation in temperature after the charge had been added. The first modification to the crucible design was to increase the thickness of the base, Figure 2b. It was hoped that this would produce a large thermal reserve in the base of the crucible which would provide enough heat to raise the slag temperature and reduce or nullify the fluctuations in temperature. At this stage the reaction temperature was measured using an optical pyrometer sighted close to the slag/carbon interface at the base of the crucible. To facilitate this a viewing hole was drilled through the thick graphite base, stopping close to the slag/graphite interface. However, difficulties were encountered in sighting the pyrometer on the base of the crucible and the viewing hole had to be widened, which meant that the thermal capacity of the crucible was reduced thus giving only partial success in nullifying the temperature fluctuations. The next modification

was to have an outer graphite cylinder shrouding the graphite crucible, Figure 2c. It was considered that the assembly would act like a resistance heated furnace and avoid local overheating or cooling at the slag graphite interface. However, with this configuration a large input power was required to obtain temperatures greater than 1 773 K and this design was abandoned.

The next design of crucible was one where the base was reduced in height but the walls thickened, Figure 2d. This meant that the mass of the crucible was roughly unchanged but it was considered that the re-distribution of the mass would help maintain a constant crucible temperature during the slag charging period. This design of crucible proved successful over a limited number of experiments but on several occasions difficulty was experienced in sighting the pyrometer. Finally the temperature measuring technique using the pyrometer was abandoned in favour of a thermocouple dipping into the melt. The pyrometer sight hole was no longer required in the base of the crucible so the final design was as shown in Figure 2d, but with a solid base to the crucible.

5.1.3 Reduction of Iron Oxide Containing Slags

Analar grade silica and calcium carbonate were mixed to give a silica: lime ratio of 2 : 1. This mixture was fired at 1 773 K in a muffle furnace; the resultant fused slag was crushed to a fine powder. Iron oxide was added as Fe_2O_3 to give an Fe_2O_3 starting composition in the slag of either 60% or 30% Fe_2O_3 by mass.

The carbon crucible was placed inside the silica tube and the system was purged with nitrogen. The crucible was then heated in stages, allowing thermal equilibrium to be achieved at each stage, until the required

37

FIGURE 2   GRAPHITE CRUCIBLES
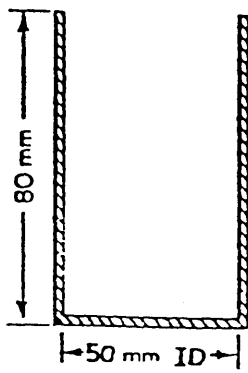
FIG.2a THIN WALLED, THIN BASE
GRAPHITE CRUCIBLE
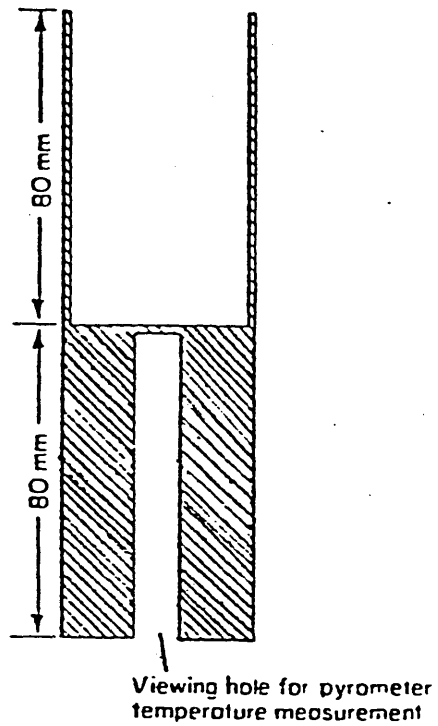
FIG.2b THIN WALLED, THICK BASE GRAPHITE
CRUCIBLE

Viewing hole for pyrometer
temperature measurement
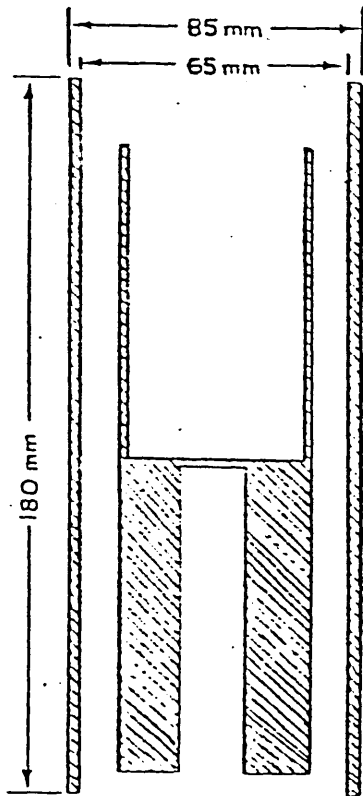
FIG.2c INNER CRUCIBLE WITH OUTER
GRAPHITE CYLINDER
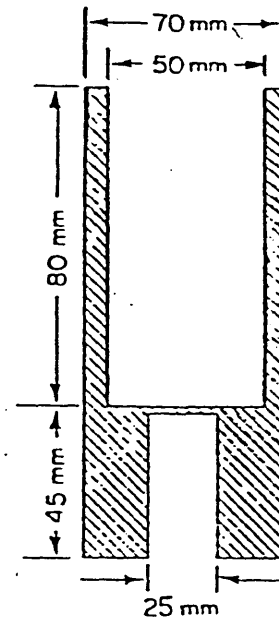
FIG.2d GRAPHITE CRUCIBLE WITH THICK
WALLS, MEDIUM THICKNESS BAS

temperature was obtained. The crucible was allowed to soak at this temperature for several minutes, after which time the weighed charge was dropped from its holding container into the carbon crucible. After the initial experiments had been carried out it was noted that a drop in temperature of between 150 $^{\circ}$C and 200 $^{\circ}$C occurred when the cold charge was added. A reheating period was allowed to permit the slag to become fully molten before the first sample was taken from the melt. To help minimise this drop in temperature the weight of the slag added to the crucible was reduced from 100 g to 50 g after these initial experiments had been completed.

It was realised that for experiments conducted at the higher temperatures this reheating period could not be allowed since the liquid slag would be seriously depleted in iron before the first sample could be taken. Use was therefore made of the drop in crucible temperature when the cold slag was added by heating the crucible in excess of the desired reaction temperature.

The degree of superheat required was determined by experience since it depended on the particular reaction temperature being studied, but in most cases it was around 200 $^{\circ}$C. When the cold charge was added to the crucible, the slag and crucible quickly attained equilibrium at the desired reaction temperature and sampling of the liquid slag could proceed.

Small samples of the melt were extracted during the experiment at varying time intervals depending on the reaction temperature. For instance, at 1 873 K a one minute sampling period was allowed whilst at 2 130 K the sampling intervals were only 15 seconds. The slag

samples were crushed to a fine powder using a ball mill and any metallic iron was removed by magnetic separation. The samples were then analysed for total iron content.

No attempt was made during the experimental run to prevent the accumulation of the iron product and it was expected that during the course of the experiment the volume of slag would decrease due to the removal of the iron oxide.

After the experiment was completed and the crucible was cold it was cut into two halves using a circular diamond saw. The two sections were dried, washed in a solution of 50% HCl - 50% H_2O, then dried in an air oven at 500 K to induce oxidation of the iron film that covered the crucible walls. Subsequent examination indicated the maximum height that the slag had reached during the experiment, and from this measurement the maximum apparent reaction surface area could be determined.

In a number of the experiments carried out a foam was observed inside the crucible which subsided towards the end of the experiment. This compounded the difficulty in making meaningful measurements of the reaction surface area. In some experiments carried out at the higher temperatures the foam came over the top of the crucible and down the outer walls. When this occurred the experiment was terminated.

5.1.4   Experimental Results

As stated in section 5.1.3, the iron oxide was added to the slag as Fe_2O_3. However the analytical determinations for each slag sample extracted during the experiments were for total slag iron, and the results have been expressed, for convenience, as "percentage FeO". This convention should not be taken to mean that any assumption has been made regarding

the state of oxidation of the iron in the slag.

For each experiment the change in FeO content in the slag with time was plotted for reaction temperatures ranging from 1 773 K to 2 135 K. Examples of the reduction curves obtained are given in Figure 3.

Although attempts were made to measure the area of reaction within the crucible, it was not possible to express the results in terms of reaction over a measured wetted area, no sensible correlation with rate of concentration change could be found. The length of the experimental times used, leading to a diminution of slag weight with time, and the fact that the iron product was allowed to accumulate may have contributed to an uncertainty in the surface area measurements, and to a poor correlation with concentration change. Attempts to obtain an order of reaction by application of the rate equation:-

$$\frac{1}{A} \frac{dN}{dt} = - k \ C^n \qquad\qquad \ldots\ldots\ldots (5.9)$$

where $\frac{dN}{dt}$ being the number of mols of iron oxide reacting per unit time.

   A = the reaction surface area

   C = the concentration of iron oxide in mols per unit volume

have led to n values varying between 0.8 and 2.5 both from experiment to experiment and within a given experiment. This result is perhaps expected since neither the volume of the slag nor the surface area of reaction is known at any given time.

However, a close examination of the reduction curves has shown that all are characterised by an induction period which in part reflects

FIGURE 3
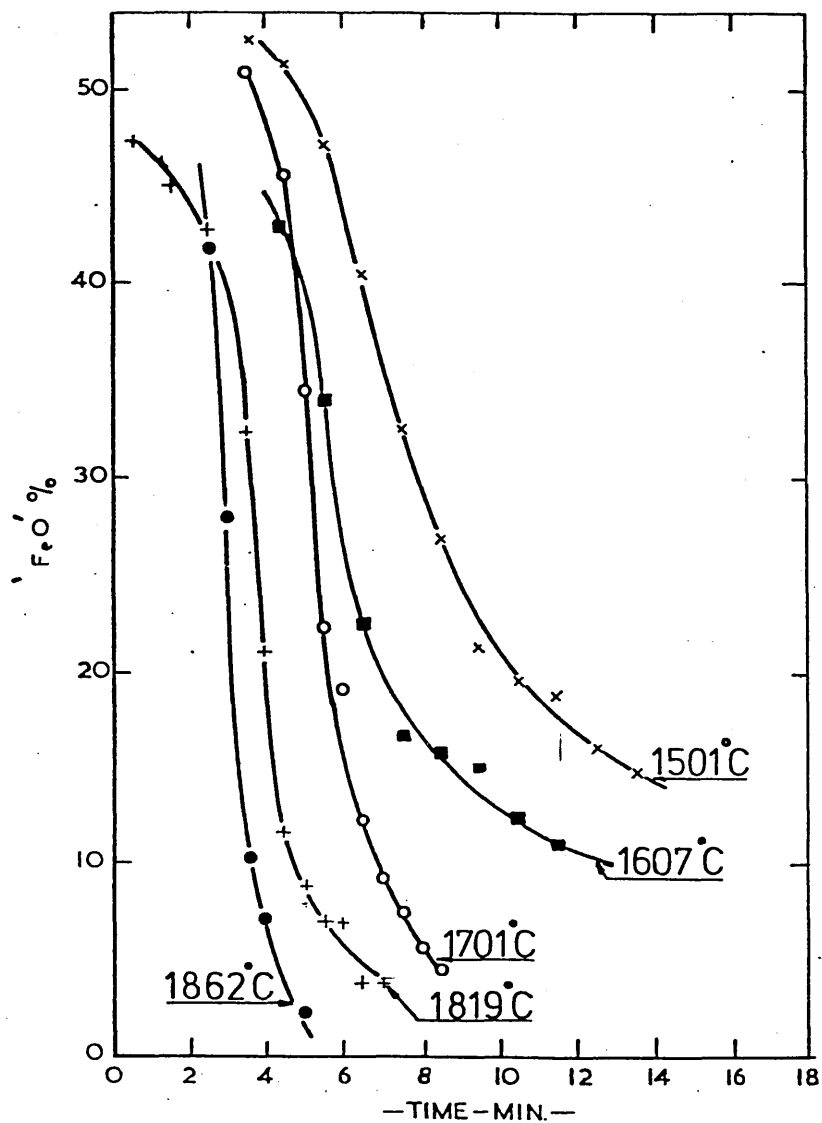
REDUCTION OF 'FeO' - CaO - SiO₂ SLAG AT VARIOUS TEMPERATURES

the uncertainty in the experimental procedure at the start of the experiment. After this induction period the experimental results can be reasonably represented by first order kinetics derived from equation 5.9 i.e. by putting $n = 1$. As $C = \dfrac{N}{V}$ where V is the volume of slag.

$$\frac{dN}{N} = - k \frac{A}{V} \; dt \qquad \qquad \dots\dots\dots (5.10)$$

If (a) is the number of mols (or weight) of iron oxide at zero time and (x) is the amount reacted after time t, then integrating equation 5.10 gives:-

$$\frac{\ln(a)}{(a-x)} = k \frac{A}{V} t \qquad \qquad \dots\dots\dots (5.11)$$

Although no theoretical justification has been found to explain this behaviour, all the results after the induction period were found to give straight lines when $\ln \dfrac{(a)}{(a-x)}$ is plotted against time. This is illustrated in Figure 4. Another feature of these results was that slags having a starting composition of 60% Fe_2O_3 gave two consecutive straight lines (although not all 60% Fe_2O_3 slags gave two straight lines), while slags having 30% Fe_2O as the starting composition gave only one straight line. Values of $K^1 = k \dfrac{A}{V}$ were calculated from these straight lines for all experiments and are given in Table 5.1 (two values K^1_1 and K^1_2 are obtained for experiments involving the 60% Fe_2O_3 slags). The influence of temperature on the constant K^1 is expressed by the Arrhenious equation:-

$$\ln K^1 = - \frac{E}{RT} + \text{constant} \qquad \qquad \dots\dots\dots (5.12)$$

FIGURE 4
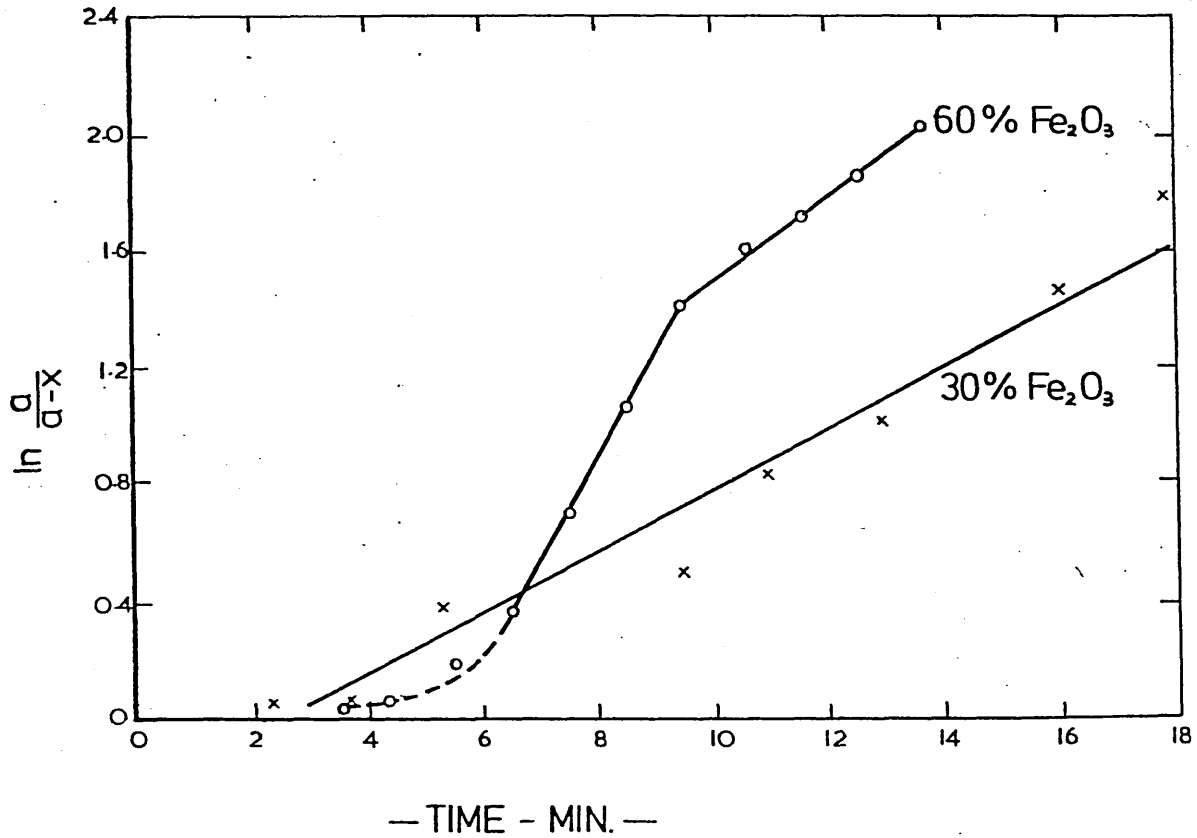
PLOT OF $\ln \frac{a}{a-x}$ AGAINST TIME FOR SLAGS CONTAINING 60% Fe_2O_3 & 30% Fe_2O_3 IN THE CHARGE AT 1500°C

Charge Weight g	Initial % Fe_2O_3	Temperature °C	K^1_1 min^{-1}	K^1_2 min^{-1}
50	60	1496	0.186	–
50	30	1500	0.110	–
50	60	1501	0.235	0.150
100	30	1547	0.130	–
100	30	1549	0.100	–
50	60	1550	0.490	0.100
50	60	1607	0.360	0.155
50	60	1615	0.391	–
50	60	1616	0.280	0.200
100	30	1620	0.215	–
100	30	1646	0.147	–
50	60	1650	0.380	0.210
50	60	1656	0.753	0.272
50	30	1671	0.214	–
100	30	1696	0.232	–
50	60	1701	0.530	–
50	60	1755	0.990	0.251
50	60	1801	0.600	–
50	60	1805	0.820	–
50	60	1819	0.470	–
50	60	1844	1.600	–
50	60	1852	1.610	–
50	60	1862	1.500	–

TABLE 5.1   VALUES OF K^1 FROM CRUCIBLE EXPERIMENTS

where   E = activation energy

            R = gas content

            T = absolute temperature.

A plot of $\ln K^1$ against $\frac{1}{T}$, Figure 5, gave two populations of points, representing on the one hand, K^1_1 values for 60% Fe_2O_3 slags, and on the other hand, the K^1_2 value for the 60% Fe_2O_3 slags plus the K^1_1 values for the 30% Fe_2O_3 slags. The apparent activation energies calculated from the slope of these lines were 31 Kcal/mole and 36 Kcal/mole respectively. The relevance of these experimental results and of their analysis to the mathematical model, is considered in section 6.6.1.

5.2   Heat and Mass Transfer Model Studies

5.2.1   Heat and Mass Transfer Analogue Theory

In its general form, the Chilton-Colburn analogy[15] describes heat and mass transfer in terms of j factors:-

Heat transfer : $\quad j_H = \dfrac{h}{U\,Cp}\,(Pr)^{\frac{2}{3}}$ .... (5.13)

Mass transfer : $\quad j_D = \dfrac{h_D}{U}\,(Sc)^{\frac{2}{3}}$ .... (5.14)

In pipe flow, these j factors are equal and are functions of the fluid flow conditions as specified by the Reynold's number. In the C.I.P. reactor, the rotation of the reactor contributes to establishing the fluid flow conditions so that we would expect the j factors to be given by an equation of the form:-

$$j_D = j_H = \int \left(Re_p \cdot Re_r \right) \qquad .... (5.15)$$

Where Re_p and Re_r are respectively Reynold's numbers for pipe flow and

FIGURE 5
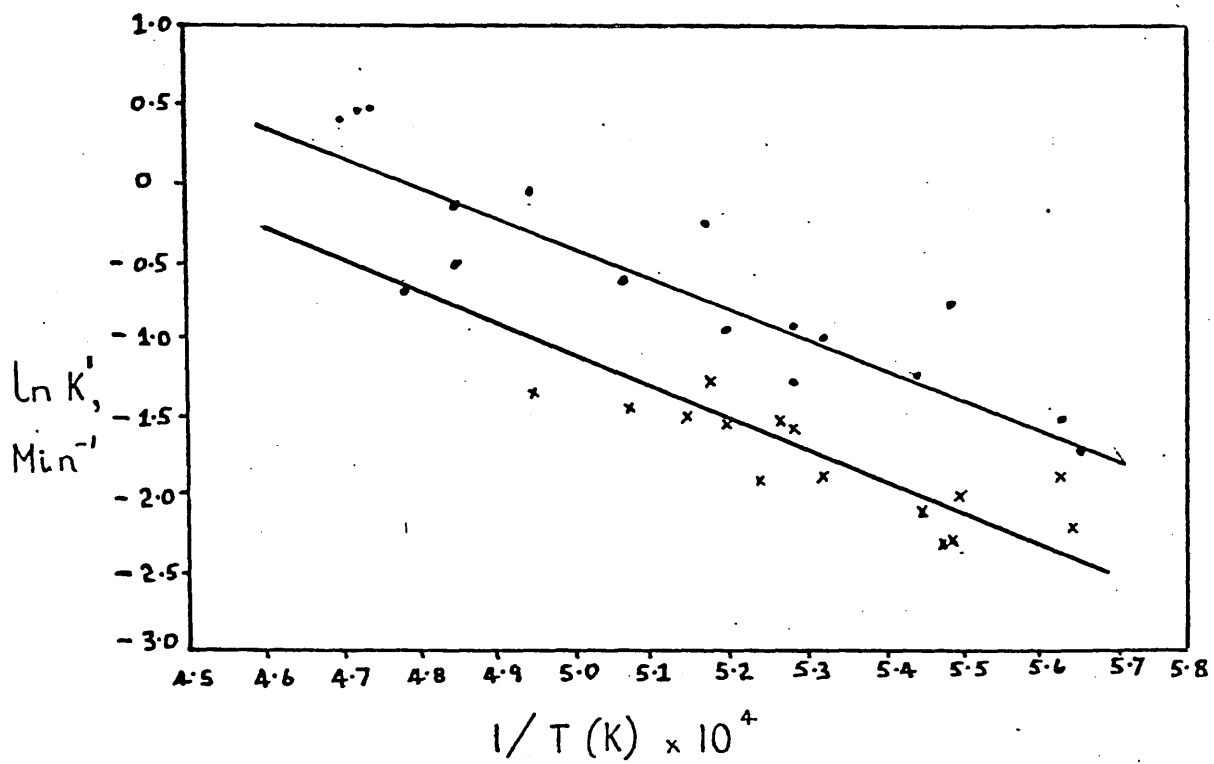
ARRHENIUS PLOT FOR CRUCIBLE EXPERIMENTS

for the rotational flow. Re_r would be defined by:-

$$Re_r = \frac{\omega d^2 \rho}{\mu}$$ .... (5.16)

It is normal to represent functional relationships of the form of equation (5.15) in terms of power expressions of the form $y = ax^n$. However, this form must be slightly modified to cope with the independent effects of axial flow and rotation, since the j factors have finite values when gas passes down the stationary reactor. Thus, it was decided to determine j factors by mass transfer (naphthalene evaporation) studies and to attempt to correlate the results using an expression of the form:-

$$j_D = j_H = a_1 Re_p^{n_1} \left(1 + a_2 Re_r^{n_2} \right)$$ .... (5.17)

These results and their analysis are described in the next sections.

5.2.2 Experimental Determination of Naphthalene Evaporation Rates

5.2.2.1 Description of the Model

The model was constructed from a perspex tube with a 6 mm wall thickness, and had a scale factor of 1/6 compared to the C.I.P. furnace. The model burner dimensions were calculated to give an equivalent burner nozzle diameter for the model compared to the pilot plant burner, as described by Bacon[10] for use with air models, such that:-

$$A_n = 0.218 \ M_n T_i^{\frac{1}{2}} - 0.068 \ G$$ .... (5.18)

Several methods of obtaining a strongly adherent and uniform layer of naphthalene inside the perspex tube were tried before a successful method was found. Using this method molten naphthalene was painted on

the inside of both ends of the tube to produce "end dams" 20 mm in length and 2 to 3 mm in height. The perspex tube was then installed inside a metal frame, the whole of which could be rotated on metal rollers, Figure 6, and the perspex tube was rotated at 75 rpm. Rotating the tube inside this arrangement allowed access to both ends of the perspex tube.

Molten naphthalene was then poured down a metal chute into the spinning perspex tube. The chute was moved slowly from the centre of the tube to the "end dam" whilst the molten naphthalene was being poured. This was then repeated from the centre of the tube to the other "end dam". This sequence was repeated until a uniform layer of naphthalene had been built up on the inside surface of the tube. Any excess naphthalene was removed from the edges of the tube and the loose particles on the naphthalene surface were removed by rotating the tube slowly by hand whilst blowing an air jet over the surface. A perspex end disc was then attached to the tube using four screws inside pre-tapped holes. A hole was machined at the centre of the end disc to allow the model burner to protrude inside the furnace model. The outside of the model burner was tapered to provide a close fit inside the perspex end disc which minimised the quantity of air entrainment into the model. The perspex model was then located and centralised in the head of a lathe before spinning commenced.

5.2.2.2 Naphthalene Sublimation Experiments

The rate of sublimation of naphthalene was determined by direct weighing rather than by a profilimetric technique. This meant that only the overall mass transfer coefficient could be determined.

49

FIGURE 6   FRAMEWORK SUPPORTING NAPHTHALENE MODEL

The length and internal diameter of the model was measured to calculate
the surface area of naphthalene exposed inside the model furnace.
Before each run the model was weighed. All the experiments were carried
out at room temperature and at atmospheric pressure. A fixed flow rate
of air was passed into the spinning model through the burner nozzle for
a given period of time, usually three hours. During this time the
temperature of the exit gas was measured every 15 minutes to enable an
average temperature of the experiment to be determined. The thermometer
was suspended in the exit gas stream approximately 5 cm away from the
end of the spinning model so that it did not interfere with the flow of
gas from the model. At the end of each run the air flow was turned off
and the model re-weighed.

One series of tests were carried out with the model stationary, the
remaining series of tests being carried out at set speeds in the lathe.
For each series of tests the speed was held constant but the flow rate
of air was altered after each run.

The loss of naphthalene in still air at the beginning and end of each
run was considered negligible, the time interval being only one or two
minutes between weighing the model and turning the air on or off.

5.2.2.3 Naphthalene Sublimation Experimental Results

The overall mass transfer coefficient, h_D, can be determined from
measurements of the weight loss of naphthalene from:-

$$h_D = \frac{W.R.\theta}{\Delta p M_N . A . t.} \qquad \dots\dots\dots\dots (5.19)$$

The dimensionless j factor for mass transfer j_D can then be determined

from equation (5.14). A range of air flows were used, firstly with the model furnace stationary, then rotating at 205 rpm, and finally rotating at 500 rpm. The air flows, average temperature of the air, the mass rate of loss of naphthalene during the experiment, the Reynolds number, mass transfer coefficient and j factors, for the three conditions 0 rpm, 205 rpm and 500 rpm are given in Tables 5.2, 5.3 and 5.4 respectively. The saturation vapour pressure of naphthalene at the average temperature of the experiment may be regarded as constant and was calculated using the equation by Sherwood and Bryant[28]. Because of local cooling due to sublimation, the surface temperature of the naphthalene will be lower than that of the air stream. However, work by Galsworthy[14] has found this drop in temperature to be negligible and has been ignored in the calculations.

5.2.3 Results and Discussion of Heat and Mass Transfer Model Studies

In order to examine the validity of a correlation for the experimental results in the form of equation (5.17), results obtained for each rotational speed were plotted separately as $\log_{10} (j_D)$ versus $\log_{10} (Re_p)$. The three separate sets of points are shown on Figure 7.

The points show a considerable amount of scatter, which is not untypical for experiments of this type. Best fit lines, drawn on the graph, for the three sets of results follow the equations:-

$$\text{for stationary reactor:-} \quad j_D = 20.32 \, Re_p^{-0.666} \quad \ldots\ldots \quad (5.20)$$

$$\text{for 205 rpm} \quad :- \quad j_D = 5.6 \, Re_p^{-0.458} \quad \ldots\ldots \quad (5.21)$$

$$\text{for 500 rpm} \quad :- \quad j_D = 21.62 \, Re_p^{-0.607} \quad \ldots\ldots \quad (5.22)$$

Temp. °C	Air Flow m_N^3/h	Wt. Loss g/h	Reynolds Number	Sat. Vap. Pressure atm·10^{-5}	P_e atm·10^{-5}	dP atm·10^{-5}	h_D cm/s	j_D
12.0	24.26	1.50	5520	2.8756	1.0809	2.3352	1.806	.0503
18.0	31.26	4.00	7113	5.3841	2.2370	4.2656	2.691	.0570
19.0	24.47	3.80	5567	5.9624	2.7154	4.6047	2.377	.0641
18.5	21.41	2.75	4871	5.6664	2.2458	4.5434	1.740	.0537
15.0	15.46	2.22	3518	3.9477	2.5103	2.6925	2.342	.1013
16.0	24.47	2.29	5567	4.3810	1.6364	3.5628	1.832	.0499
16.0	11.04	2.00	2513	4.3810	3.1662	2.7979	2.037	.1230
16.0	23.17	2.76	5273	4.3810	2.0821	3.3399	2.355	.0677
16.0	16.06	2.22	3653	4.3810	2.4173	3.1723	1.995	.0828
16.0	28.88	3.51	6572	4.3810	2.1246	3.3187	3.015	.0696
16.0	8.60	1.70	1956	4.3810	3.4571	2.6525	1.827	.1416
14.0	25.01	2.82	5690	3.5546	1.9713	2.5689	3.107	.0834
15.0	27.15	3.22	6178	3.9477	2.0735	2.9109	3.142	.0774
16.5	12.74	1.90	2899	4.6140	2.6068	3.3106	1.639	.0936

TABLE 5.2

MODEL DRUM SPEED 0 rpm

53

Temp. °C	Air Flow m^3_N/h	Wt. Loss g/h	Reynolds Number	Sat. Vap. Pressure atm.10^{-5}	P_e.10^{-5} atm.10^{-5}	dP atm.10^{-5}	h_D cm/s	j_D
18.0	13.08	3.00	2977	5.3841	4.0091	3.3795	2.548	.1209
18.0	15.8	3.17	3595	5.3841	3.5075	3.6304	2.506	.1080
17.0	17.94	4.00	4082	4.8584	3.8977	2.9096	3.932	.1456
17.0	11.48	2.50	2613	4.8584	3.8055	2.9557	2.419	.1399
17.0	19.06	4.00	4337	4.8584	3.6684	3.0242	3.783	.1318
17.0	21.37	4.50	4863	4.8584	3.6808	3.0180	4.263	.1323
17.0	25.82	5.00	5876	4.8584	3.3849	3.1660	4.517	.1162
17.0	26.90	4.50	6120	4.8584	2.9251	3.3959	3.790	.0936
17.0	29.80	5.75	6781	4.8584	3.3733	3.1718	5.185	.1156
20.0	28.54	6.00	6495	6.5982	3.6750	4.7607	3.642	.0839
17.0	11.04	2.75	2513	4.8584	4.3535	2.6817	2.933	.1764
18.0	9.99	2.75	2271	5.3841	4.8166	2.9758	2.652	.1759
18.0	14.78	3.50	3363	5.3841	4.1397	3.3143	3.031	.1357
18.0	24.84	4.72	5652	4.8584	3.3221	3.7230	3.639	.0970
17.0	22.43	4.40	5103	4.8584	3.4300	3.1434	4.003	.1186
18.0	14.29	3.38	3251	5.3841	4.1356	3.3163	2.925	.1355

TABLE 5.3

MODEL DRUM SPEED 200 rpm

Temp. °C	Air Flow m^3_N/h	Wt. Loss g/h	Reynolds Number	Sat. Vap. Pressure atm.10^{-5}	P_e atm.10^{-5}	dP atm.10^{-5}	h_D cm/s	j_D
19.0	14.78	4.00	3363	5.9624	4.7310	3.5969	3.203	.1429
19.0	19.57	5.40	4453	5.9624	4.8234	3.5507	4.380	.1476
18.0	21.41	4.25	4871	5.3841	3.4708	3.6487	3.343	.1034
18.0	24.52	5.50	5578	5.3841	3.9220	3.4231	4.611	.1243
19.0	26.23	6.00	5969	5.9624	3.9987	3.9630	4.360	.1097
20.0	11.26	3.75	2563	6.5982	5.8201	3.6881	2.938	.1715
20.0	16.60	5.50	3777	6.5982	5.7927	3.7018	4.293	.1701
18.0	13.22	3.50	3031	5.3841	4.5938	3.0872	3.254	.1617
20.0	11.49	4.20	2613	6.5982	6.3932	3.4016	3.568	.2042

TABLE 5.4   MODEL DRUM SPEED 500 rpm

It can be seen that the exponent of the 'pipe Reynolds number', Re_p, is approximately the same for the results obtained for the stationary reactor and for the reactor rotating at 500 rpm, whereas a lower exponent applies for the results obtained at 205 rpm. These differences are further shown in Figure 7 where it can be seen that lines drawn through the stationary and 500 rpm results appear to have the same slope, whereas the line drawn through the 205 rpm results appear to have a lower slope. However, the results obtained at this intermediate rotational speed seemed to be more scattered than those for the faster and slower speeds. Because of this scatter, it was decided to take the values of a_1 and n_1 from the results obtained on the stationary vessel, so that the correlation would be of the form:-

$$j_D = 20.32 \left(1 + a_2 Re_r^{n_2}\right) Re_p^{-\frac{2}{3}} \qquad \ldots\ldots\ldots\ldots (5.23)$$

Suitable values for a_2 and n_2 could now be sought by rearranging this equation in the form:-

$$\frac{j_D}{20.32 Re_p^{-\frac{2}{3}}} - 1 = a_2 Re_r^{n_2} \qquad \ldots\ldots\ldots\ldots (5.24)$$

Taking logs of both sides gives:-

$$\log_{10} \left\{ \frac{j_D}{20.32 Re_p^{-\frac{2}{3}}} - 1 \right\} = \log_{10} a_2 + n_2 \log_{10} Re_r \enspace \ldots (5.25)$$

In fact, only two values of Re_r, corresponding to the rotational speeds of 205 and 500 rpm, are available for the determination of a_2 and n_2. These two values were determined, then, by calculating average values for the left hand side of equation (5.25) for each value of Re_r, and using

FIGURE 7

The y-axis is labelled $LOG_{10} \ J_D$ and ranges from -0.6 to -1.4. The x-axis is labelled LOG_{10} REYNOLDS NUMBER and ranges from 3.2 to 3.9.

Legend:
□ 500 R.P.M
× 205 R.P.M
○ 0 R.P.M
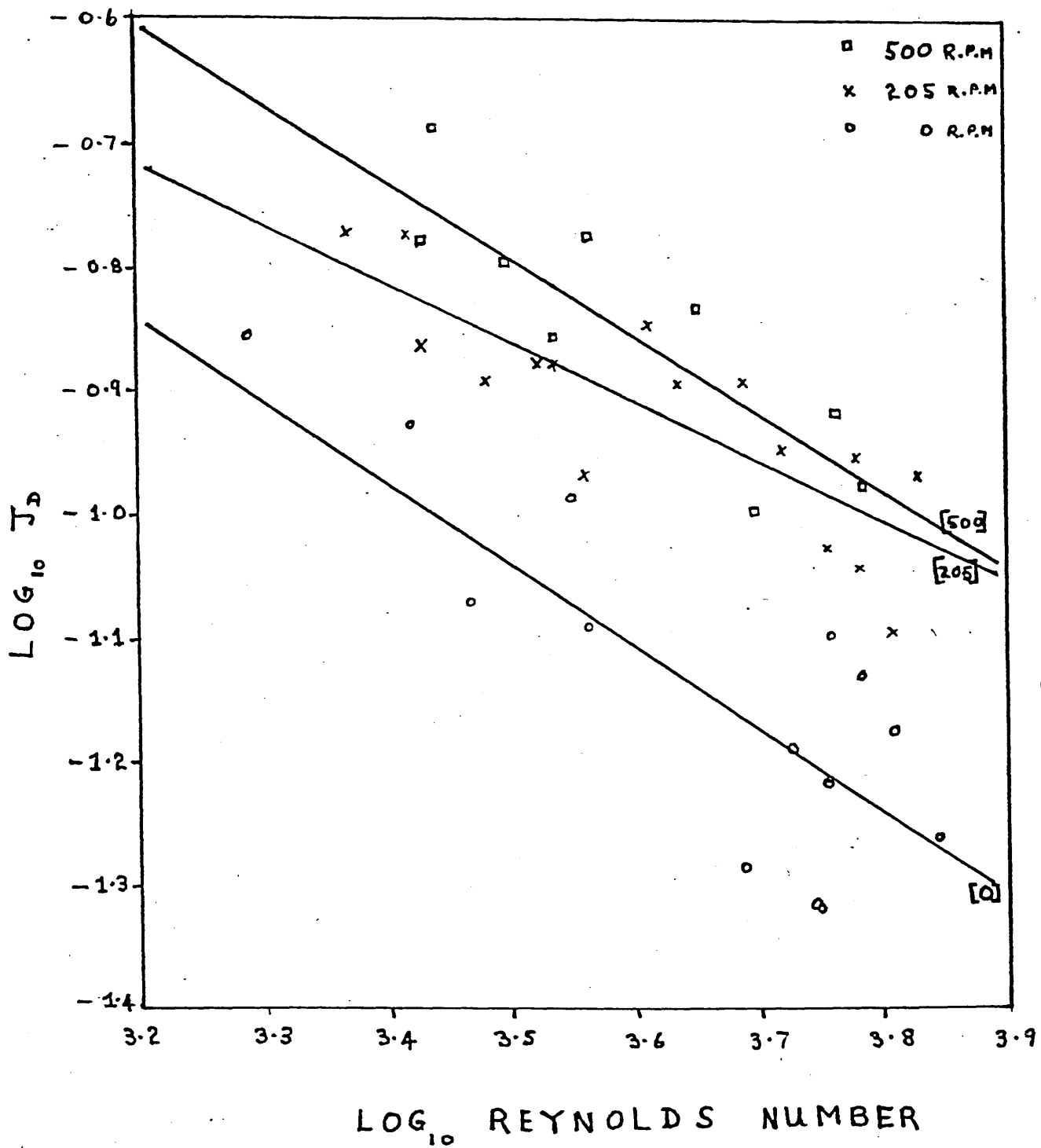
NAPHTHALENE MODEL RESULTS

these average values to calculate, from the two resulting simultaneous equations, values of n_2 and a_2. The resulting overall correlation is:-

$$j_H = j_D = 20.3 \left(1 + 0.11 \ Re_r^{0.2}\right) \ Re_p^{-\frac{2}{3}} \qquad \ldots\ldots\ldots (5.26)$$

and the results are plotted using this correlation for all rotation speeds in Figure 8.

It can be seen that the results are brought fairly well together when plotted in this way.

Heat and mass transfer coefficient values calculated from equation (5.26) for the conditions existing within the plant are discussed in relation to the plant performance in the discussion section of the thesis.

FIGURE 8
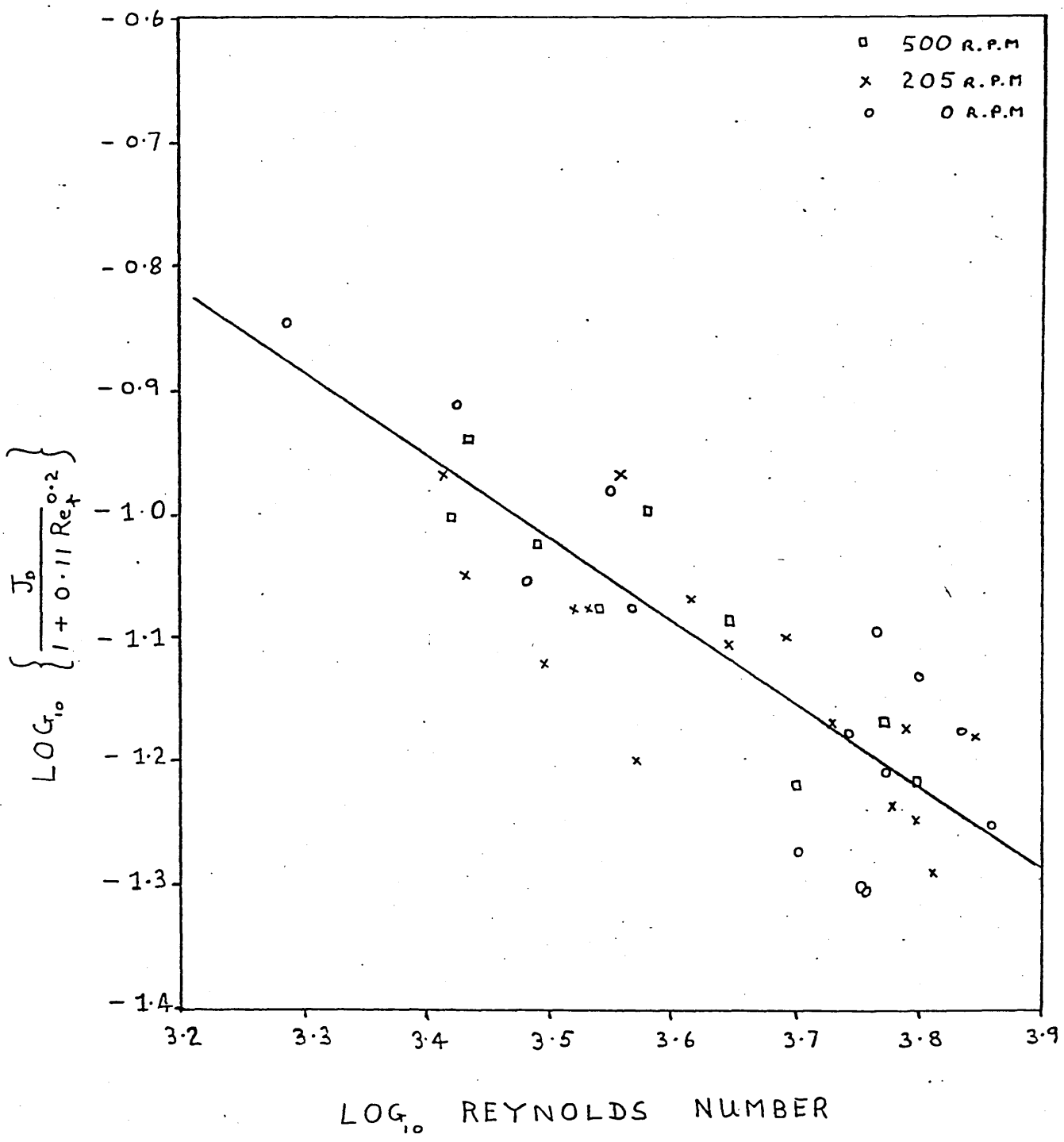
6   PILOT PLANT INVESTIGATIONS

6.1   Description of the Pilot Plant

6.1.1   Initial Design

The C.I.P. pilot plant was designed to operate with a maximum production rate of 1 tonne/hour of iron.   Figure 9 shows the basic concept of the pilot plant which consists of a centrifuge furnace 3 m long with an internal diameter of 65 cm.   Situated at either end of the furnace are static refractory lined hoods, within which the ends of the furnace rotate. The centrifuge furnace is lined with tar impregnated magnesite refractory bricks laid to a very high standard to minimise any possibility of iron being centrifuged under the high 'g' force through joints in the brick-work.   The thickness of the lining is 25 cm.

The feeding arrangements for the iron ore, coal and limestone are positioned at one end together with an oxy-oil burner, a fluidised feeder for pulverised fuel and an additional inlet for oxygen.   The oxy-oil burner is used to bring the furnace to operating temperature, and with the addition of pulverised fuel supplies auxiliary heat to compensate for the inherent heat losses in a small pilot plant.   Also positioned at the feed end of the furnace is a water seal arrangement which prevents the ingress of cooling air into the furnace.   The casting chamber is positioned at the other end of the furnace and the exhaust gases pass through this section to atmosphere.

After the furnace has been brought to the operating temperature granulated iron is charged into the spinning furnace and is centrifuged onto the refractory wall.   This iron acts as the initial protection for the refractory against slag attack until further iron units can be produced inside the furnace and centrifuged to the inner wall of the

Labels within the figure:

Molten slag and metal

Refractory lining

Gas analysis

Gas temperat measure

Water Seal

Cooling air

Oxy-oil burner and oxygen inlet

Oxygen

Oxygen

Charge of iron ore, coal and limestone

Exhaust gases

Periscope

Rotating drum

Metal and slag droplets

Cooling air

Drive unit

Motor

Metal and slag
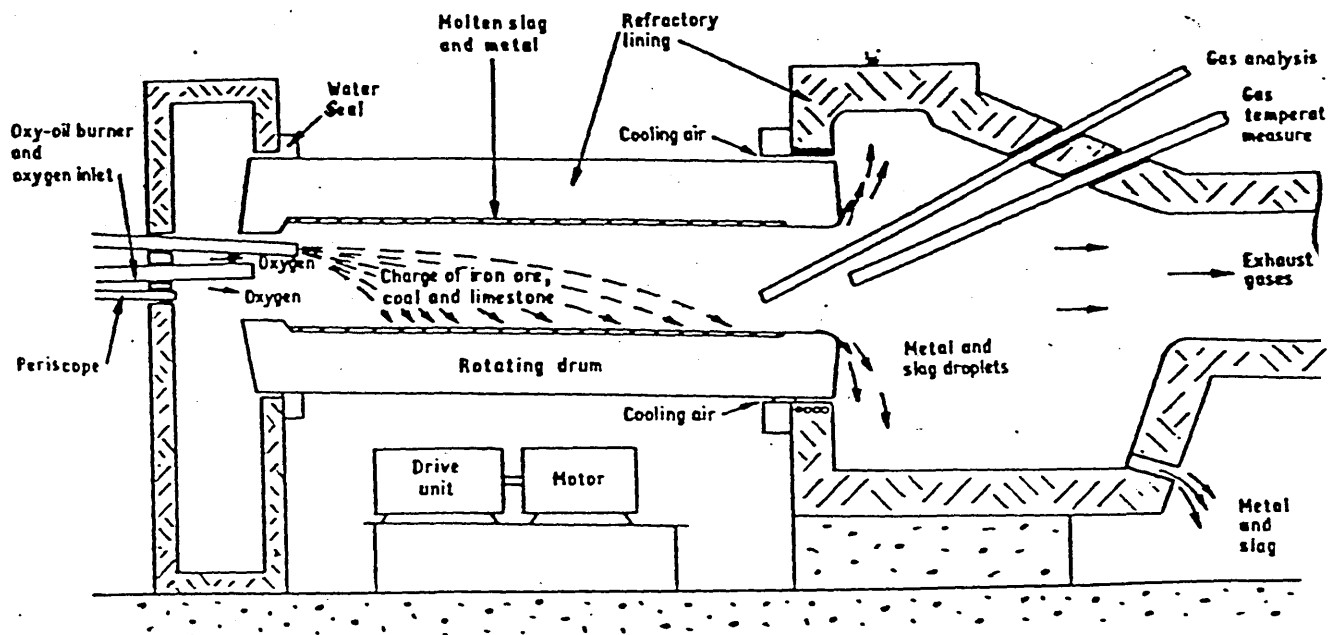
FIGURE 9   BASIC CONCEPT OF C.I.P. PILOT PLANT

furnace. A specially designed pneumatic feeder spreads a mixture of iron ore, coal and limestone evenly down a specified length of the furnace. The spreading of the charge down the length of the furnace promotes a faster melting rate of the charge and helps prevent build-up and sticking inside the furnace. The high rotational speed centrifuges the constituents of the furnace and spreads them in a uniform film around the furnace. Under the action of this centrifugal field the various liquid and solid constituents segregate into separate layers. The heaviest constituent, iron, is maintained as the outer, protective layer against the refractory surface. The liquid iron ore forms the next layer, on top of which floats the solid coal. Limestone is added to flux the slag resulting from the coal ash and the gangue in the iron ore. The depth of the rotating bed in the centrifuge furnace is controlled by the height of the dam situated at the cast end of the furnace, with 75 mm being a typical bed depth. To promote movement of the liquid bed towards the cast end, the furnace is angled at 3° to the horizontal. A typical operating speed for this size of furnace is 160 rpm.

The reduction of iron ore to iron takes place at the solid carbon, liquid iron ore interface. The iron formed is centrifuged into the iron layer which increases in depth as the reduction reaction proceeds. The iron bearing slag being depleted in iron content as it moves down the furnace. Carbon monoxide is evolved from the reduction reaction and enters the central gas core. Oxygen is added into the furnace which combusts the carbon monoxide to carbon dioxide, hence supplying heat which is radiated back to the bed to compensate for the endothermic reduction of the iron oxide and wall losses. Since the major method of

supplying heat to the bed is by radiation, pulverised fuel is added

to the central gas core, which has the effect of increasing the

emissivity of the gas core, hence increasing the amount of heat

radiated to the bed. When the holding capacity of the furnace is

exceeded, the iron spins out into the casting chamber where it dis-

charges through a tap hole and is collected.

Since ironmaking in a centrifuge furnace is unique it was considered

that the high 'g' forces on the solids and liquids of differing

densities would enhance separation of these constituents and prevent

the desired rapid chemical reaction between the carbon and liquid iron

oxide. Two solutions were postulated - one was that the self-induced

stirring motion within the bed by the carbon monoxide evolved during

the reduction reaction might be sufficient to give adequate mixing of

the reacting species; the second was mixing of the layers by varying

the rotational speed of the furnace in a cyclic manner. This type of

mixing was observed during model experiments and occurs on rapid

circumferential acceleration of the liquid and solid layers, and is

caused primarily by slip between the layers[25].

Another unique feature of this process was the use of relatively thin

liquid layers within the furnace. A liquid bed much thicker than 75 mm

is difficult to control on the pilot plant due to instabilities within

the bed, which could only be overcome by raising the rotational speed

of the furnace. Such action would be unacceptable on engineering

grounds since much finer tolerances would be required, as well as greater

safety margins. This would make the maintenance and operation of the

pilot plant impractical. The use of thin layers however bring other

problems to the process. The concept of the process relies on

transferring heat from the gas core to the bed to enable the strongly

endothermic reduction reaction to continue. This means operating with

an oxidising gas core adjacent to a bed where reducing conditions must

exist. The first consideration to this problem was that the coal layer,

being uppermost in the bed, would act as a barrier between the oxidising

central gas core and the rotating liquid bed. However, operating under

these conditions has shown that too much coal will reduce the transfer

of heat to the carbon-slag interface since the resultant coal-coke bed

is a poor conductor of heat. In addition the coal layer itself is

combusted by the oxidising species within the gas core and represents

a significant loss of carbon to the system, which is detrimental to

the fuel efficiency of the process. On the other hand if too little

coal is floating on the surface of the bed, oxidation rather than

reduction may occur within the liquid layers in the furnace. Under

these conditions, competing oxidation-reduction reactions will occur

and the net result could be one of oxidation within the bed. Data from

mathematical model runs simulating pilot plant practice was to be used

to obtain the optimum coal input rate to produce a 'balanced' condition

inside the furnace.

For safety reasons the spinning furnace is enclosed inside a metal test

house with only the minimum number of strategically positioned viewing

ports. To assist in the observations of the rotating furnace a network

of close circuit television cameras are located at either side of the

furnace and by the casting area. In addition to these a water cooled

periscope viewing device was installed at the feed end of the furnace,

viewing axially into the furnace. A television camera located at the

viewing end of the periscope provides the operators with live pictures

from inside the furnace. A rotating prism inside the periscope provides a 'static' picture of the inside of the furnace for making process observations. There is a drawback to this type of system however, since all stationary objects in the field of view, for example the burner and the feeder probes, appear to rotate.

The pilot plant is equipped with a range of measuring instruments situated around the plant. A water cooled probe for gas analysis measurement is located in one side of the static exhaust hood. The design of the plant only allows movement of this probe into the mouth of the furnace at the exhaust end. Located at the other side of the static exhaust hood is the venturi pneumatic pyrometer for measuring the central gas core temperature. The movement of this probe is restricted to the same gas sampling position as the gas analysis probe, that is just inside the exhaust end dam. The gases drawn through these probes are analysed for carbon monoxide, carbon dioxide, hydrogen and oxygen, using a mass spectrometer, and for gas temperature using the Land venturi pneumatic pyrometer logic system. A heated gas outlet line is also incorporated in the gas analysis system to keep the extracted gas mixture above its dew point so that the water content can also be measured.

The bed temperature is measured at 0.60 m and 1.80 m from the feed dam by infra red pyrometers located in the feed and exhaust hoods. The steel shell, although water cooled, is measured for any increase in temperature, e.g. penetration of the liquid bed between the brickwork, by an infra red scanning system. The signals are amplified and relayed to the central control room where they are displayed on a multi-channelled oscilloscope. The raw materials feed rates are measured

using load cells on each individual storage hopper. The oxygen flow

rate is measured using orifice plates and a rotameter measures the oil

flow rate. All the outputs from the measuring instruments are displayed

in the central control room.

The pilot plant was designed, as described above, by a design team and

its construction was supervised by the author's predecessor, as Project

Leader. Certain modifications to the plant and its operating practice

were subsequently developed by the author, and these are described in

the next section.

6.1.2   Modifications to the Pilot Plant

The initial design for the raw materials feed into the furnace was to

transfer the raw materials from their storage bunkers using rubber

belt conveyors to two holding hoppers, where coal and limestone were

mixed together, the iron ore being kept separate. Final mixing of the

raw materials occurred when they passed through two screw feeders into

a small transfer hopper, after which the mixed materials were gravity

fed to a single feeder probe and finally injected into the furnace using

a pulse of compressed air. The main problem with this feeding method

was that, although the feeder conditions were set up to feed the mixed

charge over the first 1.80 m of furnace length, because the charge was

a mixture of materials of different densities, the heaviest material,

iron ore, would fall short, and the lighter coal would accumulate

towards the furtherest point of the trajectory. This produced an iron

ore rich zone adjacent to the feed end dam and a coal rich zone towards

the centre of the furnace. To avoid this a dual feeder probe system

was designed, and, after suitable alterations to the screw feeder

discharge arrangement, the feed system was modified to feed iron ore

66

only through one of the feeder probes and the coal/limestone mixture through the second feeder probe. In this way a more uniform and controlled distribution of the raw materials feed inside the furnace was achieved.

The heat release inside the spinning furnace is achieved by combusting the carbon monoxide gas, obtained from the reaction between iron oxide in the slag and solid carbon, with oxygen in the central gas core of the furnace. Previously this oxygen had been added into the furnace through an outer annulus at the base of the oil-oxygen burner situated inside the static feeder hood. Before entering the furnace the oxygen had to pass through the "air gap" between the static feeder hood and the entrance of the spinning furnace. It was possible that not all of this oxygen would enter the furnace since the oxygen release point was some way back from the entrance to the furnace. In addition the oxygen was released around the oxy-oil flame of the burner which could alter the flame characteristics of the burner. To overcome these problems a separate, secondary oxygen probe was positioned inside the feeder hood of sufficient length to release the oxygen beyond the feed end dam of the furnace. This oxygen was now directed away from the burner flame as well as away from the pulverised fuel added downstream of the burner flame.

To prevent uncombusted oil entering the furnace and providing an explosive atmosphere inside the furnace, the burner flame is "viewed" at all times by a flame detector. Failure to monitor the flame would automatically close the oxygen and oil supply valves. The burner is ignited in the back position by a gas igniter torch and after ignition is pneumatically inserted into the furnace to a position adjacent to

the feed end dam. The flame detector must be capable of monitoring the flame with the burner in both the back and forward positions for successful burner operation. This was not always possible and difficulty was experienced, particularly during the warm-up sequence, in operating without spurious flame failure interruptions. To overcome this a second flame detector was positioned inside the feed end hood which operated in parallel with the initial detector. The system was modified so that the fuel valves remained open if either detector monitored a flame.

To facilitate these modifications on the pilot plant a complete redesign of the feeder hood was necessary because of the space limitation at the feed end of the furnace. It was noted during the earlier experiments that plant vibration was particularly excessive during the acceleration and deceleration periods in the drum speed cycling sequence. Plant vibration had also significantly increased at the higher speed levels now that the pilot plant was several years old. This level of vibration posed no problem to the rotation of the furnace as the support and rotational equipment were designed with anti-vibration pads, but it did pose a problem to the feeder platform and in particular to the load cells recording the weight of material inside the holding hoppers. The load cells provided an accurate measurement of material discharged from the hoppers and these readings were used to determine the materials feed rates into the furnace. The vibration was now preventing accurate feed rate data from being monitored, and as observed from previous experience, accurate feed rates were an essential part of the experimental programme. To prevent the vibration being transmitted through the structure of the pilot plant and into the structure of the feeder platform, the pilot plant and feeder platform were separated by cutting through all interconnecing steel work. A small amount of redesign to the feeder platform

was also necessary to ensure there was an adequate support at the positions where the cuts had been made.

6.2   Raw Materials

The raw materials used for the pilot plant experiments, iron ore, coal, limestone, were in the "as received" condition except for drying of surface moisture and screening to remove excessive lumps and fine material which could not be handled by the raw materials feed system. Some thought was given to the use of lime instead of limestone since the latter requires a large quantity of heat for decomposing into lime and carbon dioxide gas. However, the use of lime was rejected, despite the benefits to be gained on heat requirement grounds, because of the advantages to be gained by the stirring of the bath when the carbon dioxide gas is evolved from the limestone.

The raw materials, coal, iron ore and limestone were dried in a gas fired, slowly revolving kiln. The coal was screened to provide lumps in the size range 1.8 to 1.3 cm. The iron ore and limestone were also screened to remove any foreign matter, with 0.16 cm and 0.63 cm respectively being the final sizes. The pulverised fuel was purchased as a commercially prepared material, with 75 micron being the typical size. The gas oil and oxygen were obtained from commercial suppliers.

An analysis of all the materials used for the pilot plant experiments are given in Appendix 5.

6.3   Operational Procedure for the Pilot Plant

The operational procedure for the pilot plant developed as experience was gained of the plant's characteristics. The procedure was, however, developed by the author and operated under his responsibility.

6.3.1 Start-Up Procedure

For the initial warming-up stage the furnace was spun at 130 rpm and the water seal at the feed end of the furnace was flooded with water. This prevented the ingress of cold air into the furnace. The furnace was then heated at a rate of 50 ^{o}C/h using the oxy-oil burner situated at the feed end of the furnace, until a temperature of 1 500 ^{o}C was monitored at the refractory wall. The casting chamber was also heated to around 1 200 ^{o}C during this period using an air-coke oven gas burner situated in the side wall of the casting chamber. Once a furnace temperature of 1 500 ^{o}C was established, the refractory was held at this temperature and allowed to soak for at least twelve hours.

6.3.2 Batch Operating Procedure

Before the ore, coal, limestone, pulverised fuel and oxygen were added to the furnace, a charge of 500 kg of steel shot, mixed with 50 kg of coal, was added as a precursor to each experiment. The steel shot was melted to form the initial protective layer of metal over the barrel section of the refractory lining. A standard ore feed of 341 kg/h was aimed for and it was intended that a total of 1 tonne of iron ore should be added for each experiment provided that conditions within the furnace were not adversely affecting the plant life. This proviso was made because, unlike the previous earlier experiments, the output from this study was plant data and not necessarily high yields. It was recognised that certain of the conditions stipulated by the design of the experiments could lead to gross overheating and oxidation of the bed or, alternatively, low bed temperatures and build up of unmelted charge. If either set of conditions occurred then the experiment would be terminated as soon as representative plant data had been obtained.

For each experiment a drum speed of 160 rpm was chosen, and for the experiments that stipulated a variation in drum speed, i.e. bed stirring, then 160 rpm and 175 rpm drum speeds were used, with a speed change every 90 seconds at an acceleration of 1 rpm every second.

The steel shot, with the small quantity of coal, was added to the preheated furnace at the fastest possible rate without freezing of the liquid bed. The oil burner was operated at 20 g/h with the stoichiometric quantity of oxygen during the steel shot feeding operation. After the protective bed had been established the oil, oxygen and pulverised fuel input rates were adjusted to correspond with the predetermined experimental values. The raw materials iron ore, coal and limestone were then added to the furnace at their prescribed rates. The furnace was then continuously charged at these input rates until either the furnace was approaching its capacity, i.e. after ~ 3 hours continuous feeding, or until adverse conditions occurred inside the furnace, i.e. severe build up of unmelted charge or overheating of the bed. At this stage all feeding was stopped and the furnace contents were cast over the exhaust end dam and into the casting chamber by reducing the drum speed until the furnace came to rest. The liquid layers inside the furnace became unstable at 130 rpm and collapse of the layers occurred at 100 rpm, however the furnace was stopped to allow the maximum quantity of the bed contents to be cast out. A small pool of liquid was always left inside the furnace but this corresponded to only a negligible fraction of the total volume of the bed and was ignored.

The tapped material was collected in refractory lined boxes each containing 200 - 300 kg of the cast product. The liquid product was allowed to cool in the boxes, with the metal separating from the slag

under gravity. When the cast material had solidified and was
sufficiently cool, the boxes were turned upside down and the contents
removed. The slag and metal were separated by breaking up the slag
layer and the contents were then weighed and sampled for chemical
analysis.

After each experiment the cast end dam was visually inspected by
observation through the optical viewing device located in the casting
chamber and via the tap hole. If no spalling or chemical attack had
occurred, then the furnace was increased in speed until the water seal
at the feed end of the furnace was re-established ($\sim$ 135 rpm) and the
furnace was brought back to operating temperature using the oxy-fuel
oil burner. The furnace was now ready for the next experiment in the
experimental programme. If the cast end dam had deteriorated to such
an extent that the dam was lower than the preset 75 mm dam height, then
the furnace was allowed to cool down to room temperature in a controlled
manner. This meant spinning at 135 rpm (water seal made) and, by
decreasing the oil input and admitting greater and greater quantities of
air into the furnace at the feed end, cooling the furnace down at a rate
of 60 ^{O}C/h. When the furnace was cold the cast end hood was removed and
rebricking of the exhaust end dam could take place.

6.3.3 Introduction to Continuous Operation

The information and experience obtained from operating the pilot plant
in the batch mode provided the confidence to proceed with continuous
operation of the furnace, i.e. continuous feed experiments lasting in
excess of 10 hours duration. It was initially thought that operating
the furnace continuously would involve continuous feeding until the

capacity of the furnace was reached, then any continuation with the feedstock into the furnace would be balanced with material discharge. Thus, provided a liquid bed was maintained the furnace would operate with both continuous feed and continuous discharge. This, however, was not the case.

During the very early attempts at continuous operation it was noted that, at some point before the capacity of the furnace was reached, molten material would be cast from the furnace. At this point all furnace operation would stop since it was thought that premature collapse or failure of the cast end dam had occurred. However, on examination of the furnace after cool down no signs of dam failure could be seen. In an attempt to explain these events a scaled model simulation test was carried out using water as the modelling fluid and a perspex drum as the furnace to allow observations to be made. The model was operated with water feed rates which equalled the fluid capacity of the charge rates on the plant and with drum speed that provided equivalent centripetal acceleration. It was observed that before the capacity of the drum was reached, bed instabilities produced helical waves at the surface of the water, near to the feed end of the furnace. These waves would move from the feed end towards the cast end of the drum. The deeper the bed depth inside the drum then the greater the amplitude of the waves as they moved down the furnace until they reached a maximum at the cast end. It was also noted that when the "waves" at the cast end reached some critical depth, for the particular drum speed, then collapse of the liquid layers at the cast end would occur and part of the liquid contents would cast out. The liquid bed would then return to some lower, stable depth. The higher

the drum speed then the greater the depth of liquid inside the drum before bed instability occurred. These casts were termed "natural surges". Further experiments on the pilot plant verified that a similar phenomena was occurring on the plant and within the limits of the furnace bed depths and drum speeds available this phenomena could not be avoided. Hence continuous operation of the pilot plant had to be conducted with continuous feeds, but with intermittent tapping.

6.3.4   Continuous Operating Procedure.

The warm up procedure: obtaining the protective iron layer, feeding and monitoring of the raw materials input rates, and monitoring the process data was identical to that for batch operation. For continuous operation the raw materials were fed into the furnace at the feed rates decided upon after studying the results of the batch experiments and correlating them with the mathematical model predictions. The detailed reasoning leading to the choice of input rates for the continuous experiments that were considered to be the optimum for a high process efficiency with continuous furnace operation will be discussed later. The feeds were continued for several hours without interruption and experimental times of up to 10 hours were typical. Attempts to carry out experiments for much longer times usually resulted in failure of the cast end dam because of severe slag attack on the refractory material. In some instances, continuous feeds over the 10 hours could not be maintained because of feeder blockage or build up of unmelted material in the bed. On these occasions all raw materials feed would stop, i.e. iron ore, coal, limestone and secondary oxygen, until either the feeder blockage had been cleared or the bed had been remelted.

The experiments were usually conducted with casts from the furnace approximately every hour. It was usual to collect between 150 to 300 kg of melt per cast. These casts were cooled, weighed and sampled as described previously. The final cast for each experiment was carried out by reducing the drum speed until the furnace stopped. The sampling procedure was then the same as for the batch experiments.

6.3.5 Surge Casting

Carrying out continuous experiments with "natural surge" intermittent tapping, i.e. casting out part of the furnace contents when the bed depth at the cast end reached some critical value for the particular drum speed, was unsatisfactory. The timing of the casts could not be accurately determined, the quantity of material cast could not be controlled, and although the material ejected started from the cast end of the furnace it was considered, and later verified from model experiments, that unreacted iron bearing slag from the middle region of the furnace was also being dragged out of the furnace during these natural surges. This furnace practice therefore resulted in a lowering of the process efficiency.

A development of this casting technique came part way in overcoming these problems, that is by arranging the timing of the casts to happen when the cast end operators were ready and all the casting boxes were in position. This was achieved by noting the time intervals between natural surges for the particular raw material feed rates and drum speed. This provided an approximate capacity of the furnace before natural surges would occur. Only an approximation could be made since the times between natural surges and the quantity of material cast was not constant.

However, this technique was sufficiently accurate to determine when the furnace was approaching a natural surge. Before the natural surge occurred, the drum speed was lowered by 20 rpm from its normal operating speed. This meant that the bed depth inside the furnace, particularly at the cast end, was now critical for this lower drum speed and a "surge cast" would occur. The quantity of material cast could be roughly controlled by holding at this lower speed level, then quickly increasing the speed back to the experimental drum speed when casting would stop.

Using this casting technique a quantity of the liquid bed could be cast out in a controlled manner and usually approximately 200 kg of product was achieved with each cast. Casting in this manner did not overcome the problem of discharging unreacted iron ore from the central part of the furnace.

6.3.6 Rod Casting

A technique was developed to overcome the problem of discharging unreacted iron ore from the furnace and this allowed the preferential casting of iron. This technique did not require any change in the operational speed of the furnace and involved the introduction of a 5 cm diameter rod, preferably wooden for safety reasons, into the rotating liquid layers at the exhaust end of the furnace. The introduction of the rod into the liquid layers caused agitation of the layers and results initially in a small quantity of slag and metal being cast from the furnace. After this initial discharge of the slag-iron mixture a liquid sheet or wave was established with its base at the point of agitation. This liquid wave curls back into the furnace holding back the slag layer and thus preventing any further discharge of slag from

76

the furnace. Liquid metal continued to be preferentially cast from the furnace provided the rod remained inside the melt and the furnace was not depleted of iron.

This technique was developed using a scaled perspex model of the furnace with oil and water simulating the liquid layers. Experiments have shown that a higher ratio of iron is cast from the furnace if the furnace brickwork is modified to provide a "well" or deeper pool of iron at the point where the rod is inserted into the liquid layers. Control over casting was readily established using this technique since casting stopped soon after the rod is taken out of the melt. This technique has been examined on the pilot plant but still requires more test work before it becomes part of the normal pilot plant practice.

6.3.7   Pilot Plant Measurements

One of the major problems in conducting experiments using the centrifuge furnace is the lack of access inside the furnace to take meaningful process measurements. The furnace spins between two static end hoods which makes access inside the furnace very difficult, and for safety reasons the spinning furnace is housed inside a metal test house. The design of the cast hood, however, allowed two water cooled probes to enter into the gas core of the furnace at the exhaust end to just inside the cast end dam. One of the probes was used to continuously suck a sample of exhaust gas for analysis using a gas chromatograph. In later experiments a mass spectrometer was used. The second probe measured the gas core temperature at the exit of the furnace by using a commercial pyrometer, the Land venturi pneumatic pyrometer. Problems have arisen when attempting to measure the temperature of the gas on a continuous basis because of blockage of the nozzle by gas borne dust particles. Only intermittent measurements have been possible and on several occasions

even these were unsuccessful. When readings were possible, gas core temperatures in excess of 2000 ^{o}C were recorded.

The only measurements possible inside the furnace were bed temperatures at two positions, 0.60 m and 1.80 m from the feed end dam, by infra-red pyrometers located in the feed and cast hoods. These pyrometers only monitored the surface of the liquid bed and they had to view through a dirty furnace atmosphere so the values they record only gave the general trend of the bed temperature, i.e. falling or increasing, and could not be taken as precise bed temperatures.

The input rates of all the materials entering the furnace, i.e. iron ore, coal, limestone, pulverised fuel, oxygen and oil were monitored continuously during the experiment. The cast product, after cooling, was separated into slag and metal, weighed, sampled, then chemically analysed. Whenever possible a spoon sample of the material coming from the tap hole was taken for chemical analysis. Temperature measurements of the cast product was also measured using the consumable "cardboard" dip thermocouples. Sheathed Pt/Pt 13% Rh thermocouples were located at strategic points in the stationary hoods and exhaust stack to warn of any overheating that occurred in the static regions of the pilot plant. It was also possible that the steel shell of the rotating furnace could overheat locally even though it was water cooled, because of penetration into the brickwork at the joints by the liquid bed. To monitor any local overheating of the steel shell an infra-red scanning system was used to detect any increase from a preset value of the outer shell temperature of approximately 100 ^{o}C.

All the measurements taken on the pilot plant were relayed to a central

control room for interpretation and action. In addition to all these measurements, each side of the spinning furnace, the casting area and the inside of the furnace were viewed using a close circuit television network. The ability to observe the key positions of the pilot plant was crucial for safe operation of the plant. The ability to observe the inside of the furnace was perhaps the key to successful plant operation. Without this facility pilot plant operation would be carried out blind and important process observations, particularly those regarding the changes in bed condition, could not be made. The development of a prefocused periscope, with a built-in air jet to ensure the input lens remains clean, and the use of a television camera with a videcom tube for viewing with intense light, made continuous observations inside the furnace possible. The periscope also has a prism located inside the optical tube which could be made to rotate in the opposite direction to the furnace which, when the speeds are matched in the correct ratio, effectively froze the bed rotation. However, the contrast of the objects inside the furnace was impaired and also stationary objects, e.g. the feeder probes, appeared to be rotating, so this facility was only used on specific occasions.

A thermocouple was embedded into each of the eight bearing housings situated on the roller bearing support pedestals and these temperature readings were also displayed in the control room. It was important that the bearing temperatures did not exceed 80 $^{\circ}$C since above this temperature the lubrication provided by the high temperature grease would diminish.

6.3.8   Bed Sampling

One of the major problems during continuous operation was to assess, at regular intervals, the course of the experiment with regards to iron

production. Analysis of the exhaust gas, which was constantly sampled, acted as a guide to how well the experiment was proceeding but this could be misleading. Analysis of slag sampled from material cast from the furnace provided useful information, but even this was limited since its exact location inside the furnace was not known.

A method was devised by which samples of material could be extracted from the liquid layers just inside the cast end dam. Sampling from this point provided material which had had the maximum residence time inside the furnace. A wooden pole, 3 cm diameter was used and of sufficient length to reach inside the furnace when held outside the casting chamber. A metal sleeve was inserted and fixed at the sampling end of the pole. A metal cup, 2.54 cm internal diameter and 4.5 cm deep was attached to the metal sleeve. The mouth of the cup was set at right angles to the wooden pole. By suitably marking the wooden pole it could be inserted into the furnace until the metal cup was approximately 0.5 cm from the refractory.

With the liquid iron and slag layers established inside the furnace, sampling was carried out by inserting the pole into the furnace with the mouth of the sampling cup pointing upwards. When the pole was in position (with the cup inside the liquid layers but still in the upright position) the pole was rotated to bring the mouth of the cup into the liquid layers and facing the direction of furnace rotation. The pole was then immediately withdrawn from the furnace with a sample of the melt inside the cup.

A wooden pole was chosen because it is relatively light and easily manageable, since the pole length was over 3 m. In addition to this if

the pole was to catch for any reason inside the furnace and withdrawal was impossible, then the pole would snap and burn away with no damage to the furnace or to the operator. With experience the whole sampling procedure took less than 10 seconds and the sample pole and cup could be reused several times.

6.3.9 Determination of Process Yield from Plant Experiments

Liquid iron and slag are tapped from the furnace, collected, cooled, then weighed and analysed. The yield from the process is ideally determined from the equation:-

$$\text{Iron yield} = \frac{\text{Iron Cast} - \text{Iron in Initial Steel Shot}}{\text{Total Iron in Ore}} \times 100$$

However, experience showed that it was very difficult to collect all the iron from the furnace at the end of an experiment because a quantity of iron usually remained inside the furnace and on the inner walls of the casting chamber. Recovery of this iron was usually not possible which meant that for the batch type experiments, where only a limited quantity of iron ore was charged, any iron not collected would greatly underestimate the process yield. This problem was not so acute for the continuous experiments where a greater quantity of iron ore was charged during the experiment. Thus an alternative method of calculating the process yield was developed based on the iron content of the slags collected during the first cast from the batch experiments. It was usual to collect all the slag from an experiment since very little slag remained inside the furnace, and what remained inside the casting chamber could easily be broken and collected. Thus from a knowledge of the total iron units added with the iron ore, and the total iron units collected in the slag, the difference between these two values should

represent the iron units produced from the ore. This value would represent the maximum yield from the process since no account has been taken of any iron ore which may have been lost in the exhaust duct. This, however, was found to be relatively small and represented only a small fraction of the input materials.

A knowledge of the iron content of the slags sampled from the furnace during continuous operation could also be used to indicate process efficiencies. The rate of addition of the slagmaking materials are known, e.g. gangue content of the coal and the analysis of the iron ore and the limestone. Thus for a given input rate of raw materials the degree of reduction could be estimated from the total iron content of the slag after an allowance had been made for refractory pick-up by the slag (determined from the MgO level in the slag). The same technique could be used for the bulk slags, where a representative analysis is known.

Mass balances were carried out on each experiment by collecting, weighing and analysing all the material cast from the furnace during the experiment and, where possible, collecting the material from inside the furnace and casting chamber after the experiment. However, because of the difficulty of removing all of the solidified material, particularly from the inner walls of the casting chamber, some of the material collected at the start of an experiment actually originated from the previous experiment. It was not possible to accurately proportion the collected material to different experiments, therefore a standard procedure was adopted where, during the continuous experiments, all material collected during an experiment would, for mass balance purposes, be assigned to that experiment.

6.4. Batch Experiments

In section 4 it was described how the mathematical model describing the C.I.P. process had been developed prior to the author's involvement, to such an extent that it could predict the input conditions of iron ore, coal, pulverised fuel and oxygen, at which successful ironmaking should have been achieved. Ironmaking could not be achieved, however, but it was not known whether this was due to errors in the mathematical model, or due to an inability to operate the plant in the manner required by the model's predictions.

The author concluded that more information was required from the process itself over a wide range of operating conditions, which could serve as a comprehensive test for the predictions made by the mathematical model. Comparison between the predictions and the measured plant performance would demonstrate the true value of the model as a generator of the operating conditions for successful ironmaking. The mathematical model had shown that whilst some process variables had a significant effect on the process yield, e.g. coal stoichiometry, for a particular set of input conditions, others were less important. The range in input conditions used on the pilot plant had been limited up to this time, since the planned purpose of the early experiments had been to optimise process operation with the aim of producing consistently high yields. Consequently all correlation studies comparing practices used on the pilot plant with the predictions of the mathematical model had been limited to this narrow area.

The author, therefore, decided to conduct a factorial series of batch experiments over a sufficiently wide range of conditions to encompass operation with fluid highly oxidised beds through to operation with a

semi-molten bed in which unmelted material would build up. It was anticipated that the results of these experiments, together with the light that they would throw on the mathematical model, would allow conditions to be established under which continuous operation could be extended from the maximum time then achieved - three hours - up to the ten hour maximum imposed by the storage capacity of the feed hoppers. Only if this extension could be achieved would it be possible to carry out a true assessment of the centrifugal ironmaking process as a producer of iron.

A series of sixteen individual experiments which, together formed a factorial experiment, was designed in which the coal, oil, pulverised fuel and oxygen input rates were varied, and the effects of stirring the bed, were evaluated. The actual values of these operating variables required careful choice, since experiments had to be designed which were within the scope of the pilot plant without endangering its working life. The compromise chosen was to limit the range of oxygen inputs but to allow a wide range of inputs for coal, oil and pulverised fuel.

Three main target input levels, high, medium and low were chosen for the feed rates of coal, oil, pulverised fuel and oxygen, except that in experiments in which two of the input levels were at their medium value, the other variable was set either at its medium level or at an extra high level, or at an extra low level, thus accentuating any resulting variation in the plant's performance. The full range of input conditions, with the values chosen for the feed rates, are given in Table 6.1. This Table also shows that two experiments were carried out at one given set of input conditions with the bed stirred and not stirred. The iron ore input rate was held at a constant 341 kg/h throughout the series of experiments.

Experiment No.	Oxygen Flow		Pulverised Fuel		Stoichiometric Ratio Coal : Ore		Oil Flow	Stir	Remarks
	Planned Level	Value Chosen m_N^3/h	Planned Level	Value Chosen m_N^3/h	Planned Level	Chosen Ratio	g/h		
88	High	382	Low	45	High	1.8	10	Yes	Completed
89	Low	354	Low	45	High	1.8	20	No	Completed
90	V. High	396	Mid	68	Mid	1.5	15	Yes	Completed
91	V. Low	340	Mid	68	Mid	1.5	15	No	Completed
92	Low	354	High	102	High	1.8	20	Yes	Completed
93	High	382	Low	45	Low	1.2	20	Yes	Completed
94	Mid	368	V. Low	34	Mid	1.5	15	No	Completed
95	Low	354	High	102	Low	1.2	20	Yes	Completed
96	High	382	High	102	High	1.8	20	No	Completed
97	Mid	368	Mid	68	V. High	2.0	15	Yes	Completed
98	High	382	High	102	Low	1.2	10	No	Dam Failure
99	Mid	368	Mid	68	V. Low	1.0	15	No	Completed
100	Mid	368	Mid	68	Mid	1.5	15	Yes	Completed
101	Mid	368	V. High	136	Mid	1.5	15	Yes	Plant Failure
102	Low	354	Low	45	Low	1.2	10	No	Completed
103	Mid	368	Mid	68	Mid	1.5	15	No	Completed

FIGURE 6.1   DESIGN OF THE FACTORIAL EXPERIMENT

It was an intrinsic part of the factorial experiment that plant

conditions other than those being intentionally altered should remain

constant from experiment to experiment, therefore a standard base

practice was observed. All experiments were carried out on a batch

basis, i.e. the experiment would be terminated and the furnace contents

cast out before the volume of contents became so great that molten

material would be ejected over the cast end dam. A cast dam, 75 mm

high was used throughout the series of experiments, sometimes requiring

rebricking between experiments. The results obtained are presented in

the next section.

6.5   Results of the Batch Experiments

Only fifteen of the planned sixteen experiments were carried out fully,

one experiment could not be completed despite two attempts to establish

the required operating conditions. Table 6.2 summarises the materials

inputs for these experiments, both the target and achieved values, plus

the weight and chemical analyses of the cast slag and metal. Graphs

showing the output gas analysis, bed temperatures and duration of each

experiment are given in Figures 10 to 39. The time prior to start of

each graph was occupied by the start-up procedure and the initial 'hump'

on some of the bed temperature graphs is produced by the steel shot,

charged at the start of each batch experiment (see sections 6.3.1 and

6.3.2).

The results of the experiments were used to test, and then improve, the

predictive ability of the mathematical model. The details of the

procedure involved being presented in section 6.6. Tables 6.2 and 6.3

(pages 87 and 88) contrast the measured plant performance with the

TABLE 6.2 MATERIAL INPUTS FOR FACTORIAL EXPE

Expt. No.		Total Oxygen nm³/h	P.F. kg/h	Oil gals/h	Carbon Stoich.	Ore kg/h	Coal kg/h	CaCO₃ kg/h	Stir	Steel Shot kg.	Ore kg	Coal kg	CaCO₃ kg	P. kg
		: RATE OF MATERIAL INPUT								TOTAL INPUT				
88	AIM	382	45.36	6.5	1.8x	341	311	73	Yes	509	430	556	146	13
	ACTUAL	382	60.0	6.5	1.92x	320	311	73	Yes					
89	AIM	354	45	15	1.8x	341	311	73	No	509	423	516	135	11
	ACTUAL	354	59	15	1.77x	362	324	77 -	No					
90	AIM	396	68	11.3	1.5x	341	259	67	Yes	500	778	748	196	18
	ACTUAL	396	69	11.3	1.54x	343	268	70	Yes					
91	AIM	340	68	11.3	1.5x	341	259	67	No	500	653	610	160	116
	ACTUAL	340	59	11.3	1.53x	332	257	66	No					
92	AIM	354	102	15.5	1.8x	341	311	73	Yes	500	306	358	94	120
	ACTUAL	354	100	15.5	1.74x	306	270	63	Yes					
93	AIM	382	45	14.8	1.2x	341	207	60	Yes	500	620	502	131	102
	ACTUAL	382	51	14.8	1.42x	310	223	65	Yes					
94	AIM	368	34	11.5	1.5x	341	259	67	No	500	709	570	152	106
	ACTUAL	368	47	11.5	1.52x	332	255	66	No					
95	AIM	354	102	15.7	1.2x	341	207	60	Yes	500	662	428	114	142
	ACTUAL	354	75.4	15.7	1.25x	352	223	65	Yes					
96	AIM	382	102	15.7	1.8x	341	311	73	No	500	260	242	64	106
	ACTUAL	382	81.5	15.7	1.9x	318	306	72	No					
97	AIM	368	68	11.5	2.0x	341	345	78	Yes	500	301	302	80	80
	ACTUAL	368	66	11.5	2.05x	328	340	76	Yes					
98	AIM	382	102	7.4	1.2x	341	207	60	No	500	797	514	137	198
	ACTUAL	382	86	7.4	1.26x	345	220	62	No					
99	AIM	368	68	13.6	1.0x	341	173	53	No	1000	650	548	106	120
	ACTUAL	368	60	13.6	1.06x	325	174	53	No					
100	AIM	368	68	13.6	1.5x	341	259	67	Yes	500	640	658	132	120
	ACTUAL	368	60	13.6	1.54x	320	254	66	Yes					
102	AIM	354	45	8.8	1.2x	341	207	60	No	400	614	588	129	100
	ACTUAL	354	40	8.8	1.15x	320	185	54	No					
103	AIM	368	68	13.8	1.5x	341	259	67	No	450	620	500	124	126
	ACTUAL	368	64	13.8	1.5x	324	248	64	No					

Expt. No.	Plant/ Model	Gas Analysis % Vol.						Slag Analysis %			Carbon Burn-off kg/h	Temperature °C			Iron kg/h			Yield %
		CO	CO_2	H_2	H_2O	O_2	N_2	Fe_T	CaO	SiO_2		Gas	Carbon – Slag Interface	Iron Layer	Added	Reduced	Oxidised	
88	Plant	23.7	28.1	5.1	28	0	15.1	16.1	29.5	22.9	29.6	1995	1793	1736	204.8	250.4	77.3	87.0
	Model	25.4	34.5	3.8	30.1	0.02	6.1	25.6	34.9	26.7					204.8			84.1
89	Plant	20.1	22.5	7.3	39	0	10.9	17.9	30.6	21.2	45.4	1844	1437	1267	231.6	228.8	45.9	84.0
	Model	29.2	24.5	5.9	25.7	0	14.7	32.2	29.0	23.9					231.6			78.0
90	Plant	19.5	27.9	5.2	35	0	12.3	21.4	26.1	21.3	11.8	2039	1841	1766	219.5	341.6	171.6	83.0
	Model	27.5	31.8	4.3	29.3	0.03	7.0	35.2	25.6	23.6					219.5			77.5
91	Plant	23.4	29.1	5	29	0	13.5	20.8	26.1	23.9	44.9	1782	1327	1177	213.7	182.6	22.8	72.0
	Model	28.1	26.4	5.6	26	0	13.9	37.5	23.5	22.2					213.7			74.8
92	Plant	32.5	20.4	9.1	24.4	0	13.6	25.9	21.7	22.2	4.3	1637	1425	1258	195.8	235.1	110.5	82.0
	Model	33.7	19.9	0.4	24.3	0	12.9	40.6	22.8	19.6					195.8			68.8
93	Plant	18.6	29.7	5	38	0	11.7	45.6	10.9	11.0	1.5	2283	1766	1678	193.1	300.2	213.5	53.0
	Model	14.0	36.5	1.6	29.4	2.1	16.4	50.0	17.3	13.3					193.1			44.8
94	Plant	7.0	22.4	2.8	44	0	19.6	13.7	30.9	28.7	55.5	2222	1898	1629	212.4	214.5	31.9	93.0
	Model	16.2	34.0	1.8	25	0.7	22.3	25.3	34.7	27.0					212.4			86.0
95	Plant	20.5	27.3	5.6	37.9	1.2	8.7	40.2	14.0	16.1	1.0	1890	1564	1478	225.2	305	180.7	40.0
	Model	29.0	27.1	5.5	27.9	0	10.5	48.1	18.0	15.2					225.2			55.2
96	Plant	28.7	14.0	9.1	30	0	18.2	35.4	16.2	17.2	50.0	1799	1193	1056	204.6	156.4	17.5	53.0
	Model	31.8	20.8	7.6	24.9	0.01	14.9	38.9	24.9	19.3					204.6			67.0
97	Plant	23.6	32.7	4.4	29	0	9.2	10.4	31.8	23.5	22.4	1689	1489	1337	209.9	262.6	102.5	92.0
	Model	31.9	25.8	7.7	28.8	0.01	5.8	33.3	28.4	23.0					209.9			96.3
99	Plant	7.9	29.4	2.6	47.6	1.3	11.3	45.9	6.7	13.4	33.5	2170	1885	1704	208.0	172.3	101.8	42.4
	Model	22.4	32.0	2.9	26.2	0	16.3	56.1	11.9	11.2					208.0			33.9
100	Plant	15.7	28.0	5	44	1	5.6	6.3	34.3	29.3	6.0	1950	1750	1671	205.8	305.8	153.4	96.0
	Model	24.5	29.4	4.1	27.9	0	14.1	36.8	26.3	21.2					205.8			73.9
102	Plant	17.7	32.4	5	40	1.0	4	28.4	19.0	24.1	38.4	2263	1972	1754	205.3	183.4	95.3	75.5
	Model	15.6	42.2	1.5	28.3	1.8	10.6	53.1	14.1	12.7					205.3			40.5
103	Plant	20.4	32.9	4	36	1	5	44.0	12.3	13.0	43.4	1808	1420	1250	211.7	196.8	43.4	39.0
	Model	31.3	25.4	6.3	25.9	0	11.1	37.5	25.2	20.9					211.7			73.3

TABLE 6.3   COMPARISON OF PLANT AND MATHEMATICAL MODEL OUTPUT

predictions made by the mathematical model after it had been improved in this way.

Summaries of the results of each experiment are presented below, highlighting any important observations that were made. Photographs taken from the feed end during some of the batch experiments are presented in Appendix 6.

Experiment 88

This was a stirred experiment with the bed surface temperature falling initially from 1 750 $^\circ$C to 1 580 $^\circ$C. For the last $1\frac{1}{2}$ hours of feeding the bed temperature was fairly level at 1 580 $^\circ$C (Figure 11). Feeding was intermittent and two build ups of unmelted material were noted after about one hour and two hours from the start of the feeding period. The experiment was terminated after the second build up had been melted, the slag and metal collected were fluid and the metal contained 2.58% carbon. The slag contained 16.1% total iron and the yield was calculated to be 87%. For the main part of the experiment the exhaust gases contained between 40 and 55% CO_2 and 20 to 30% CO, (Figure 10).

Experiment 89

This was an unstirred experiment with the temperature of the bed remaining constant at 1 600 $^\circ$C for the majority of the experiment but falling to 1 450 $^\circ$C over the last fifteen minutes of the experiment, (Figure 13). Feeding was interrupted by a build up which occurred about one hour after the start of the experiment and the experiment was terminated half an hour later when a second build up occurred. Three collapses were necessary to discharge the contents of the furnace with reheating in-between. Even after three collapses some material stayed inside the furnace. The metal tapped at a low temperature of 1 253 $^\circ$C. Excess coal was cast with the slag and the metal contained 1.8% carbon.
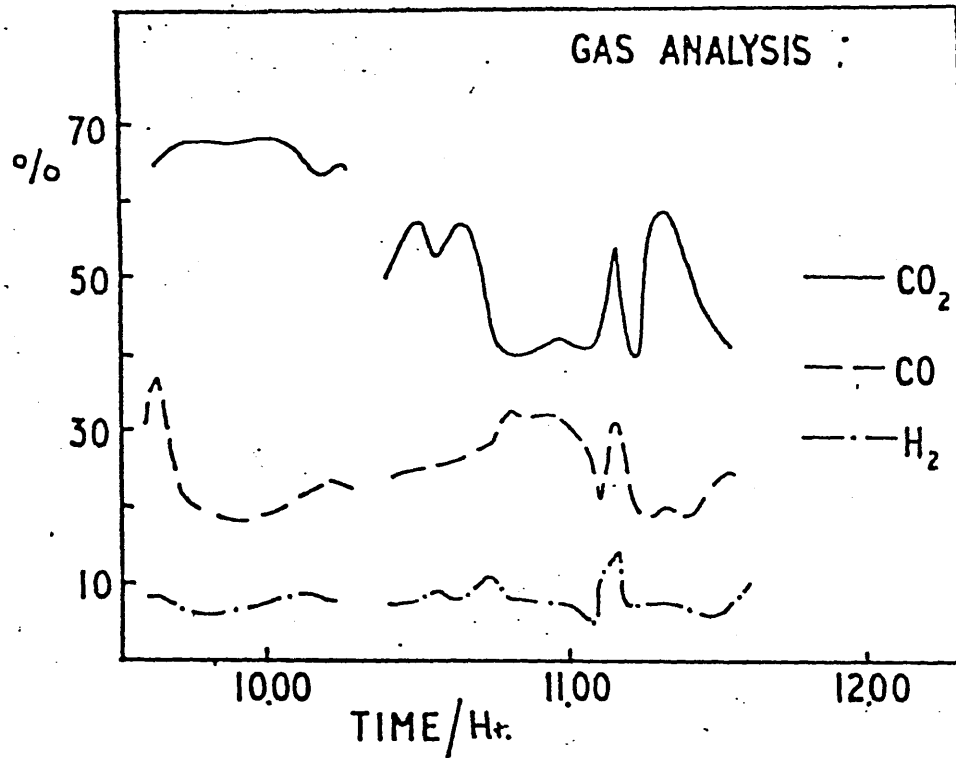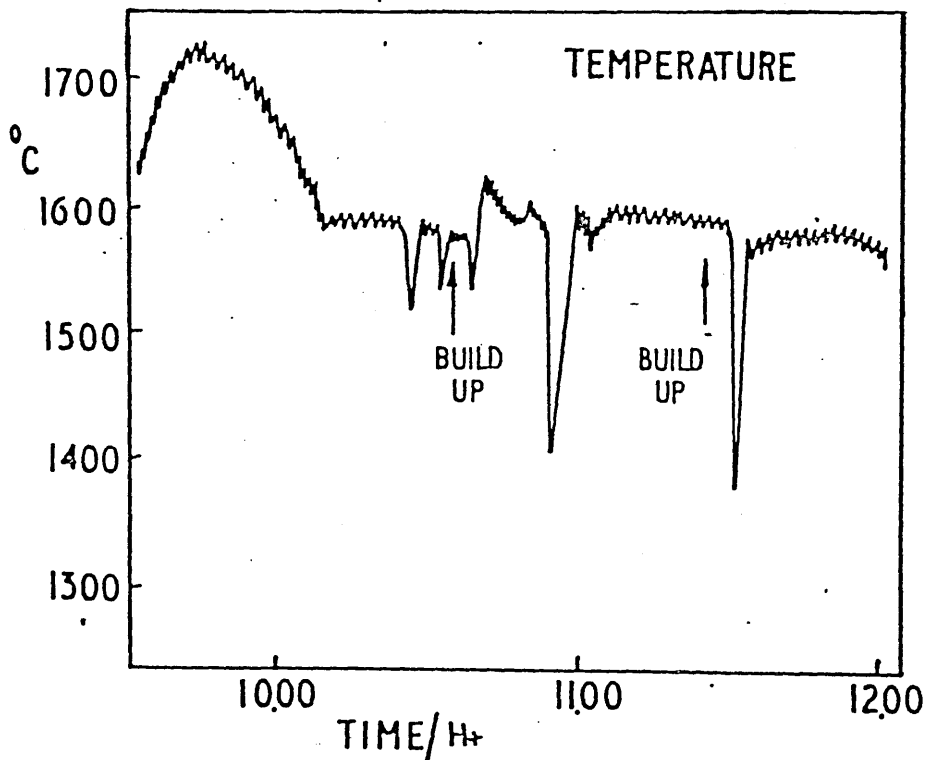
89

EXPERIMENT 88

FIGURE 10

FIGURE 11

EXPERIMENT 89
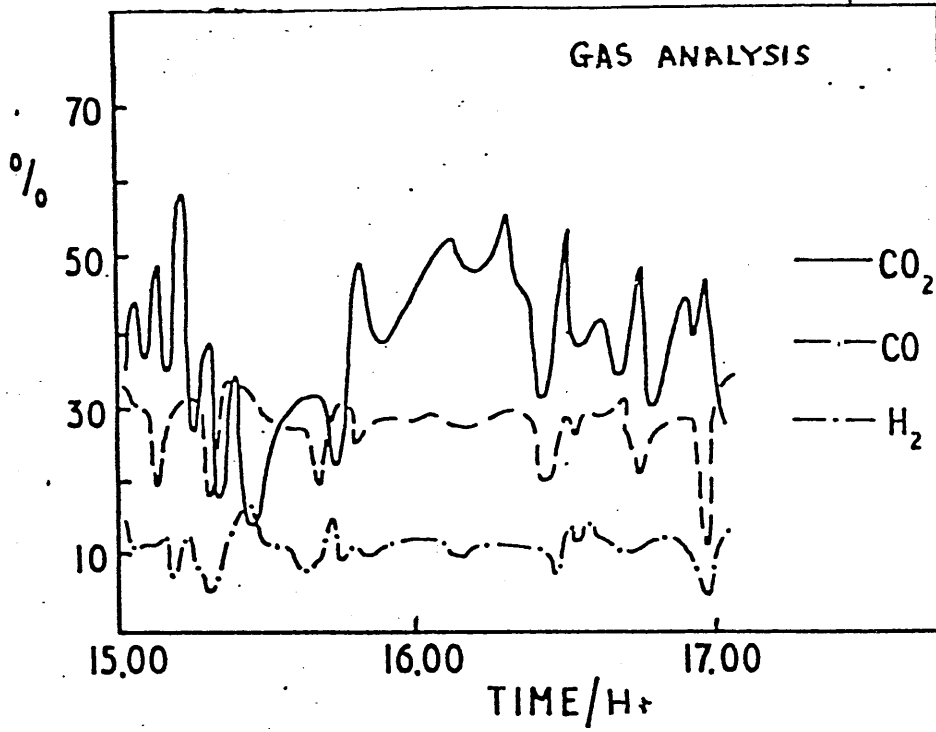
FIGURE 12
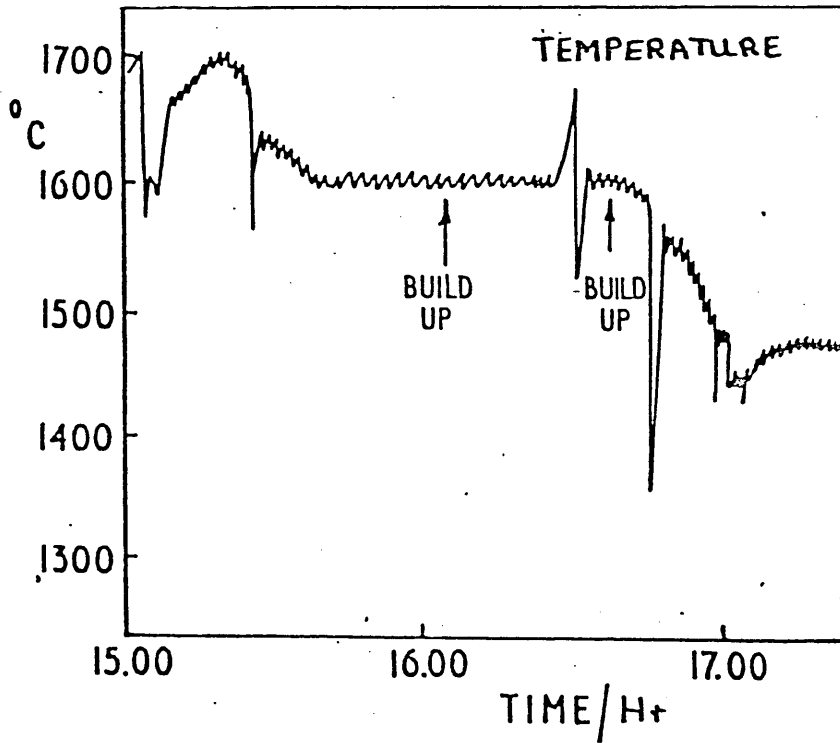
FIGURE 13

The composition of the slag was comparable with that of experiment 88, the slag containing 17.8% total iron. The calculated yield for the experiment was 84%. The analysis of the waste gases was also similar to experiment 88 with an average CO_2 content of 40% and a CO content of 27% (Figure 12).

Experiment 90

This was a stirred experiment with a lower coal input compared to the previous two experiments. Some slight build up occurred after one hour of feeding probably due to a lower starting temperature than usual, but this did not reoccur as the experiment continued and average process temperatures in the order of 1 550 ^{o}C were measured, rising slowly as the experiment progressed (Figure 15). The temperature of the metal on collapse was 1 420 ^{o}C and more metal was cast than could have possibly been produced during the experiment. This extra metal must have been the residue from the previous cold experiment 89. The high process temperatures were also reflected in the analysis of the waste gases which contained on average 60% CO_2 and 20% CO (Figure 14). The metal produced by the experiment was low in carbon (0.07%) and the slag contained 21.37% total iron. The calculated yield for the experiment was 83%.

Experiment 91

This was an unstirred experiment with a low starting temperature of about 1 550 ^{o}C (Figure 17). Slight build up occurred after one hour but feeds were only interrupted for a few minutes. At the end of the experiment excess coal was observed with the tapped product and although the temperature of the slag was measured at 1 400 ^{o}C no metal was cast. This indicated that any iron which had been produced was frozen inside

EXPERIMENT 90

GAS ANALYSIS

FIGURE 14
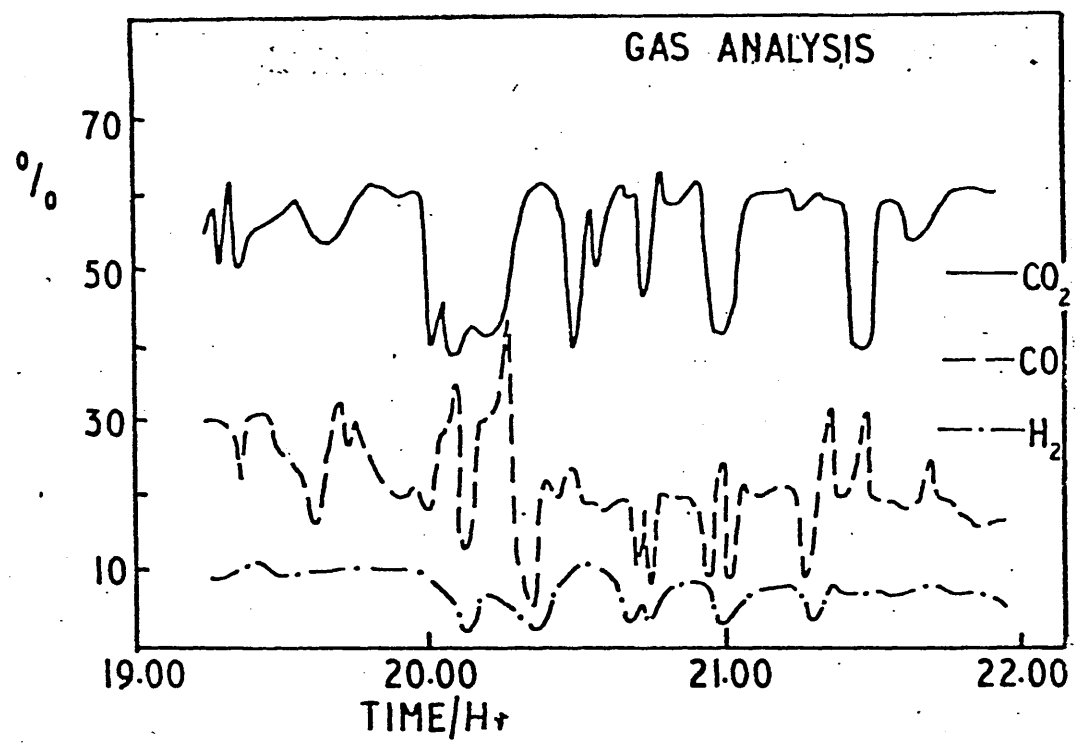
TEMPERATURE
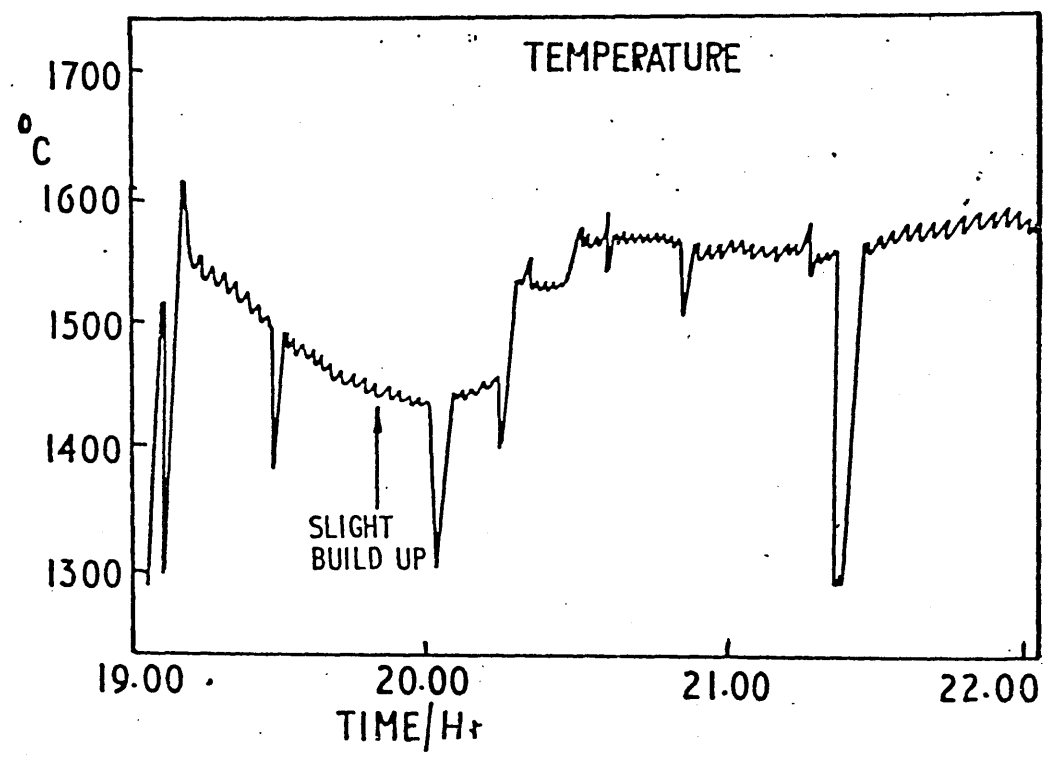
SLIGHT
BUILD UP

FIGURE 15
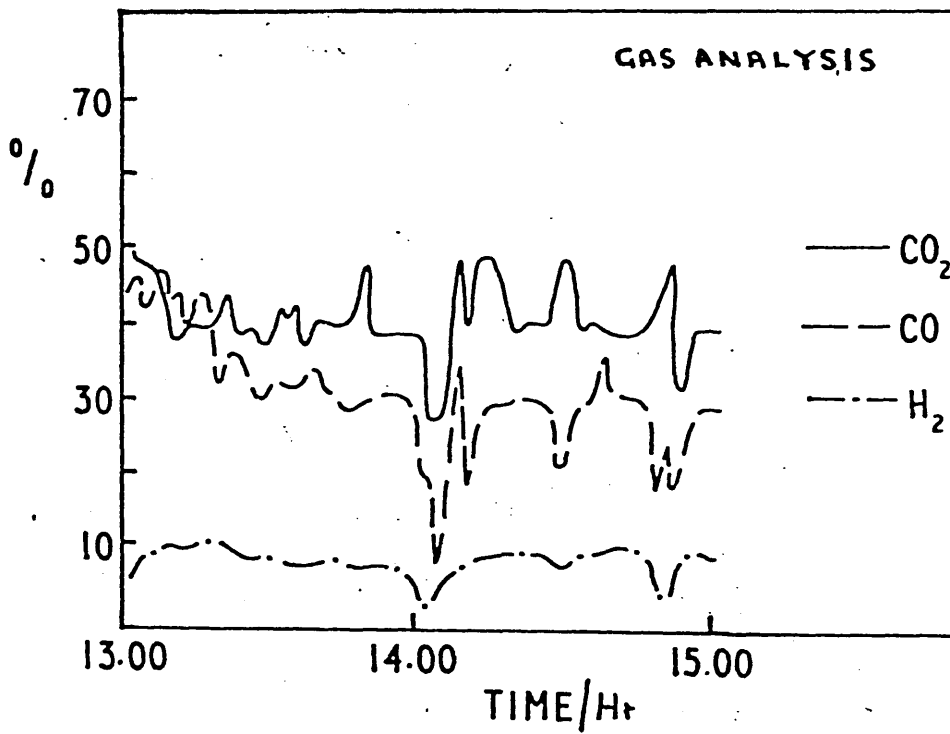
EXPERIMENT 91

FIGURE 16
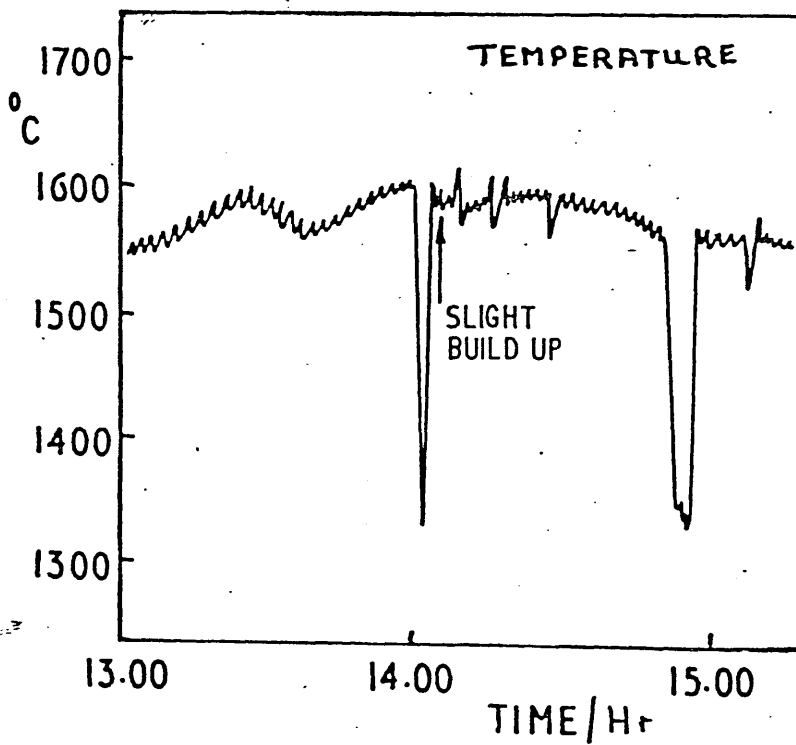
FIGURE 17

the furnace. The temperature of the bed throughout the experiment was fairly level at 1 575 ^{o}C although towards the end of the experiment the bed temperature was falling slightly. The composition of the waste gases were reasonably constant throughout the experiment and averaged at 40% CO_2, with between 25 and 30% CO (Figure 16). The slag cast on the first collapse contained 21% total iron and the calculated yield for the experiment was 72%.

Experiment 92

This was a stirred experiment with a high coal and a low oxygen addition. The temperature of the bed was falling throughout most of this experiment reaching a level for the last hour at 1 420 ^{o}C (Figure 19). Charging had to be stopped on two occasions to melt out a build up and the experiment was terminated when it was felt that the low process temperatures were making the experiment untenable. In order to discharge the contents of the furnace it was necessary to heat the furnace without making additions of ore and coal. Two collapses were made, the temperature of the first collapse being 1 390 ^{o}C and that of the second 1 460 ^{o}C. The metal that was cast contained 0.57% carbon and the associated slag 25% total iron. Between the first and second collapse significant oxidation occurred and the second slag that was cast contained 60% total iron. The composition of the exhaust gases was reasonably constant throughout the experiment, the CO_2 content being around 39% and the CO content about 25% (Figure 18). The calculated yield of the experiment was 82%.

Experiment 93

This was a stirred experiment but with high oxygen and low carbon additions. Conditions inside the furnace were extremely hot with the bed temperature starting off at 1 500 ^{o}C and increasing throughout the

95
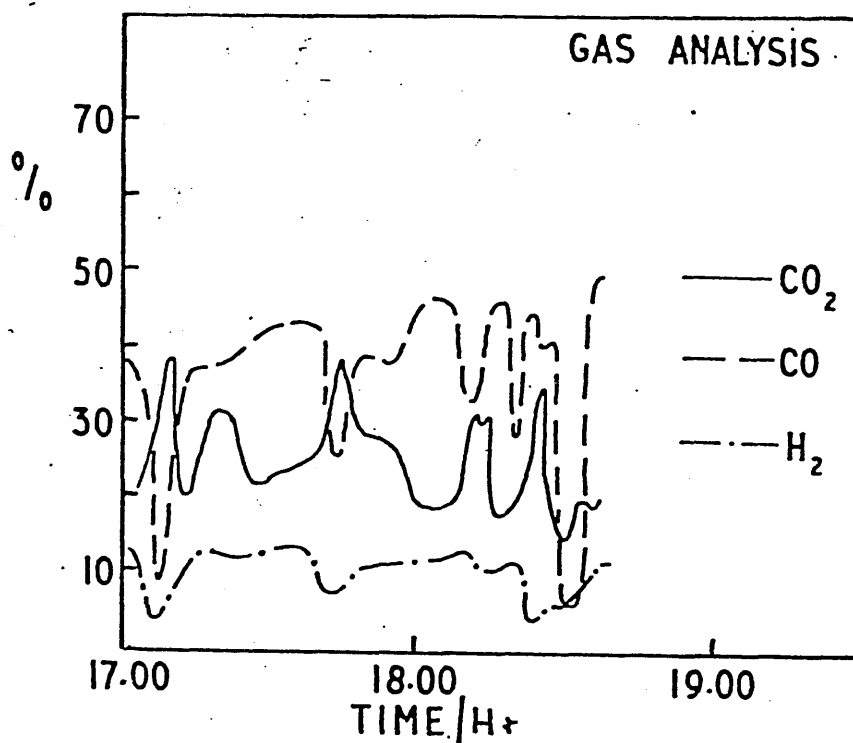
EXPERIMENT 92

FIGURE 18

FIGURE 19

EXPERIMENT 93

GAS ANALYSIS

70

%

50

30

10

CO₂
CO
H₂

10.00   11.00   12.00

TIME/Hr

FIGURE 20

TEMPERATURE

1700

°C

1600

1500

1400

1300

10.00   11.00   12.00

TIME/Hr
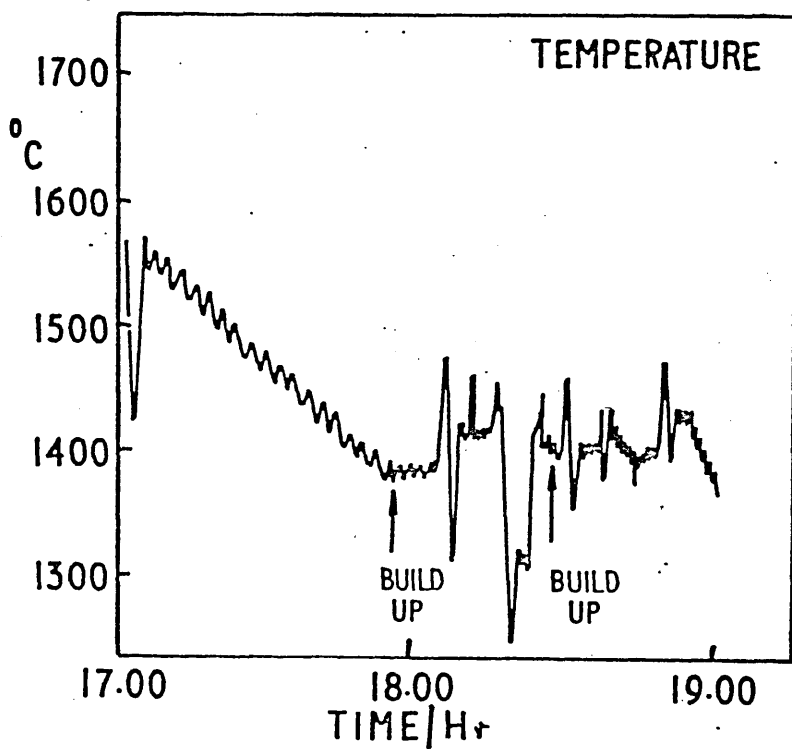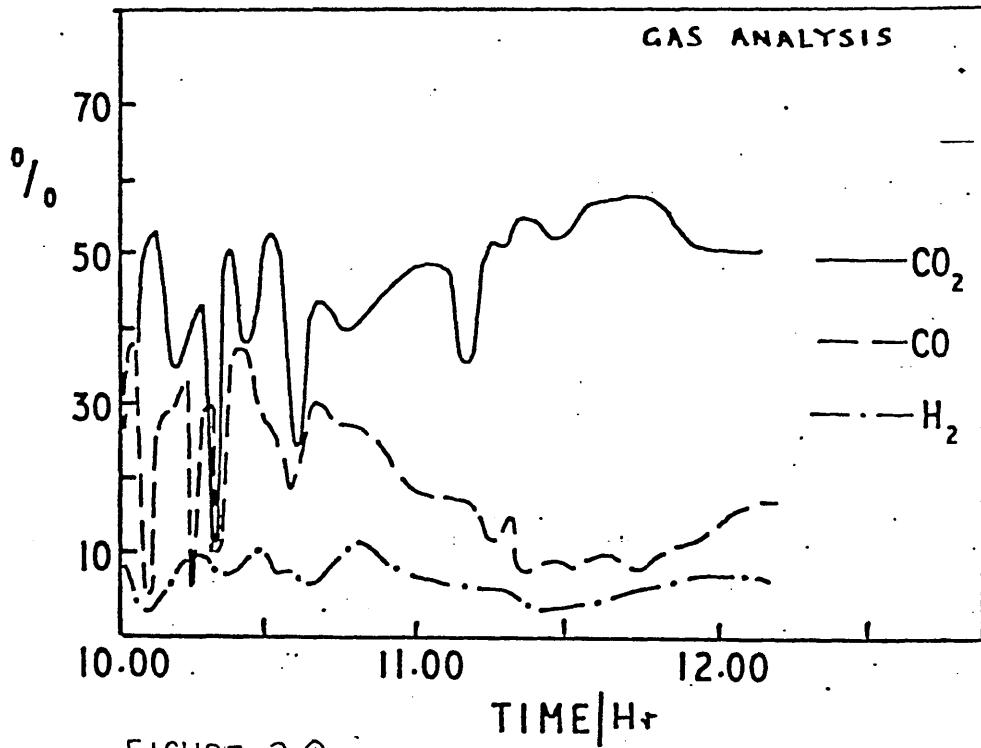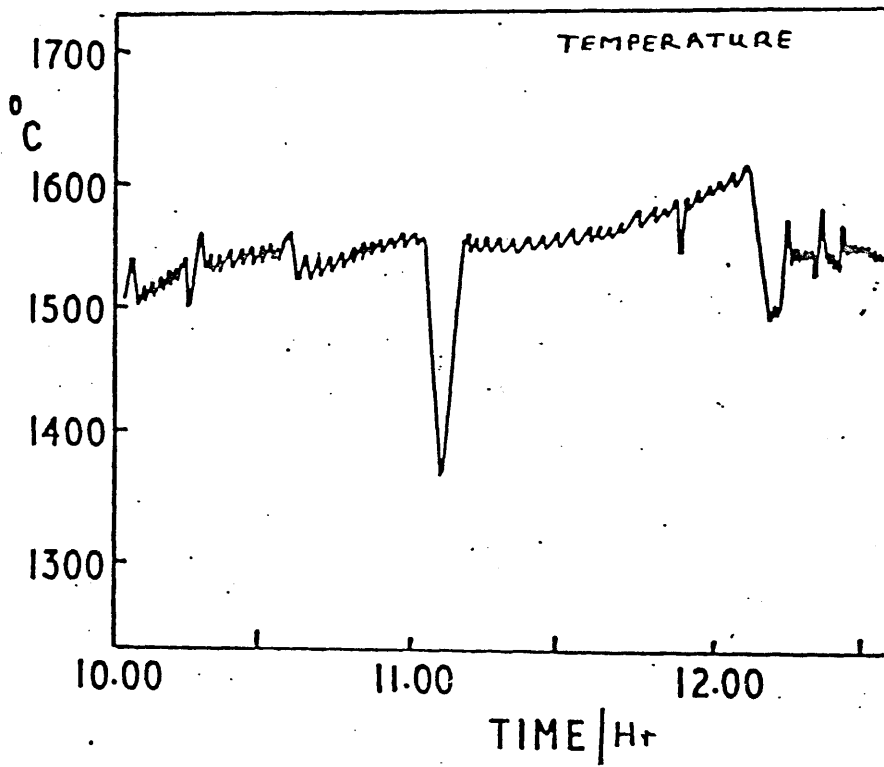
FIGURE 21

experiment to end in excess of 1 600 ^{o}C (Figure 21). There were no signs of build up during the experiment. The temperature of the metal cast was in excess of 1 500 ^{o}C but the total iron content of the slag was high at 46%, indicating oxidising conditions and a poor yield, which was calculated to be 53%. During the experiment the CO_2 content of the exhaust gas increased from 47% to 60% and the CO content of the gases reduced from 30% to 15% (Figure 20).

Experiment 94

This was an unstirred experiment with steady conditions throughout. A slight build up was noted after about one hour but was not sufficient to stop feeding. The analysis of the waste gases was constant throughout the experiment, the CO_2 content being 50% and the CO content about 10% (Figure 22). The bed temperature showed signs of fluctuation throughout the experiment but was on average 1 575 ^{o}C, although there was a marked fall in temperature produced during the last hour (Figure 23). When the experiment was terminated the metal and slag were cast cleanly from the furnace, the metal containing 1.34% carbon and the slag 13.7% total iron. The calculated yield for the experiment was 93%.

Experiment 95

This was a stirred experiment with a low carbon addition. The bed temperature rose continuously during the experiment which was terminated after two hours, when the bed temperature was in excess of 1 700 ^{o}C (Figure 25). Observations of the bed after one hour's operation showed a hot furnace with little sign of coal. No build up occurred and the composition of the exhaust gases had a CO_2 content between 40 and 60% and the CO content between 20 and 30% (Figure 24). Two collapses were necessary at the end of the experiment. The temperature of the metal on

EXPERIMENT 94
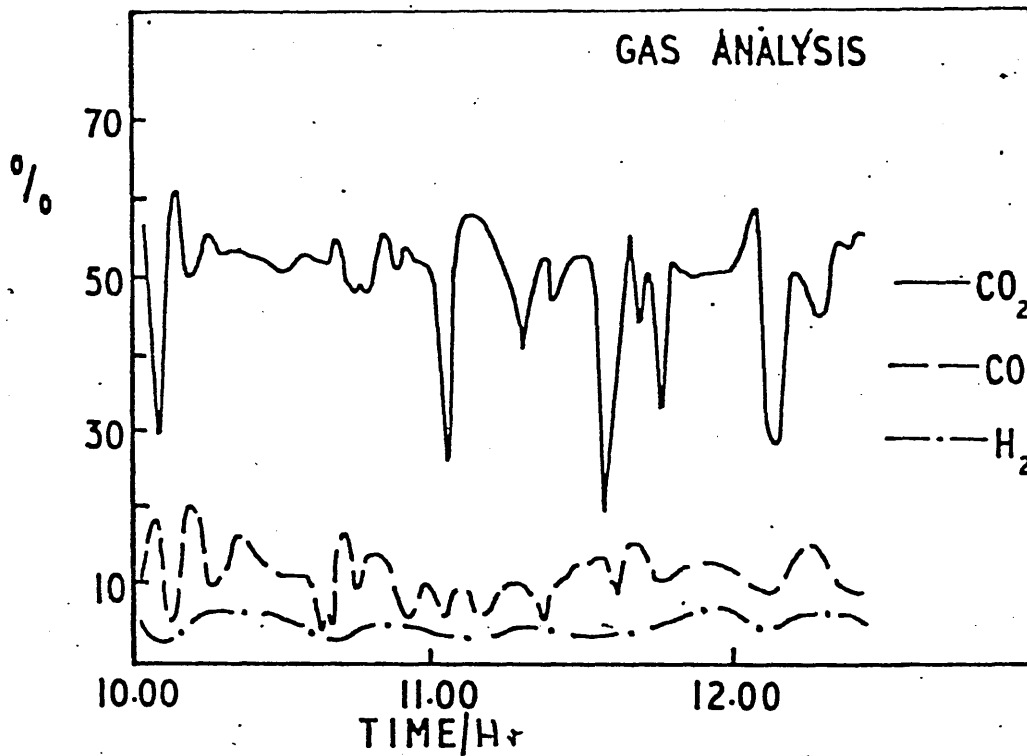
FIGURE 2 2
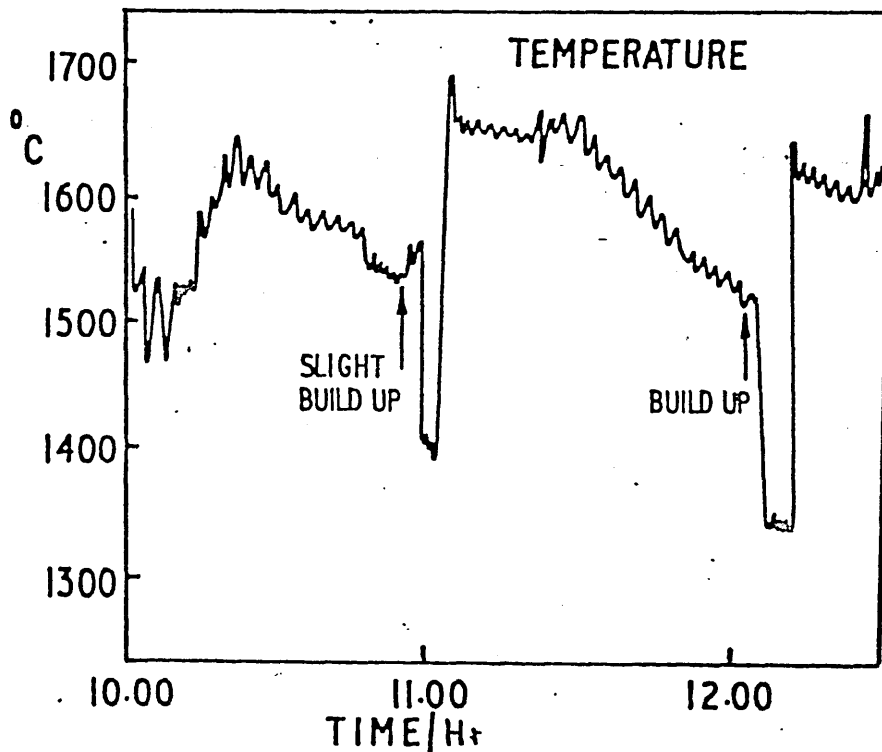
FIGURE 2 3

EXPERIMENT 95
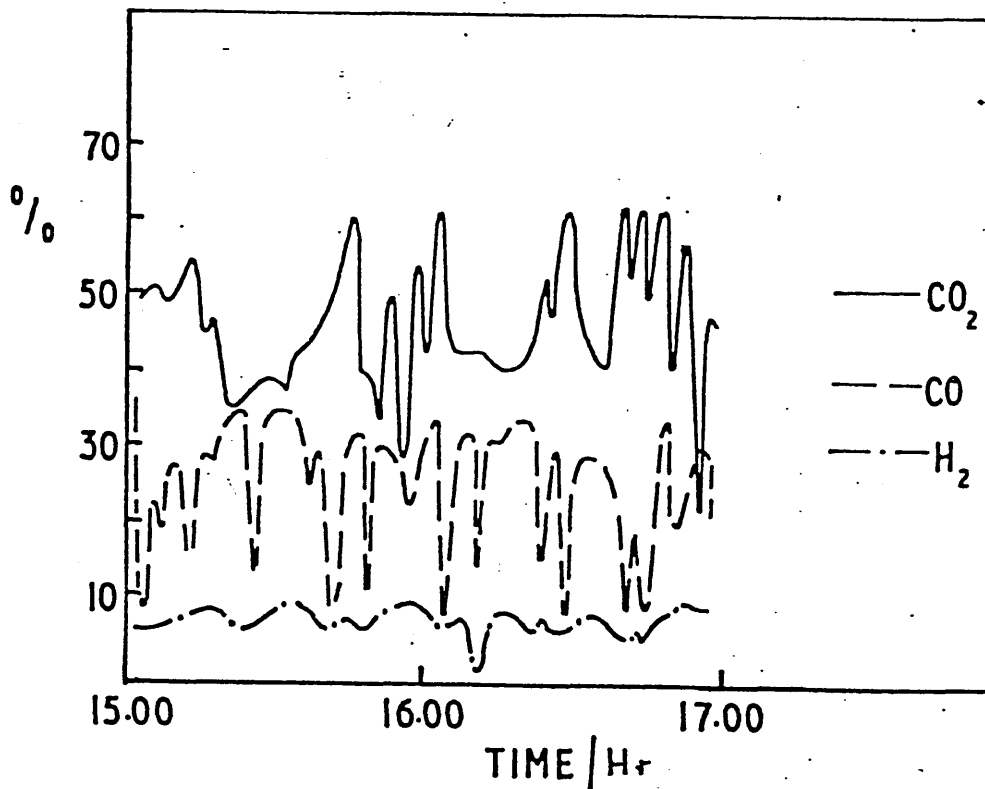
FIGURE 24

FIGURE 25

100
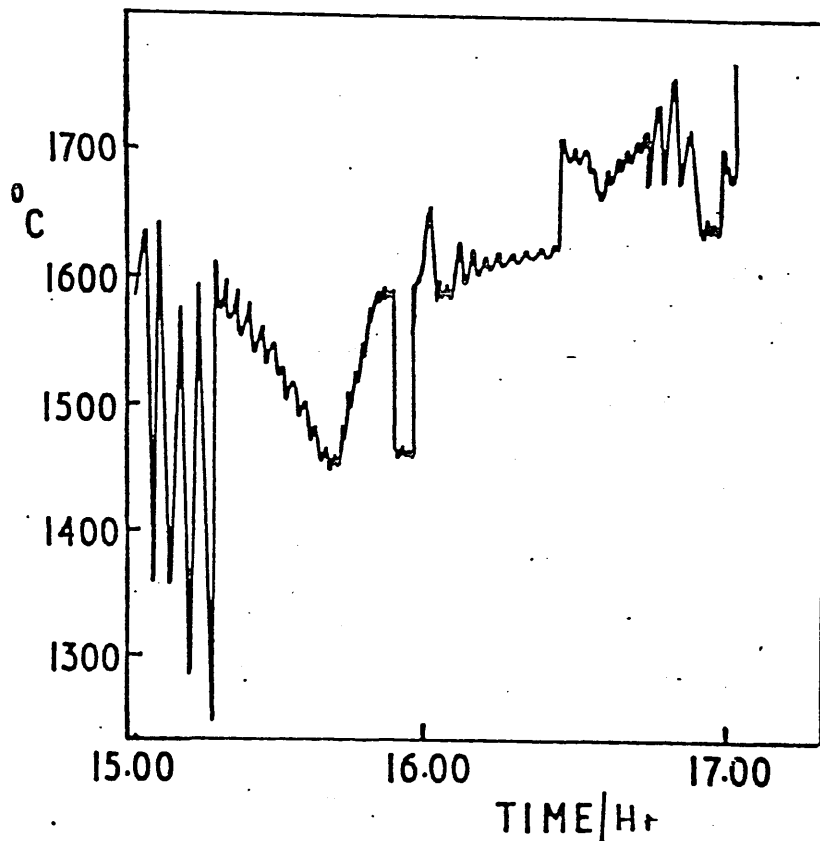
the first collapse was 1 510 ^{o}C and that of the second collapse

1 700 ^{o}C. The carbon content of the metal varied between 0.02% carbon

and 0.7% carbon, the slag contained 40.16% total iron. 825 kg of metal

were cast which approximated to the same number of iron units added

during the experiment. The yield calculations based on the slag analysis

however indicated that the yield was only 40%, and it is probable that

part of the iron cast was residue from experiment 94.

Experiment 96

This was an unstirred experiment with a high carbon input. Build up

occurred after about half an hour of feeding which proved difficult to

remelt. The build up reoccurred shortly after restarting feeding. The

bed temperatures were extremely low throughout the experiment apart from

the time when the build up was being remelted (Figure 27). The exhaust

gases contained 40% CO_2 and 30% CO during the first part of the experiment

but altered so that during the last half an hour of the experiment they

contained 20% CO_2 and 35 to 40% CO (Figure 26). Only small quantities

of slag and metal were cast at the end of the experiment and the product

was so viscous that, on slowing the furnace to cast the contents they

built up on the stationary exhaust hood roof and stopped the rotation

of the furnace completely. The metal contained 0.69% carbon and the

slag 35.4% total slag iron. The yield for the experiment was calculated

to be 53%.

Experiment 97

This was a stirred experiment with a very high carbon input. Build up

of unmelted material occurred persistently throughout the experiment

and the process temperature dropped rapidly from 1 550 ^{o}C to below

1 300 ^{o}C (Figure 29). Due to instrument failure, gas analysis was not

EXPERIMENT 96
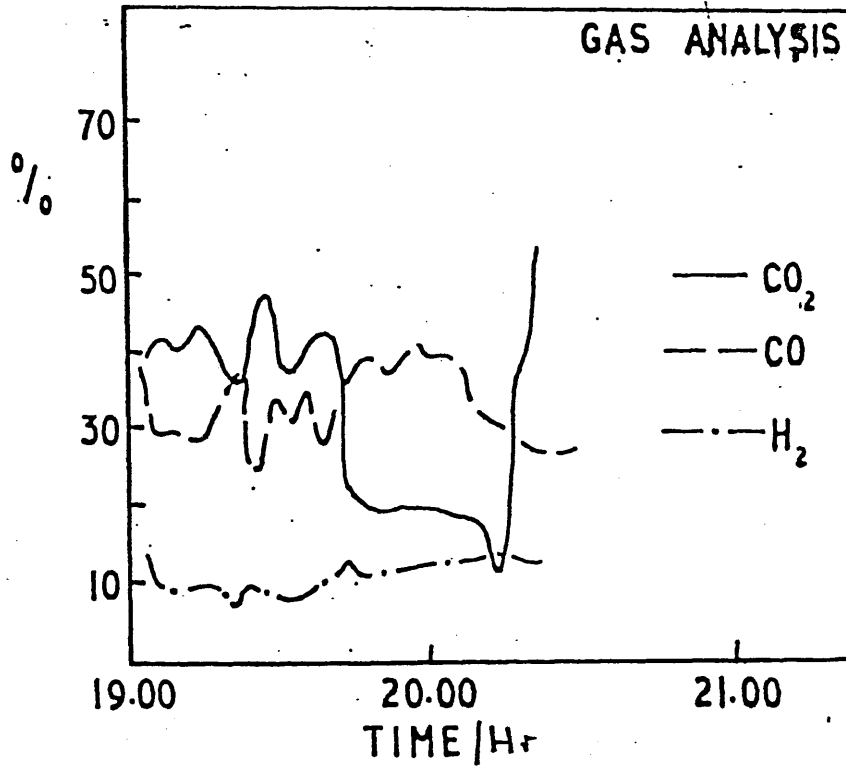
FIGURE 2 6

FIGURE 2 7

EXPERIMENT 97

GAS ANALYSIS

— CO$_2$
--- CO
-·- H$_2$

TIME/Hr

FIGURE 28

TEMPERATURE

BUILD
UP

BUILD
UP

TIME/Hr
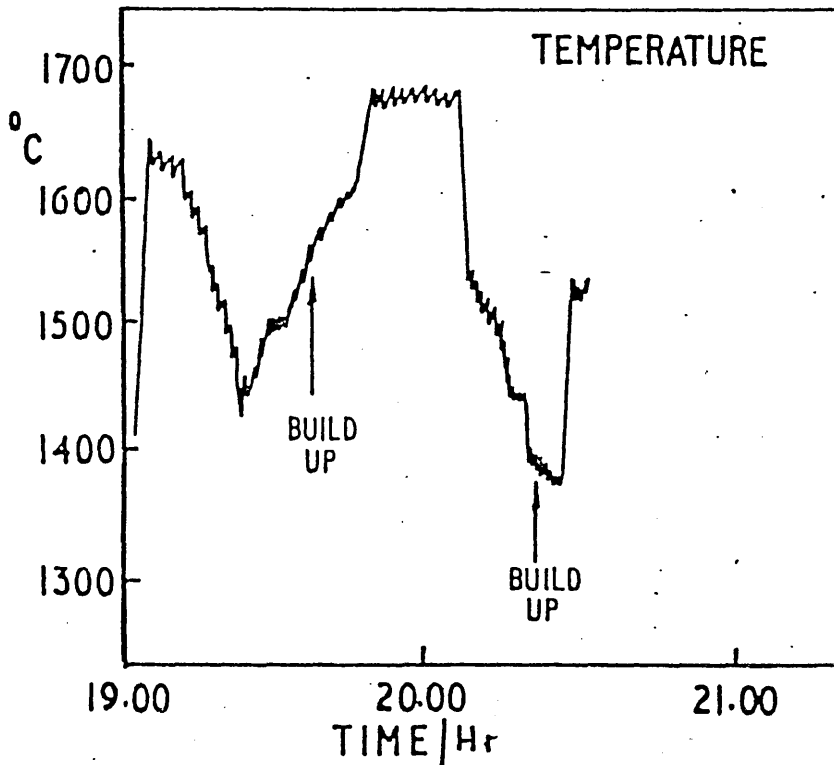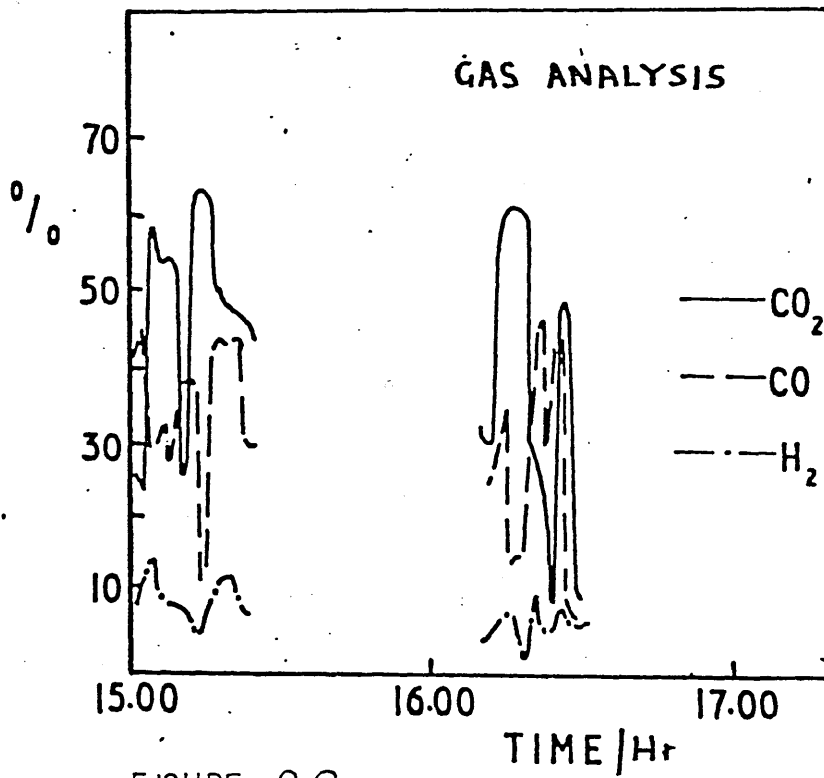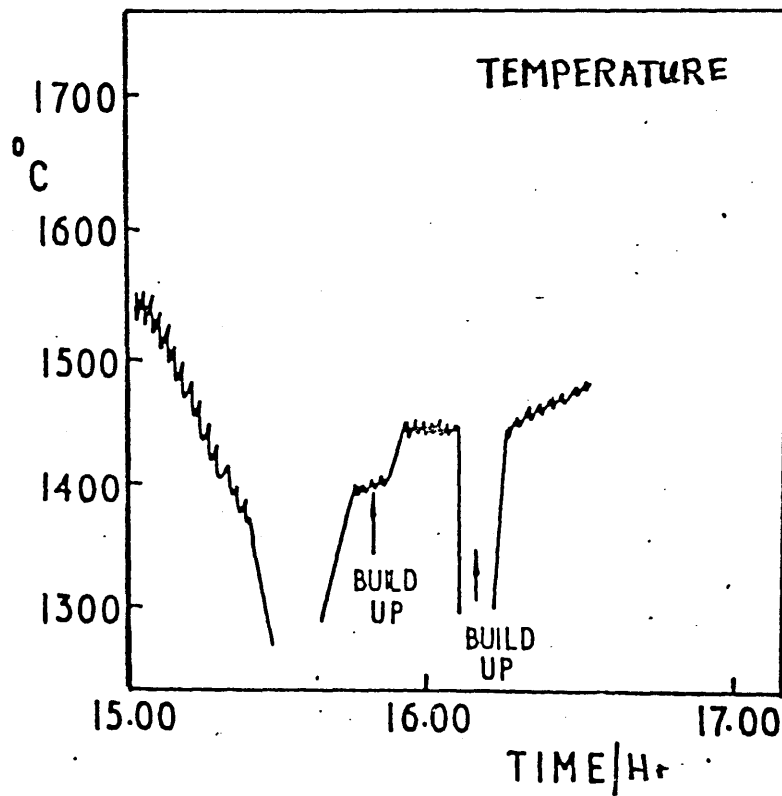
FIGURE 29

possible except for short periods when the CO_2 content was measured between 30 and 60% and the CO content between 40 and 50% (Figure 28). On the first collapse only a small quantity of metal was cast, containing 1.4% carbon, at a temperature of 1 370 ^{o}C. The slag contained 10.4% total iron which gave a calculated yield of 92%, possibly due to the short duration of the experiment, which exaggerated the effect of the small amount of reduction carried out initially by carbon dissolved in the melted layer of steel shot at the start of each batch experiment.

Experiment 98

This was a stirred experiment with a low carbon input. Continuous feeding was possible throughout the experiment and no build up occurred. The temperature of the bed rose steadily during the experiment, starting at 1 600 ^{o}C and finishing at 1 640 ^{o}C (Figure 31). The CO_2 content of the exhaust gases varied between 50 and 60% during the experiment (Figure 30). During this experiment the casting dam failed. The cast iron contained 0.40% carbon and the slag contained 51.7% total iron, representing a zero yield for the experiment.

Experiment 99

This was an unstirred experiment using mid-values of oxygen, pulverised fuel and oil, together with a very low carbon input. The bed temperature rose steadily during the experiment from 1 400 ^{o}C to 1 500 ^{o}C (Figure 33) and no build up occurred. The composition of the exhaust gases was steady during the experiment, with the CO_2 content being 60 to 65% and the CO content between 10 and 20% (Figure 32). A fluid collapse was obtained with the metal temperature being 1 550 ^{o}C. 935 kg of metal (which was almost equivalent to the initial protective layer) and 122 kg of slag containing 46% total iron were cast. Observations during the

# EXPERIMENT 98
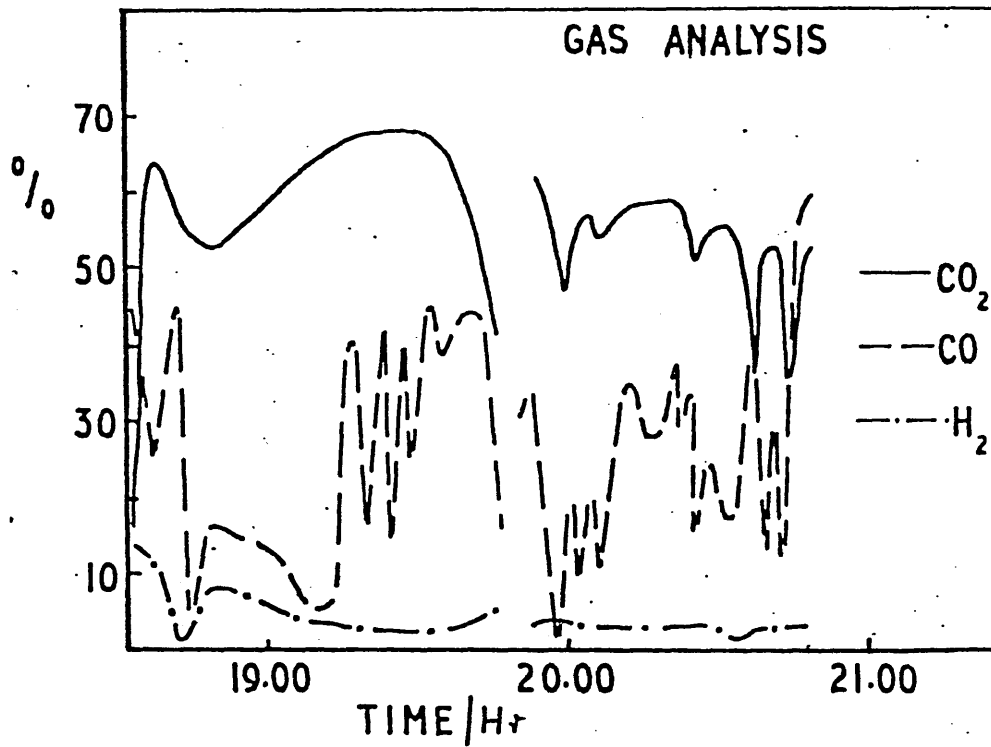
FIGURE 30
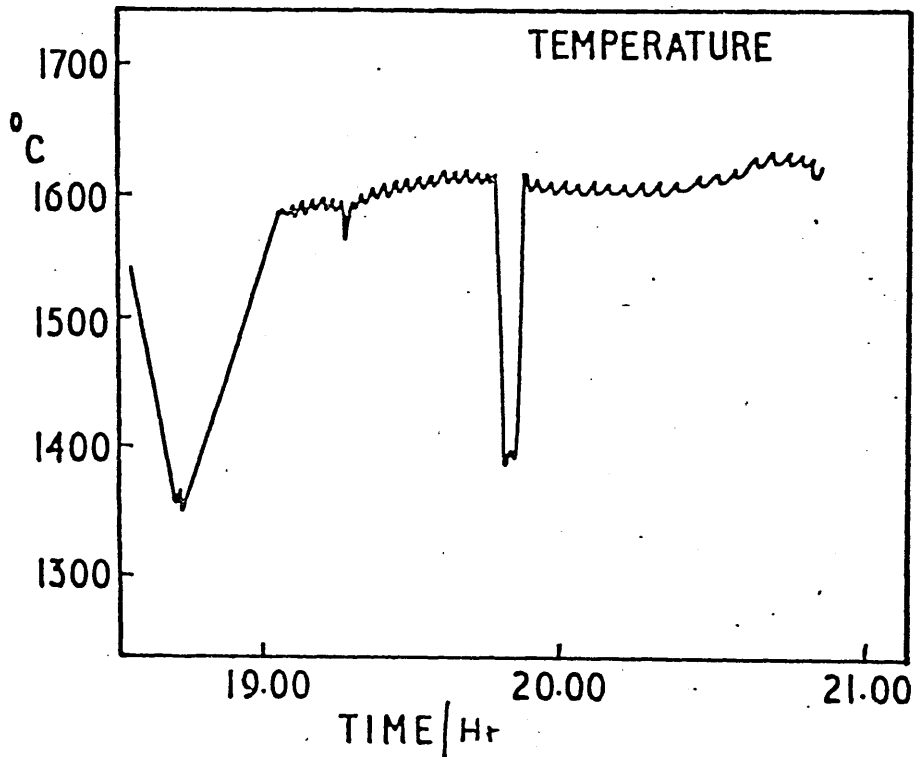
FIGURE 31

EXPERIMENT 99
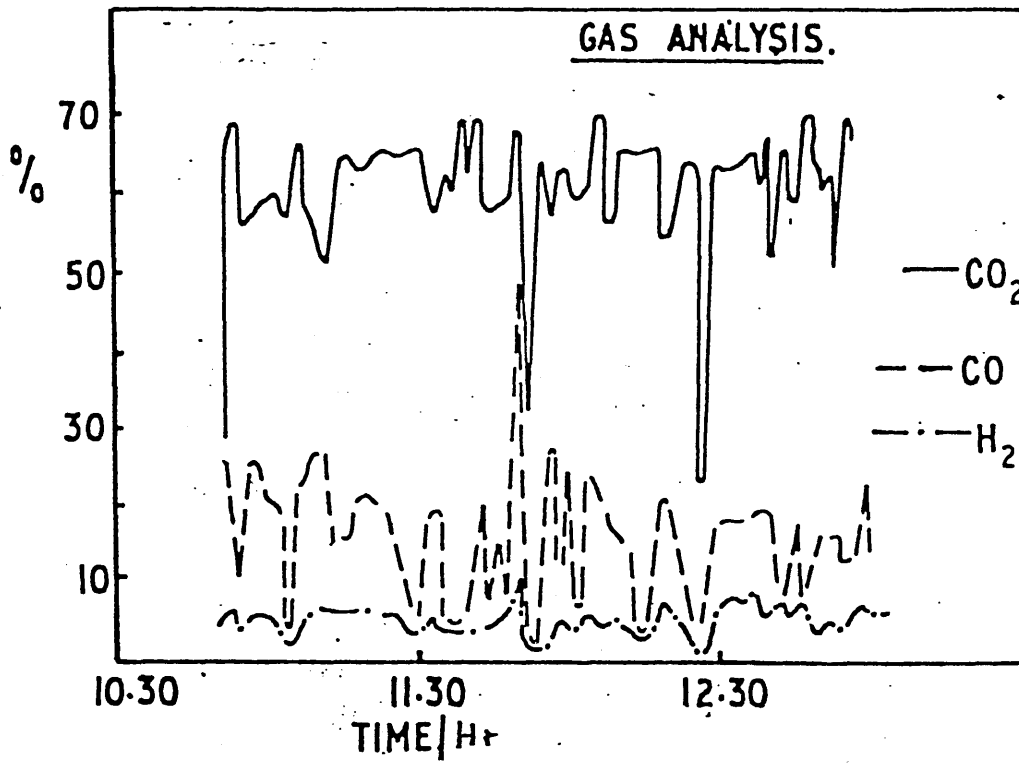
FIGURE 32
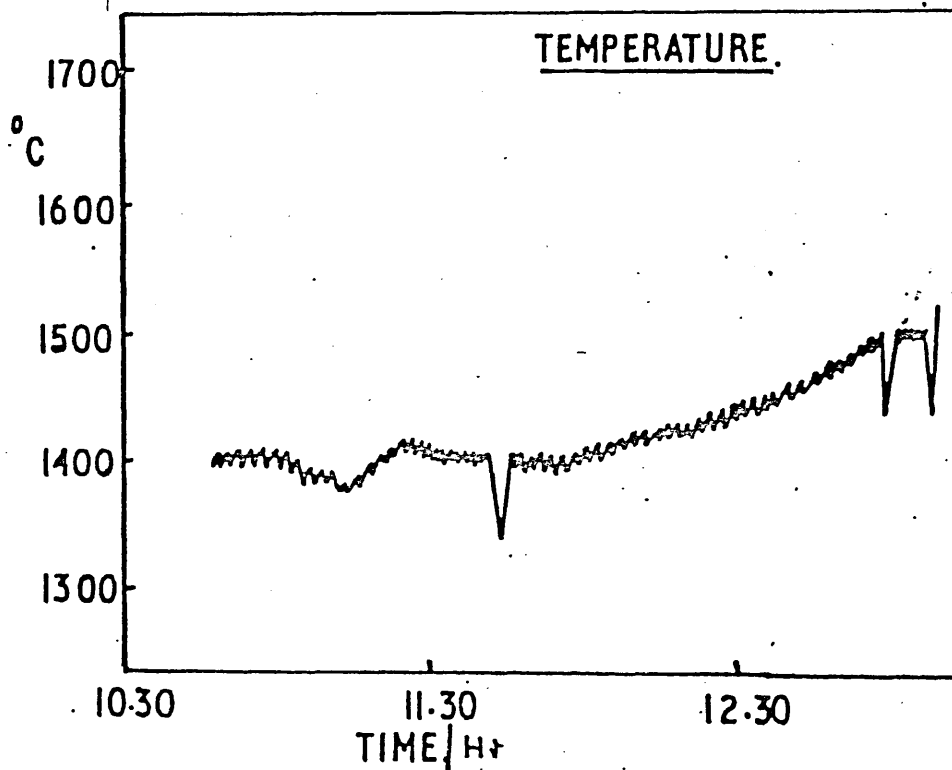
FIGURE 33

experiment had indicated a hot, reactive system, but there was no visual evidence of coal particles on the bed. The yield from the experiment was 42.4%.

Experiment 100

This was a stirred experiment using mid-values of oxygen, oil and pulverised fuel, together with a carbon input equivalent to 1.5 x stoichiometric requirements. One build up of unmelted material occurred after one hour twenty minutes of feeding and took eight minutes to remelt. The measured bed temperature was low, being 1 320 ^{o}C (Figure 35), but observations indicated a higher bed temperature, a foaming bed and reactive conditions. The CO_2 content of the exhaust gases was around 50%, and the CO content around 30%, throughout the experiment (Figure 34). When the experiment was terminated the product was very foamy and much of the material remained inside the casting chamber. The small amount of slag that was cast contained only 6.29% total iron and accordingly the calculated yield was high at 96%.

Experiment 101

This experiment was started on a number of occasions, but on each attempt the experiment was prematurely terminated. On one occasion there was an engineering breakdown of the drive system during the warm-up period; on each of the other occasions the cast end dam failed catastrophically during the course of the experiment and before useful data could be obtained. The conditions inside the furnace did not appear to be any more aggressive towards the cast end dam than experienced in the other experiments, but after the third failure of the cast end dam it was decided to move on to the next experiment in the series.

EXPERIMENT 100
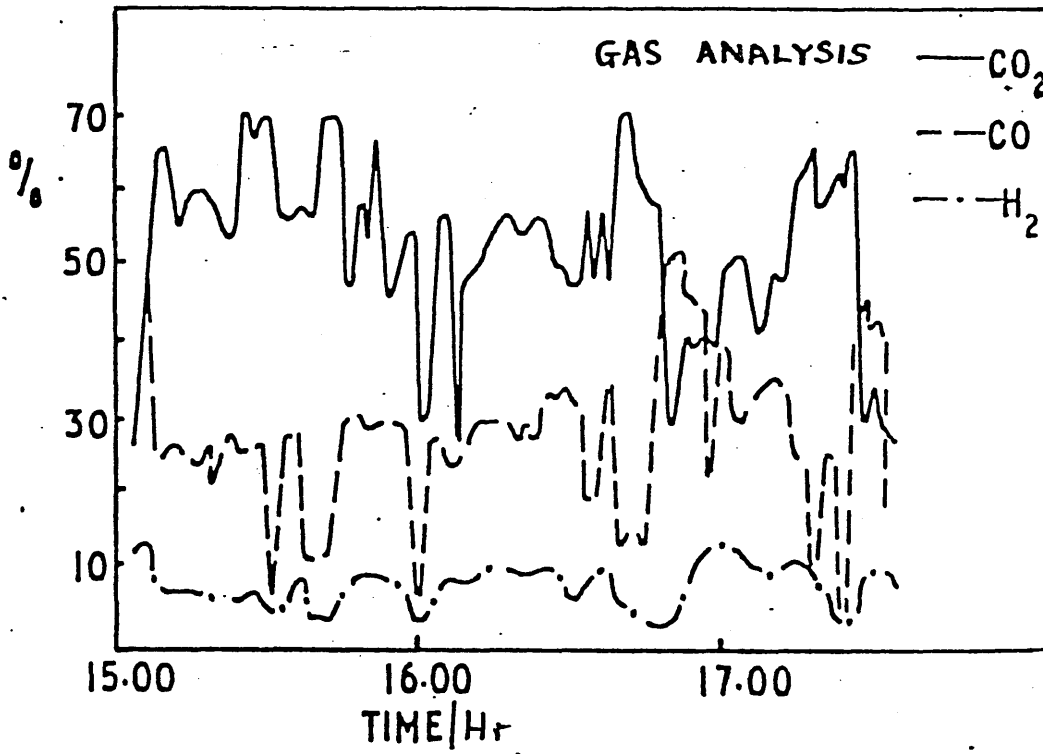
FIGURE 34
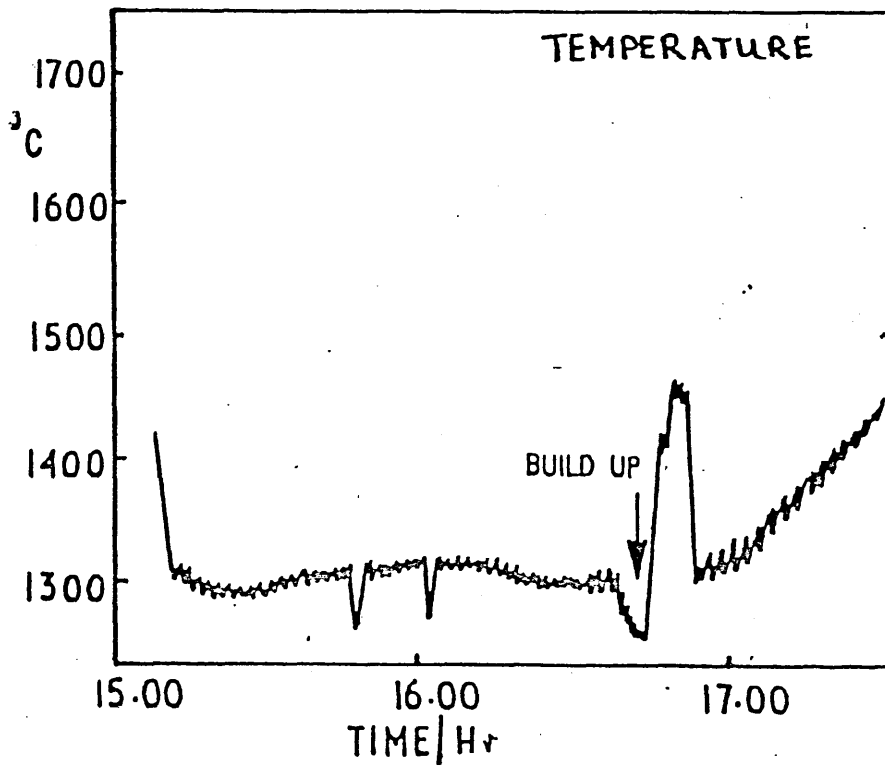
FIGURE 35

Experiment 102

This was an unstirred experiment using low levels of oxygen, oil and pulverised fuel and carbon input. A build up occurred shortly after the start of the experiment but once this had been melted, feeding was restarted and no further interruptions occurred. Conditions were steady once this initial interruption was overcome but low bed temperatures, around 1 400 $^{\circ}$C, were monitored (Figure 37). The exhaust gases contained, on average, 50% CO_2 and 28% CO (Figure 36). At the end of the experiment the product that was cast was fluid but slightly foamy. Once again a large proportion of the cast remained inside the casting chamber, the level of the hearth rising markedly. The slag that was cast contained 28.4% total iron and the yield from the experiment was calculated to be 75.5%.

Experiment 103

This was an unstirred experiment with identical inputs to those used in experiment 100. No build up was experienced throughout the experiment and the plant conditions were steady. Continuous feeding was possible throughout the experiment and the furnace temperature was constant at 1 450 $^{\circ}$C (Figure 39). The exhaust gases contained 50% CO_2 and 30% CO (Figure 38). At the end of the experiment a slag containing 44% total iron was cast and a yield of 39% was calculated. The collapsed material caused the furnace to sieze and again a large quantity of material remained inside the furnace and the casting chamber.

6.6   Analysis of the Batch Results

6.6.1   Technique for Refining the Mathematical Model

The mathematical model had been developed in such a way that a number of its parameters could be adjusted in the light of operating experience.

EXPERIMENT 102

GAS ANALYSIS.

FIGURE 36

TEMPERATURE.
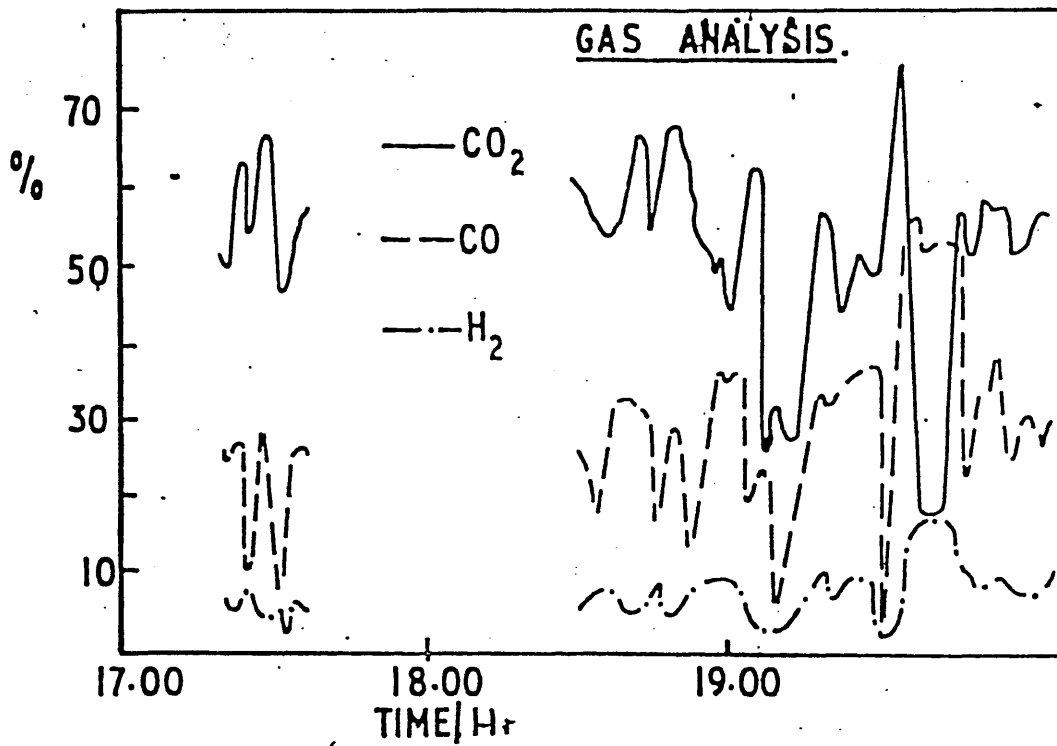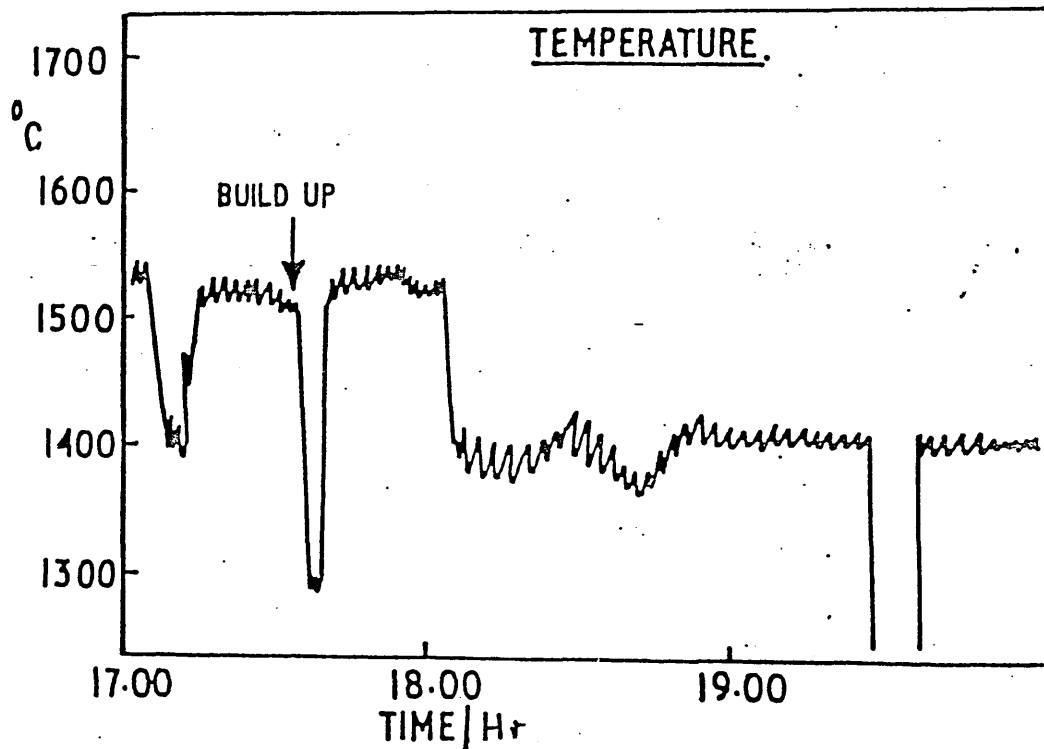
FIGURE 37

EXPERIMENT 103
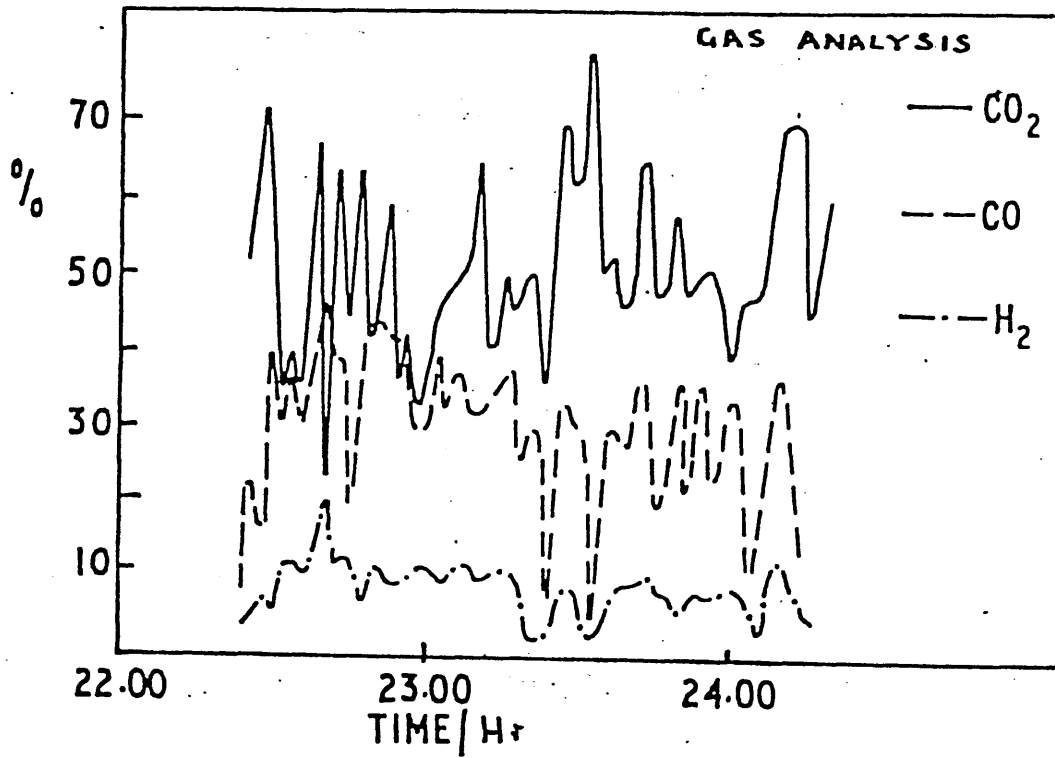
FIGURE 38
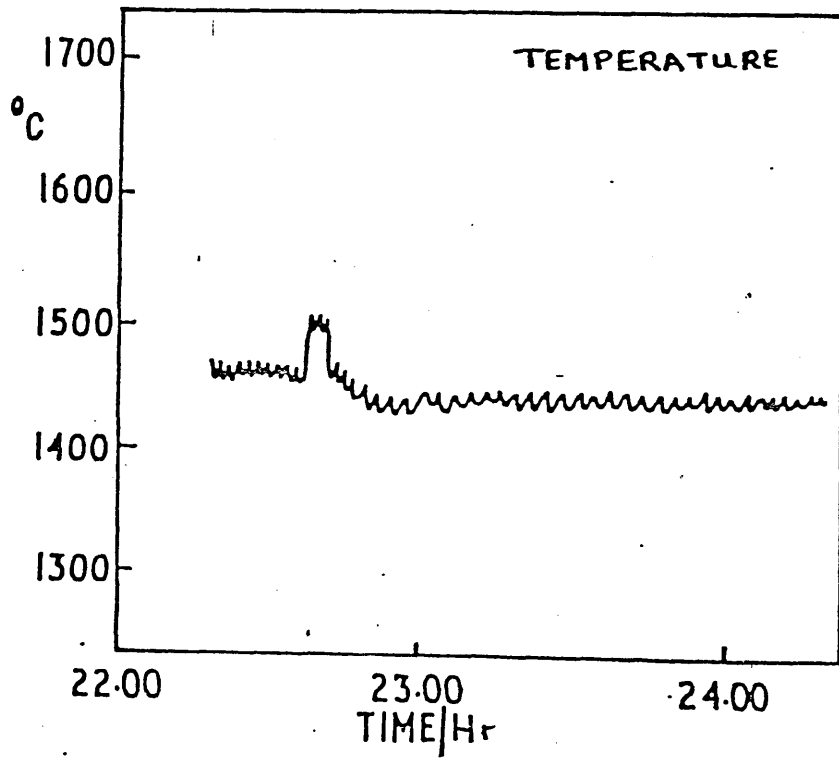
FIGURE 39

The first column of Table 6.4 lists these parameters, and the second column states the initial value of each parameter that had been incorporated into the mathematical model before the start of the work reported in this thesis. The use of these values in the model resulted in predictions of plant performance quantitatively and qualitatively at variance with observations on the pilot plant. Once the results of the factorial experiments had been obtained, then a systematic empirical campaign commenced to obtain more realistic values of these parameters for use in the mathematical model.

The value of each parameter was changed in turn and the resulting effect on the predictions of the model examined. Where a significant change was observed, a number of further changes in the value of the parameter were made until an optimum value could be identified by comparison with the actual performance of the pilot plant on the factorial experiments. The results of the campaign are shown in Table 6.4 where the third column shows the range of values tried for each parameter, and the final column shows the value finally identified as the optimum. The campaign is described in more detail below.

6.6.2   Mass Transfer Coefficient Values

The mathematical model determined the mass transfer coefficient in the gas phase from the standard pipe flow correlation (see section 4.1). This value was then systematically changed by multiplying it by an increasing factor x 2, x 3, x 4, x 5, x 10, and the resulting effects on predicted bed temperature, carbon coverage and yield were examined. Increasing the multiplying factor increased the yield and the bed temperature but tended to decrease the bed coverage - for values below 4, the predicted yield and bed temperature were significantly below the

Parameter	Initial Value Incorporated into the Mathematical Model	Range of Values Examined	Optimum Value
Mass Transfer Coefficient	Standard pipe flow correlation.	x 2 to x 10 the pipe flow correlation value.	x 5
Heat loss to water cooled probes (W)	1.76×10^5	1.76×10^5 to 2.1×10^5	1.76×10^5
Activation Energy (Kcals $gmol^{-1}$)	-69 Kcals $gmol^{-1}$	-69 Kcals $gmol^{-1}$	-69 Kcals $gmol^{-1}$
Reaction Rate (g atoms $cm^{-2} s^{-1}$ at 1500 $^{\circ}$C and 25 mass % FeO)	2.8×10^{-5}	2.0×10^{-5} to 4×10^{-4}	3×10^{-5}
Reaction Cut-off Temperature ($^{\circ}$C)	2000 $^{\circ}$C	1800 $^{\circ}$C to 2000 $^{\circ}$C	1800 $^{\circ}$C
Thermal Conductivities (W/m^{K})			
Iron Layer	29.3	29.3	29.3
Slag Layer	2.1	1.05 to 2.5	2.1
Coke Layer:-			
(i) Unstirred	2.0×10^{-1}	3.0×10^{-3} to 1.05	4.2×10^{-1}
(ii) Stirred	41.87	41.87	41.87
Distribution of Charged Material	Uniform along the furnace length.	Triangular Distribution	Uniform Spread

TABLE 6.4   REFINING OF THE MATHEMATICAL MODEL

113

values observed, whereas values above 5 resulted in increasingly

complete carbon burn-off and erroneously predicted an uncovered, very

hot slag layer. For this reason, a value of 5 was chosen as the

optimum value, and the appropriateness of this value was subsequently

confirmed from the naphthalene mass transfer studies, as discussed later

in section 7.3.

6.6.3 Heat Losses to Water Cooled Probes

Plant measurements had been originally used to determine the value of

the heat losses to the water cooled probes. However, a number of

computer predictions resulted in much higher gas temperatures than those

observed in the corresponding factorial experiment, and an increase in

the heat loss parameter was sought as a means of producing a more real-

istic prediction. Very little change in the predicted gas temperature

resulted, however, the original value was retained as the optimum.

6.6.4 Reaction Kinetics

As discussed in section 5.1.1, the rate of reaction, $\frac{dN}{dt}$, was described

in the kinetic experiments in terms of the first order form of equation

(5.1):-

$$\frac{dN}{dt} = A.K.C \qquad \ldots\ldots\ldots (6.1)$$

where A is the nominal slag/carbon interfacial area, K is a nominal

rate constant, and C is the molar concentration of FeO in the slag.

The work described in section 5.1 had shown that the nominal rate

constant obeyed the Arrhenius equation up to temperatures in excess

of 1 800 $^{\circ}$C, so that the reaction rate per unit area, r_T, at temperature

T, can be described by the equation:-

$$r_T = A \left(e^{\frac{-E}{RT}} \right) . C \qquad \ldots\ldots\ldots (6.2)$$

The mathematical model expressed this relationship in terms of a base

rate, r_o, at temperature $T = 1\ 723\ K$ and for a slag containing 25

mass % FeO, this base rate being shown in Table 6.4. A rate constant,

k_o, can be determined from this base rate by applying the equation:-

$$r_o = k_o\ C = A \left(e^{\frac{-E}{RT_o}} \right) . C . \qquad \ldots\ldots\ldots (6.4)$$

Thus $\dfrac{r_T}{r_o} = \exp \left\{ \dfrac{-E}{R} \left(\dfrac{1}{T} - \dfrac{1}{T_o} \right) \right\} \qquad \ldots\ldots\ldots (6.4)$

so that $r_T = k_o \exp \left\{ \dfrac{-E}{R} \left(\dfrac{1}{T} - \dfrac{1}{T_o} \right) \right\} . C . \qquad \ldots\ldots\ldots (6.5)$

The value of the activation energy, E, used in the model is shown in

Table 6.4. It was taken from previous work[27] that had studied the

kinetics of the reaction up to 1 500 ^oC. The work described in

section 5.1 of this thesis had not been able to provide an improved

value of the activation energy, due to foaming in the crucible, but

had confirmed that the rate of the reaction continued to increase with

temperature up to about 1 850 ^oC. This was important since one possible

interpretation of the experimental data, involving oxygen transfer

through a CO/CO_2 gas film lying between the carbon and the slag,

suggested that the reaction rate should decrease quite markedly as the

temperature approached 1 900 ^oC.

Uncertainties about the kinetic of the reaction at temperatures above

1 500 ^oC had been allowed for in the mathematical model by incorporating

a 'cut-off' temperature after which the rise in the reaction rate with temperature was assumed to cease. The value chosen for this temperature made no difference to the performance of the mathematical model over the first 80 'slices' because the predicted bed temperatures were too low. Over the remaining 100 slices, however, the use of a cut-off temperature of 2 000 $^{\circ}$C produced instabilities in the performance of the mathematical model. The reduction reaction could occur unrealistically quickly, completely consuming sections of the carbon bed and thus opening up the slag layer for increased heat transfer. This increased heat transfer rate could exceed the rate at which heat was consumed by the reaction causing the bed temperature to rise further, and thus further increasing the reaction rate. As a result, high yields and high bed temperatures were predicted under most operating conditions - even under conditions which, in the actual batch experiments, had resulted in portions of the bed freezing - leading to the build up of solid rings around the inside of the furnace.

The performance of the mathematical model was much more realistic when a cut-off temperature of 1 800 $^{\circ}$C was used. The consumption of carbon by the reduction reaction was reduced in the region beyond the first 80 slices. Although this resulted in a slight increase in predicted carbon oxidation rates, it still predicted more complete coverage of the slag layer by the carbon bed. This greater coverage naturally led to lower heat transfer rates and hence lower reaction rates. Unstable performance of the mathematical model was completely damped out, leading to the prediction of process yields and bed temperatures that were closer to those observed.

Of greater importance, however, was the greater reliability that could

be placed on the model's ability to predict conditions under which

extremes of temperature necessitated stopping the operation of the plant.

As mentioned earlier, a cut-off temperature of 2 000 $^{\circ}$C could predict

high operating temperatures under conditions in which solidified rings

of material actually built up on the inside of the furnace. Such

erroneous predictions no longer occurred when the cut-off temperature

was set at 1 800 $^{\circ}$C. On the other hand, the higher cut-off temperature

had also failed to predict how the furnace behaved under highly oxidising

conditions - the only conditions under which extremely high temperatures

had been found to occur in the actual batch experiments and had necess-

itated stopping the operation of the plant to avoid excessive refractory

attack. Once again, erroneous predictions were made by the model because

it over estimated the rates at which the reduction reaction would con-

sume both oxygen and process heat at temperatures in excess of 1 800 $^{\circ}$C.

Thus a cut-off temperature of 1 800 $^{\circ}$C was used in the mathematical

model and, as discussed later, the use of this temperature was, in fact,

supported by the laboratory experiments and by qualitative observations

made on the plant.

6.6.5   Thermal Conductivity of the Coke Bed

As stated in section 4.1, in the description of the mathematical model,

reference (26) was used as the source for values of the thermal conduct-

ivity of the coke in the bed. This reference gave a range of values

depending upon the coke type, and upon the temperature. Neither of

these was known to any accuracy, so coke thermal conductivity values

had to be assumed in the model. The situation was further complicated

because it had been envisaged that cycling the rotation speed of the furnace between two set limits would cause a shearing action between the liquid slag layer and the carbon bed floating on top of it. This shearing action could cause the carbon particles in the bed to rotate and also to sink into the slag layer* both of which phenomena would enhance the transfer of heat through the carbon layer from the gas to the slag. Thus it was necessary to assume two different thermal conductivity values for the coke layer, one for the unstirred bed, and one for the bed stirred by cycling the rotation speed. Data presented in reference (26) suggested that coke thermal conductivities were typically about 0.2 W/mK, and this value was used initially in the mathematical model. The resulting predicted slag layer temperatures were unrealistically low. On the other hand, when values greater than 0.42 W/mK were used, slag layer temperatures higher than the range observed were predicted. Consequently the value 0.42 W/mK was used for unstirred coke beds. The enhancement of the heat transfer process by the shearing action discussed above was accounted for by increasing the coke thermal conductivity value to 41.87 W/mK. This value gave predictions that were in keeping with the experimental observations, and was therefore used whenever the mathematical model was used to predict the performance of the stirred furnace.

----

*FOOTNOTE   Both these phenomena had been observed in early model experiments, involving water, paraffin and vermiculite, that had been carried out in the development of certain patents[25].

In fact it was found that the thermal resistance of the coke layer was of relatively little importance in the stirred experiments, although the predicted performance of the furnace could be affected quite strongly by values assumed for the thermal conductivity of the slag layer. The initial value used in the mathematical model was 2.1 W/mK, whereas values only slightly in excess of this figure gave extremely high slag and metal temperatures, and greatly exaggerated reduction and oxidation rates. On the other hand quite large reductions below this figure produced relatively little effect. Thus this initial value was used throughout the predictions made by the mathematical model.

6.6.6   Feeding Distribution of Solids

The initial mathematical model had assumed that the solids could be thrown into the furnace in such a way that they fell evenly along the entire length of the bed. Test on the solids feeding equipment conducted outside the furnace did not support this assumption, suggesting that the actual distribution was more triangular in form, the apex of the triangle falling some halfway along the furnace. However, attempts to incorporate such a distribution into the mathematical model were unsuccessful. In all cases very low bed temperatures were predicted below the apex of the distribution triangle, and in some cases actual build up of solid material was predicted at that point. These predictions were at variance with the observed performance of the plant, so the triangular solids distribution profile was abandoned, a uniform distribution being assumed in all cases. The correctness of this decision was partly supported by the results of certain rough investigations that were conducted on the furnace. When solid material was thrown into a stationary unfired furnace and collected in a series of shuttered compartments, a humped

distribution was found to occur, and no material was thrown out of the end of the furnace. However, when solids were thrown into the operating furnace, no change having been made in the operation of the feeder mechanism, solid material was observed to be thrown out of the end of the furnace. Moreover, careful observation within the furnace under these conditions supported the assumption that the solids were fed evenly to the operating furnace since no distribution hump could be observed under any set of operating conditions.

6.6.7 Testing of the Improved Mathematical Model

As stated in section 6.6.1, the improvements in the mathematical model were achieved by comparing its predictions of the furnace's performance during each batch experiment with the actual performance observed. At the end of this progressive modification process, the mathematical model was able to predict fairly accurately the ways in which the furnace would respond to different operating conditions. The accuracy of these predictions is demonstrated below, where, for each batch experiment, the observed performance of the plant is summarised in tabular form and set alongside a summary of the prediction made by the mathematical model.

Experiment No. 88

Plant Observations	Model Predictions
This was a stirred experiment with bed surface temperature falling during the experiment from 1 750 °C to about 1 580 °C. Two build ups were noted after about 1 hour and 2 hours from start of experiment.	The model predicted a build up situation starting at 75 divisions. The iron and slag temperatures were high (1 736 °C tapping temperature for iron) and some oxidation occurred. The gas analysis predicted

120

Experiment No. 88 cont'd

Plant Observations

The first build up started about
80 cm into the furnace. Although
temperatures were falling slowly
throughout, on termination after
2 hours the metal and slag collected
were still fluid and metal compos-
ition was 2.58% carbon.

Calculated Yield = 87.0%

Model Predictions

was very close to the plant
results.

Calculated Yield = 87%

Experiment No. 89

Plant Observations

This was an unstirred experiment
with bed surface temperatures
constant at 1 600 ^{o}C for part
of the time, but falling after
$1\frac{1}{2}$ hours, and on termination of
the experiment three collapses of
the bed, with reheating periods
in-between, were required to
discharge the furnace contents.
Even after three collapses some
material stayed in the furnace,
and the metal tapped at 1 250 ^{o}C
(dip temperature) and 1.8% C.
Excess carbon was noted floating
on the collected slag.

Calculated Yield = 84%

Model Predictions

The model predicted that most of
the furnace bed would be covered
in carbon, and that build up would
occur. Little oxidation of the
iron bed was predicted, together
with a tapped iron product at
1 267 ^{o}C. The gas analysis pre-
diction was again close.

Calculated Yield = 78.9%

Experiment No. 90

Plant Observations	Model Predictions
This was a stirred experiment with bed temperature increasing slowly throughout. Some slight build up occurred after $\frac{1}{2}$ hour probably due to a lower than usual 'start' temperature, but this did not repeat as the experiment warmed up. The collapsed metal was very fluid (dip temperature 1 420 ^{o}C) and more metal was cast than could possibly have been produced during the experiment. This extra metal was the residue from the previous 'cold' experiment 89.	The model predicted high slag and iron temperatures with very slight build up at the end of the furnace. It also predicted a high degree of iron oxidation, but the competing reduction reactions were sufficient to maintain a good positive yield. The gas analysis predicted was reasonably close to the plant measurement. The temperature of the tapped iron product was 1 766 ^{o}C.

Calculated Yield = 83%   Calculated Yield = 77.5%

Experiment No. 91

Plant Observations	Model Predictions
This was an unstirred experiment with a fairly low 'start' temperature of 1 550 ^{o}C. Slight build up occurred after 1 hour, but feeds were only interrupted for a few minutes. At the end of the experiment excess coal was observed with the tapped product,	The model predicted complete coverage of the bed with coal and a very low iron temperature at the exit end of the furnace of 1 117 ^{o}C. The predicted gas analysis was again close to the plant values which in turn were fairly steady throughout the experiment.

Experiment No. 91   cont'd

Plant Observations	Model Predictions

and although the slag cast was at

a dip temperature of 1 400 ^{o}C no

metal was cast. This indicated

that the iron product was frozen

in the furnace.

Calculated Yield = 72%   Calculated Yield = 74.8%

Experiment No. 92

Plant Observations   Model Predictions

This was a stirred experiment with   The model predicted low slag and

excess coal and low oxygen. The   metal temperatures and consider-

bed temperatures were falling   able build up. The exit iron

throughout most of the experiment   temperature predicted was 1 258 ^{o}C,

although the metal was cast at   and part of the poor yield was

0.57% carbon and a dip temperature   owing to oxidation occurring in

of 1 390 ^{o}C. Feeds had to be   the first half of the furnace where

stopped on two occasions to melt   carbon layer burned off. The gas

out the build up, and the reason   analysis predictions were very close.

for a reasonably fluid cast was

$\frac{1}{2}$ hour of reheating in the furnace

with ore and coal feeds off immed-

iately prior to casting.

Calculated Yield = 82%   Calculated Yield = 68.8%

Experiment No. 93

Plant Observations

Again this was a stirred experiment, but with high oxygen and low carbon additions to the bed (1.2 times stoichiometric). Conditions were very hot in the furnace with the bed temperature increasing throughout and no signs of build up. The metal cast had a dip temperature in excess of 1 500 $^{\circ}$C, but the slag iron content was high at 46%, indicating oxidising conditions and a poor yield.

Calculated Yield = 53%

Model Predictions

The model predicted high temperatures (2 283 $^{\circ}$C in the gas and 1 678 $^{\circ}$C in the iron at exit) and oxidising conditions. It predicted a high iron reduction rate but also a high competing oxidation rate. The gas analysis was again reasonably close between plant and model.

Calculated Yield = 44.8%

Experiment No. 94

Plant Observations

This was an unstirred experiment with slight build up. The build up was only noticed during observation breaks and was not sufficient to stop the feeds. Gas analysis was very steady during the experiment although the indicated bed temperature was fluctuating. From the operating viewpoint this was clearly a 'balanced' case with

Model Predictions

A close examination of the detailed model predictions indicated complete coal coverage over the first 100 divisions of the furnace, partial coverage again in the last part. This was an unusual prediction, which seemed partly to be borne out by the plant experiment. The slag and iron temperatures at the exit were high at 1 708 $^{\circ}$C and 1 629 $^{\circ}$C respectively.

Experiment No. 94 cont'd

Plant Observations

partial coal coverage of the furnace. Observations showed coal coverage in the first half but either a coal shortage or 'sunk' coal in the second half. A fluid cast of metal and slag was obtained with the initial carbon content of the iron at 1.3%.

Calculated Yield = 93%

Model Predictions

The gas analysis correlation was not very close for this experiment.

Calculated Yield = 86%

Experiment No. 95

Plant Observations

This was a stirred experiment with low carbon input rates. The bed temperatures were rising continuously during the experiment which was terminated after 2 hours when the bed temperature was in excess of 1 700 $^{\circ}$C. Observations after 1 hour of operation showed a very hot furnace with little signs of coal. No build up occurred and cast metal temperatures were at a dip temperature of 1 510 $^{\circ}$C on the first collapse and 1 700 $^{\circ}$C on the second. 852 kg of metal were cast

Model Predictions

The model predicted no build up, a high degree of iron oxidation, but only a moderate metal exit temperature of 1 478 $^{\circ}$C. The gas analysis predictions were fairly close. The model predicted that the bed would not be covered with coal over most of its length.

Experiment No. 95 cont'd

Plant Observations

which was about the same as the

total iron units added for the

experiment. Since the yield was

poor, some iron cast was undoubtedly

residue from 94.

Calculated Yield = 40%

Model Predictions

Calculated Yield = 55.2%

Experiment No. 96

Plant Observations

This was an unstirred experiment

with a high coal input of 1.8

times stoichiometric. The bed

temperatures were falling sharply

through the feeding periods and

observations after $1\frac{1}{2}$ hours of

operation showed build up in the

first half of the furnace and low

temperatures. Little slag or metal

was cast at the termination of the

experiment, and the iron was so

viscous that it siezed up the

furnace on slowing down by building

· up on the stationary exhaust hood

sufficiently to stop the drum.

Calculated Yield = 53%

Model Predictions

The model predicted very low exit

iron temperatures at 1 056 $^{\circ}$C, and

also complete coverage of the bed

with carbon and a bed build up

situation. The gas analysis

predictions were quite close. Very

little iron was produced after 135

divisions of furnace length because

of low bed temperatures.

Calculated Yield = 67.9%

Experiment No. 97

Plant Observations

This was a stirred experiment with a very high coal input 2 times stoichiometric. The bed temperature dropped rapidly in the early part of the experiment and then fluctuated, and there were two stoppages of feed to clear build up. Observations after $1\frac{1}{4}$ hours indicated a cold furnace with excess coal in the first half particularly. Little metal was cast in the first collapse, and the dip temperature was 1 370 ^{o}C. The calculated yield was high owing to the short duration of the experiment. The bed would probably have frozen if the experiment had continued.

Model Predictions

The model predicted a lower yield than that obtained from the plant and a low exit iron temperature of 1 337 ^{o}C. Excessive build up was also predicted from half way down the furnace length which resulted in the low bed temperatures towards the exit end of the furnace.

Calculated Yield = 92%

Calculated Yield = 76.3%

Experiment No. 98

Plant Observations

This was an unstirred experiment which suffered from a dam failure fairly early on. The effect of this failure could be seen during

Model Predictions

No correlation attempted owing to the dam failure on the plant. The model did, however, predict high bed temperatures with an

Experiment 98   cont'd

Plant Observations	Model Predictions
observations taken at 1 hour,	oxidised bath. High carbon burn
1 hour 50 minutes, 2 hours and	off rates were predicted, together
$2\frac{1}{4}$ hours from the start of feeding.	with a high exit gas temperature.
The feeds were maintained over	A low yield was predicted.
this period, and observations	
indicated that the coal was	
'stretched out' as the slag	
velocity tended to increase with	
continuous casting of slag from	
the end of the furnace. This	
clearly leads to a high temp-	
erature and highly oxidising	
conditions in the slag, and con-	
sequently a poor yield.	
Calculated Yield = Zero %	Calculated Yield = 21%

Experiment No. 99

Plant Observations	Model Predictions
This was an unstirred experiment	The model predicted no build up
using mid-levels of oxygen, p.f.,	and a high metal temperature of
and oil along with a very low coal	1 704 ^{o}C. Both were experienced
input of 1.0 x stoichiometric. The	on the plant. The gas analysis
bed temperature rose gradually from	predictions did not correlate too
1 400 ^{o}C to 1 500 ^{o}C and no build	well with the plant but the pre-
up occurred. The collapse was	dicted yield was close to the actual.
fluid with a dip temperature of	The bed was only partially covered

Experiment No. 99   cont'd

Plant Observations

1 550 $^{\circ}$C.   935 kg of metal (which
was about the same as the initial
addition of steel shot) and 122 kg
of slag at 46% Fe^T were cast.   Some
of the cast remained inside the
casting chamber.

Note: The recorded measurement of
bed temperature for this experiment
and for the subsequent experiments
100, 102 and 103 may be low, prob-
ably owing to a fault on the
pyrometer.

Calculated Yield = 42.4%

Model Predictions

with coal and oxidation of the bed
occurred resulting in the low yield.

Calculated Yield = 33.9%

Experiment No. 100

Plant Observations

This was a stirred experiment
using mid-levels of oxygen, oil
and p.f. along with a coal input
of 1.5 x stoichiometric.   One build
up occurred about $\frac{2}{3}$ of the way
through the two hour experiment and
took about 8 minutes to melt out.
The indicated bed temperature was
low, but observations indicated
high bed temperatures, a foaming

Model Predictions

The model predicted a high reduction
rate competing with a high rate of
oxidation.   A slight build up was
also predicted, towards the cast
end of the furnace, but with high
slag/metal temperatures, over most
of the furnace length.   The gas
analysis correlation between plant
and model was quite close but a
lower yield was predicted.   The

Experiment No. 100   cont'd

Plant Observations	Model Predictions
bed, and reactive conditions. This was borne out by the very foamy cast product which dipped at 1 520 ^{o}C. Much of the material stayed inside the furnace. The small amount of cast slag analysed at 6.29% Fe^T and the calculated yield was high.	oxidation of the bed took place mainly over the middle section of the furnace where the bed was not covered by coal, and this resulted in the somewhat low yield.
Calculated Yield = 96%	Calculated Yield = 74%

Experiment 102

Plant Observations	Model Predictions
This was an unstirred experiment using low levels of oxygen, oil and p.f. along with a coal input of 1.2 x stoichiometric. Three build ups occurred during the experiment but each one was slight and easily melted out. The bed temperature was steady at 1 400 ^{o}C and the collapse was fluid but slightly foamy. Again a lot of material stayed inside the casting chamber, the level of the hearth rising markedly. The slag cast contained 28.44% Fe^T.	The model predicted no build up with higher slag/metal temperatures than were experienced on the plant. There was a good correlation with the gas analysis but the predicted yield was lower than the calculated plant yield. The predicted yield was low because of only a modest rate of reduction of the ore coupled with some oxidation of the iron.
Calculated Yield = 75.5%	Calculated Yield = 40.5%

Experiment No. 103

Plant Observations

This was an unstirred experiment using mid-levels of oxygen, oil and p.f. along with a coal input of 1.5 x stoichiometric. No build up was experienced and the plant conditions were very steady with continuous feeding and a level bed temperature of 1 450 $^{\circ}$C. The drum seized on collapse of the bed and again a lot of material remained inside the drum and the casting chamber. The slag analysed at 44% Fe^{T} and the yield was low.

Calculated Yield = 39%

Model Predictions

The model predicted build up over the latter part of the furnace, resulting in lower bed temperatures than were measured on the plant, although the iron temperature inside the furnace must have been low since none was cast out of the tap hole on collapse. The gas analysis correlation was quite close but a higher yield than that measured on plant was predicted. The model predicted only a low level of oxidation, hence the relative high yield value.

Calculated Yield = 73%

The agreement achieved, as outlined above, between the observed performance of the furnace and the predictions of the mathematical model will be discussed further in section 7.6, but was considered sufficient for the mathematical model to contribute significantly to the planning of those plant operating conditions under which continuous operation could be achieved. The discussions and judgements that were involved in planning the operating conditions for the continuous experiments are considered in the discussion section of the thesis - section 7.5, the continuous experiments are described in the next sections.

6.7 Conditions for the Continuous Experiments

As stated in section 6.4, the purpose of the factorial series of experiments was only secondarily to improve and confirm the mathematical model. The prime purpose of the experiments was to seek conditions under which the plant could be operated continuously, improving the mathematical model, however, being seen as one of the necessary tools for this purpose. Thus from observations made during the factorial experiments, from the predictions made by the improved mathematical model, and from accumulated operating experience of the plant's performance, a set of operating conditions were drawn up for the three continuous experiments to be conducted. The operating procedures that were used have been described in section 6.3, which also explained how the start up and operating procedures used in the continuous experiments differed from those used in the batch experiments. Batch experiments were conducted with and without variable speed stirring of the bed but, as discussed later, both the plant results and the mathematical model showed the furnace's performance to be improved by stirring. Thus variable speed stirring was used in all the continuous experiments.

The feed rates chosen for the continuous experiments are shown in Table 6.5. The input rates for experiments 118 and 119 were identical, but observations made during these experiments indicated slight changes could be made with advantage, as discussed in section 7.5. These changes were made before experiment 122 was carried out.

TABLE 6.5

Experiment No.	Ore kg/h	Coal kg/h	Limestone kg/h	Pulverised Fuel kg/h	Oxygen nm^3/h	Oil g/h
118	341	237	60	75	360	15
119	341	237	60	75	360	15
122	341	249	60	100	385	15

The batch experiments had been terminated by dropping the rotation speed of the furnace gradually to zero, whence the entire contents of the furnace were cast out. Obviously, the contents of the furnace could not be removed in this way during the continuous experiments so, as described in section 6.3.5 a system of surge casting was developed for the continuous experiments. This system was developed in conjunction with model work that showed the furnace capacity to increase with its speed of rotation so that a significant reduction in this speed, once the furnace was near its normal operating capacity, resulted in the controlled casting of part of the furnace contents. Not only were the liquid contents cast out, but also a proportion of the carbon bed, as was discovered in a series of special surge casting tests carried out on the furnace between the end of the factorial experiments and the start of the continuous experiments. Consequently the coverage of the slag layer by the carbon bed was drastically reduced each time the furnace was surge cast. In order to stop resulting increases in slag oxidation, a single additional charge of 50 kg of coal was made to the furnace each time it was surge cast, over and above the feed rates shown in Table 6.5.

6.8   The Results of the Continuous Experiments

The progression of each of the three continuous experiments is set out schematically in each of Figures 40 to 42. Each Figure shows, at the top, the feed rates of ore, coal and pulverised fuel (PF) that were actually used at different times during the experiment. The totals of these three materials charged to the furnace are then shown graphically, as they increased throughout the period of the experiment. Below this graph, arrows indicate the times at which bed samples were taken (see section 6.3.8), and at which the furnace was surge cast; and then a graph

133

shows how the bed temperature changed during the experiment. Once the initial start up period was completed, these graphs show that average bed temperatures of about 1 500 ^{o}C were maintained in each experiment. The drops in temperature indicated each time the furnace was surge cast are more apparent than real. The radiation pyrometer measuring the bed temperature was sighted through the cast end. This opening was obscured during the surge cast by finely divided carbon that had fallen from the bed, and by a mist of fine liquid drops thrown away from the main liquid streams leaving the furnace. Thus the pyrometer was not able to read the bed temperature over the surge cast period and this gives rise to the apparent troughs in the temperature trace.

Below this trace, four longitudinal charts show:-

(i)   The iron content in the slag that was separated from each bed sample.

(ii) The appearance of material emerging from the tap hole of the casting chamber over the time periods indicated between the arrows.

(iii) The weight of slag emerging during each of these time periods, and its iron content.

(iv) The weight of iron emerging during each of the indicated time periods together with its carbon content.

The final graph shows gas analysis samples taken from the cast end of the furnace.

Certain of the quantitative data shown in the Figures is set out again with greater precision in Tables 6.6 to 6.8, together with more complete chemical analyses. Finally, Tables 6.9 to 6.11 show complete mass balances

for each experiment, highlighting in separate sub-tables the weighed

yield of iron obtained.

Apart from this quantitative data, qualitative observations were made

during each experiment, and these are described below.

6.8.1   Experiment No. 118

The total duration of this experiment including the initial iron shot

feeding period was 10 hours. The feeding of the raw materials was con-

tinuous over this period apart from the intended stoppages to allow

surge casting to be carried out. A total of 1865 kg of iron ore and

1761 kg of coal were charged into the furnace. The input rates were

reasonably uniform over the feeding periods and were close to the

intended values.

The bed temperature was reasonably steady throughout the experiment, the

average bed temperature being 1 550 $^\circ$C. During the ore feeding periods

the exhaust gas analysis showed 55 - 60% CO_2 with 25 - 30% CO. The

nitrogen level was 15 - 20%, with the oxygen level peaking at 2%. Gas

analysis was not available during the surge casting periods when the

probe was completely withdrawn from the furnace to prevent material

build up on its water cooled surface. High nitrogen levels of up to 70%

and oxygen levels of 17% were occasionally monitored. These corresponded,

however, to the formation of solid blockages in the mouth of the probe

when the resulting enhanced suction in the sampling line tripped the

threshold pressure in the condenser and filtering system, causing air to

leak into the line.

Six surge casts were carried out during the experiment but for the first three nothing emerged from the tap hole of the casting chamber at the time of casting. However, small quantities of slag ran out of the tap hole between the casting times, as indicated in Figure 40. The first time this occurred it was thought that no material had been cast at the moment of the contrived surge cast but that a minor involuntary surge cast had occurred subsequently. It was soon realised, however, that the material had been cast into the casting chamber at the time of the contrived surge cast, but took some time to emerge from the tap hole. This took place for the first three surge castings in this experiment, and then an actual involuntary surge cast took place to be followed immediately by contrived surge cast number 4. Surge casts 5 and 6 produced reasonable quantities of material from the tap hole almost instantaneously, and this material contained metallic iron for the first time in this experiment. Surge cast 6 was conducted virtually 8 hours after the start of the experiment.

At this time, the plant was fully under control and no operating problem had arisen, other than the foreseen limitation of hopper capacity. The experiment was therefore terminated in a controlled manner, by arranging two collapses of the bed, of the type used to conclude the batch experiments. Over one metric tonne of metal was collected at the first collapse (see Figure 40, and Tables 6.6 and 6.9), this being the greatest amount of metal that had been obtained from the furnace up to that time.

Except in the initial stages, the casting and sampling procedures functioned as expected, the slag samples showing that reduction was occurring during the early stages of the experiment even though no iron was cast from the furnace until surge cast 5. The iron contents of the

136

slag sampled from the furnace remained more or less in the same range throughout the experiment, but the iron contents of slag cast from the furnace at the latter stages of the experiment showed increasing quantities of iron. As will be discussed later, this was thought to be due to a drawback to the surge casting technique.

It was found that very little material could be cast or sampled from the furnace during the very early stages of the experiment - the first sample produced no material whatsoever - and this was realised to be due to the extremely shallow bed present in the furnace at this time.

By the end of the experiment, a total of 1245 kg of metal had been collected from the furnace, its carbon content varying from 0.56% to 2.37%. After the initial quantity of iron shot, used in the start up procedure, had been subtracted (see mass balance in Table 6.9) this quantity of iron represented no more than 520 kg of iron obtained by the reduction of the iron ore charged to the furnace - a yield of 43%. However, 390 kg of iron remain unaccounted for in this overall external mass balance. Observations inside the furnace showed that a shallow layer of iron remains within the furnace however stringent the final collapses of the bed. Moreover, although as much material as possible had been physically removed from the inner walls of the casting chamber, slag is significantly easier to remove than iron. Thus it is likely that the bulk of the iron that has been unaccounted for comprises metallic iron that had remained inside the furnace, or had been sprayed onto the inside of the casting chamber from where it could not be removed. If this assumption is correct, the iron yield becomes 75%, a figure much more in keeping with the iron contents of the slag samples obtained from the furnace during the experiment.

TABLE 6.6

EXP. No. 118

AIM	To reduce iron ore continuously for a minimum period of fo... from an appraisal of the Factorial Experiment and incorpo... induced surge cast.			
INPUT:-	ORE kg/h	COAL kg/h	$CaCO_3$ kg/h	P.F.
Desired input	341	237	60	6
Actual input(Av)	335	227	57	8
Total input	1 865 kg	1 761 kg	335 kg	56

	DESCRIPTION OF OUTPUT	TIME h	WEIGHT kg	C
	Minor Surge	13-12/13-42	55 kg Slag	–
	Bed Sample 2	13-20	Slag	–
	Dribbles	13-42/15.08	84 kg Slag	–
	Bed Sample 3	14-05	Metal	0.87/1.2
			Slag	–
	Bed Sample 4	14-35	Metal	.005/.37
			Slag	–
	Bed Sample 5	15-00	Metal	1.11/1.3
			Slag	–
	Dribbles	15-08/16-15	65 kg Slag	–
	Bed Sample 6	15-40	Metal	.16/2.35
			Slag	–
MATERIAL	Bed Sample 7	16-10	Metal	.92/1.08
CAST &			Slag	–
CHEMICAL	Nat. Surge	16-15/16-20	34 kg Slag	–
ANALYSIS	Surge	16-20	20 kg Slag	–
	Bed Sample 8	17-08	Slag	–
	Bed Sample 9	17-45	Metal	.10/.16
			Slag	–
	Dribbles	16-20/17-55	215 kg Slag	–
	Surge	17-55	128 kg Slag	–
	Dribbles	17-55/18-40	30 kg Metal	2.37
			40 kg Slag	–
	Bed Sample 10	18-52	Metal	0.09/1.5
			Slag	–
	Dribbles	18-40/19-00	10 kg Slag	–
	Surge	19-08	40 kg Metal	0.56
			105 kg Slag	
	1st Collapse	19-20	1 175 kg Metal	0.86
			94 kg Slag	–
	2nd Collapse	19-45	46 kg Slag	–

YIELD	Weighed Yield = 43 % Using the assumption that the unaccounted for iron (se... the casting chamber, yield = 75 %

TABLE 6.9 MATERIAL BALANCE FOR

EXP. No. 118

	IRON SHOT (750 kg)	ORE (1865 kg)	COAL (1761 kg)	CaCO$_3$ (335 kg)	P.F. (567 kg)	OIL (450 kg)	TOTAL
ASH			141.9		36.28		
Fe^T	708.8	1188	18.7	2.0	3.66		1921.16
Fe^M	708.8						708.8
C	21.9		868		337.7	385.6	1613.2
Mn	2.8						2.8
Si	10.1						10.1
S	1.27	0.19	11.8		4.08	4.05	21.39
P	5.2	0.56					5.76
CaO		18.65	9.08	179.56	2.39		209.68
MgO		3.73	1.42	0.67	0.62		6.44
Al$_2$O$_3$		9.32	34.76	1.34	10.15		55.57
SiO$_2$		121.2	68.82	7.37	17.23		214.62

	Minor Surge. Box 10 55 kg Slag	Dribbles. Box 7 84 kg Slag	Dribbles. Box 2 65 kg Slag	Natural Surge. Box 11 34 kg Slag	Surge. Box 18 20 kg Slag	Dribbles. Box 4 215 kg Slag
Fe^T	10.12	18.81	11.44	8.9	6.0	89.0
S	0.034	0.105	0.06	0.048	0.036	0.07
CaO	12.59	20.58	18.33	8.80	4.8	22.57
MgO	7.04	7.22	5.85	2.55	1.48	7.74
Al$_2$O$_3$	4.45	11.50	5.85	2.65	1.44	23.22
SiO$_2$	14.24	21.5	16.51	7.41	4.08	28.38

INPUT

Iron units from   (i)   SHOT Fe^M = 708.8 kg

(ii)   ORE   Fe^T = 1188   ⎫

(iii)   COAL etc   ⎬ 1212.36 kg

         Fe^T = 24.36 ⎭

OUTPUT

Assume shot remains as shot

Metallic iron weighed = 1229.02 kg ⟨ 708.8 kg (SHOT) / 520.22 kg (ORE)

Iron Assoc. with slag = 302.09 kg

Iron unaccounted for = 390.05 kg

Weighed Yield = $\dfrac{520.22 \times 100}{1212.36}$ = 42.9 %

Assume the 390.05 kg of iron unaccounted for ex

∴ Iron made = 520.22 + 390.05 = 910.27 kg

Yield = $\dfrac{910.27 \times 100}{1212.36}$ = 75.08 %

6.8.2   Experiment No. 119

This experiment was intended as a direct repeat of experiment 118. As such, the course of the experiment was very similar except that it only lasted for 3.5 hours, Figure 41. The early termination of the experiment was caused by the failure of the cast end dam which deteriorated to such an extent that it could no longer retain the liquid bed. The material input rates and bed temperature profile were similar to those in experiment 118, with, once again, apparent troughs in the temperature readings during surge casting. The exhaust gas analysis was reasonably steady throughout the experiment, although there were two long delays - one to repair the water cooled probe, the other to remove a blockage inside the probe. The analysed composition of the exhaust gases differed slightly from that measured in the previous experiment, the nitrogen and oxygen levels being higher at about 30% and 4% respectively. These higher levels suggested that the water seal was not functioning as well as in the previous experiment, allowing more air to enter the furnace. This additional air did not lower the bed temperature to any appreciable extent, but did result in lower CO levels - of about 15%.

Even before the first surge cast was carried out on this experiment, a quantity of slag ran out of the tap hole. This event illustrates the slight uncertainty, which is discussed further later, surrounding the collection of data from the pilot plant on which precise mass balances could be based. It was suspected that the slag might have originated from the previous experiment 118 but, in keeping with the convention that had been adopted about the collection of data for mass balances (see section 6.3.9), the slag was included in the mass balance for experiment 119.

Two surge casts were carried out, the yields of slag being 34 kg and 39 kg, containing 15.1% and 13.7% of iron respectively. There was a constant but small flow of slag between the two surge casts, 60 kg in total. It was felt that this slag was from the first surge cast but had been sprayed over the inner surfaces of the cast end chamber from which it drained gradually. After the second surge cast it was noticed that the cast end dam was in poor condition so that no further raw materials were added except the small quantity of coal always added immediately after a surge cast had been carried out, and the decision was made to end the experiment. Consequently, two bed collapses were carried out to empty the furnace, the bed being reheated for a short period between the two collapses in order to increase the fluidity of that material which had remained inside the furnace after the first collapse. 1095 kg of metal were cast in the first collapse and 105 kg of slag. The second collapse produced a further 125 kg of metal and 35 kg of slag. The masses and analyses of the material cast from the furnace during this experiment are detailed in Table 6.7. Also included in this Table, and in the mass balance shown in Table 6.10 is 70 kg of metal which was removed as a solid lump from the floor of the cast end chamber immediately after the completion of the experiment.

Table 6.7 also shows the results of the five bed samples that were taken during the experiment, their total iron contents ranging from 4.9 to 19.4%. The mass balance in Table 6.10 shows a loss of 12.86 kg of iron during the experiment but an iron yield from the charged ore of almost 80%. Once again this iron yield is in keeping with the bed analyses obtained during the experiment.

Ore rate , kg/h	342
Coal rate. kg/h	222
P F rate .k g /h	-9 5 -

Accumulative ore   kg

Accumulative coal, kg

1000

Accumulative P F . kg

Iron shot
750 kg

Q. 750

5   500

250

1100   12.00   13 00

Bed sample   Bed sample
A   B

1700

1600

9; 1500

£   1400

1300

1200
1100   **1200**   **BS.A**   **b s a**
Bed samples   17.4 7.   7 3 7.
7. FeT

Description of
material discharged

Material output and
chemical analysis:—   Weight of slag t kg

7. FeT in slag

Weight of metal;kg

7. C in metal ,
11 00   12.00

60
Exhaust gas analysis:-

CO-

CO

10 00   **1030**   1100   **11 30**   1200   **13.00**
TIME, hour

TABLE 6.7

EXP. No. 119

AIM	As Experiment 118			
INPUT:-	ORE kg/h	COAL kg/h	$CaCO_3$ kg/h	P.F. kg/h
Desired input	341	237	60	68
Actual input (Av)	340	230	58	92
Total input	1 091 kg	1 002 kg	184 kg	317 kg
	DESCRIPTION OF OUTPUT	TIME/h	WEIGHT kg	C	S
	Bed Sample A	12-20	– Slag	–	0.1:
	Bed Sample B	13-20	– Slag	–	0.3(
Material Cast	Remelt	13-25/14-10	140 kg Slag		0.0!
and Chemical	Surge	14-10/14-20	34 kg Slag		0.1:
Analysis	Spoon Sample	14-10	– Slag		0.1!
	Bed Sample C	14-22	– Slag		0.2:
	Remelt	14-20/15-30	60 kg Slag		0.0!
	Bed Sample D	15-00	– Slag		0.1]
	Bed Sample E	15-27	– Slag		0.18
	Surge	15-30	39 kg Slag		0.1(
	Spoon Sample	15-30	– Slag		0.1:
	Dribbles	15-40	20 kg Slag		0.0!
	1st Collapse	15-45	1 095 kg Metal	0.87	
			105 kg Slag		0.2]
	Dribbles	–	15 kg Slag		0.1(
	2nd Collapse	16-10	125 kg Metal	–	–
			35 kg Slag		0.1(
	Casting Chamber		70 kg metal		
Yield	Weighed Yield = 80 %				

T A B L E *b-IQ* M A T E R I A L   B A L A N C E Fop

EXP. No. 119

	IRON SHOT (750 kg)	ORE (1091 kg)	GOAL (1001.8 kg)	CaCO₃ (184.2 kg)	P.F. (317 kg)	OIL (243 kg)	TOTAL	Remelt. Box 15 140 kg Slag	Surge. Box 16 34 kg Slag	Remelt. Box 10 60 kg Slag	O ρ
ASH			80.74		20.29						
FeT	708.8	649.9	10.65	1.10	2.04		1417.5	57.4	5.13	15.72	5
FeM	708.8						708.8				
C	21.9		493.8		188.8	208.3	912.8				
Mn	2.8						2.8				
Si	10.1						10.1				
S	1.27	0.109	6.71		2.28	2.19	12.56	0.134	0.039	0.059	0.
P	5.2	0.327					5.53				
CaO		10.91	5.17	98.73	1.34		116.15	16.2	9.55	13.38	11.
MgO		2.18	0.81	0.37	0.34		3.70	6.6	3.33	5.40	4.
A l₃0₃		5.45	19.78	0.74	5.68		31.65	10.2	2.92	4.62	3.
SiOs		70.91	39.15	4.05	9.64		123.75	25.9	9.83	13.5	10.

INPUT

    Iron units from (i)   **SHOT Fe^ = 708.8 kg**

             (ii)   **ORE FeT = 643.9**   ▶ SS1.65

             (iii) **COAL,FeT = 11.75**
                etc.

OUTPUT

    Assume shot remains as shot

    Metallic Iron Weighed =   **1273.okg** – w 708'8 **kg (SHOT)**

    Iron Assoc, with Slag =   **131.04 kg**   **kg (ORE)**

    Iron Unaccounted for =   82.86 kg

Weighed Yield = 56~4.8 x 100 = 7 9 ⁒
$$\frac{}{6 \; 61.65}$$

6.8.3   Experiment No. 122

This ironmaking experiment lasted for 9.5 hours, with continuous

feeding except for the normal stoppages required during surge casting,

Figure 42.   The feed rates were very close to their intended values,

except that the ore feed rate was slightly low at 330 kg/h rather than

the intended 341 kg/h.   A total of 2549 kg of iron ore was charged before

the experiment was terminated.

Bed temperatures monitored during the experiment varied between 1 500

and 1 600 $^{\circ}$C, except for the usual apparent temperature troughs occurring

during surge casting.   The exhaust gases contained 48 to 60% CO_2, 24 to

30% CO, low nitrogen levels of 4 to 14% and up to 3% oxygen.   Four surge

casts were carried out during the experiment, the first one immediately

yielding 94 kg of slag and 130 kg of metal followed by a further 125 kg

of slag and 10 kg of metal, these latter quantities having been delayed

temporarily on the inner surfaces of the cast end chamber.   The three

remaining surge casts followed a similar pattern although the second

and fourth surge casts produced only slag.   Five bed samples were taken

during the experiment, their iron contents varying between 10.8 and 12.5%.

The experiment came to an abrupt halt with the total collapse of the feed

end dam, whereupon much of the bed contents were discharged into the feed

end chamber.   The emergency shut down procedure was put into operation

and the remaining bed contents were discharged into the cast end chamber,

630 kg of metal and 50 kg of slag being collected in this way.   A second

bed collapse was then carried out, a further 85 kg of metal and 165 kg

of slag being removed.   Subsequently, 950 kg of metal were extracted

from the feed end chamber but no slag.   Not all the material cast during

the emergency shut down procedure had been collected in the casting boxes

then in place and a further 50 kg of metal had also to be extracted from the casting box support ring.

The separate amounts of material collected during the experiment together with their analyses, are shown in Table 6.8, as are the analyses of the bed samples. The mass balance for the experiment is shown in Table 6.11. It showed that 161.5 kg of iron could not be accounted for, but that 1138.7 kg of iron had been produced from the charged ore, representing a weighed yield of 69%. If it is assumed, as is likely, that the iron unaccounted for represents relatively finely divided metal that could not be extracted after the experiment's abrupt termination, then the calculated yield of iron from the ore is increased to 79%, a figure more in keeping with the slag analyses obtained from the bed samples.

F I G U R E 4 . 2   EXP. 122

Rate of Raw Material Addition* kg/h			Coat addition afref swr^e.	
Ore	330–	322-		■330
Coal	-244-	246		247
P.F.	86	-7 2	K	-9 2-

ACCUMULATIVE WEIGHT, kg

2S00

2000   Acc. Ore wgt kg
             A«-c. Coal W$t Kg
1500   Acc. P.F. wgt. kg   981

1000   750 kg Iron Shot   516

500 -   T80

                              m

Time of Bed Sample and Analysis,*4 FeT   {B S1 at 15.3 7. | в S 2 at 10.8 *4

Time of Surge Cast   Surge 1

Description of Output   Surge   Dribbles
                                                                 Cast

Weight of Slag, kg   125

Analysis,*/. FeT   447

Weight of Metal,kg   T30

L   1   1

1700   BED SURFACE TEMPERATURE

1600

1500
*C
1400

1300

i?oo4
   9.00   9.30   10.00   11.00 · 11.30   11.30   1200   1230   13.00   13.30   14.00   14.30   15.00

EXHAUST GAS ANALYSIS
60

        CO
7.
   36

9.00   930   10.30   11.00   1130   12.00   12.30   13.00   13.30   14.00   14.30   15.00
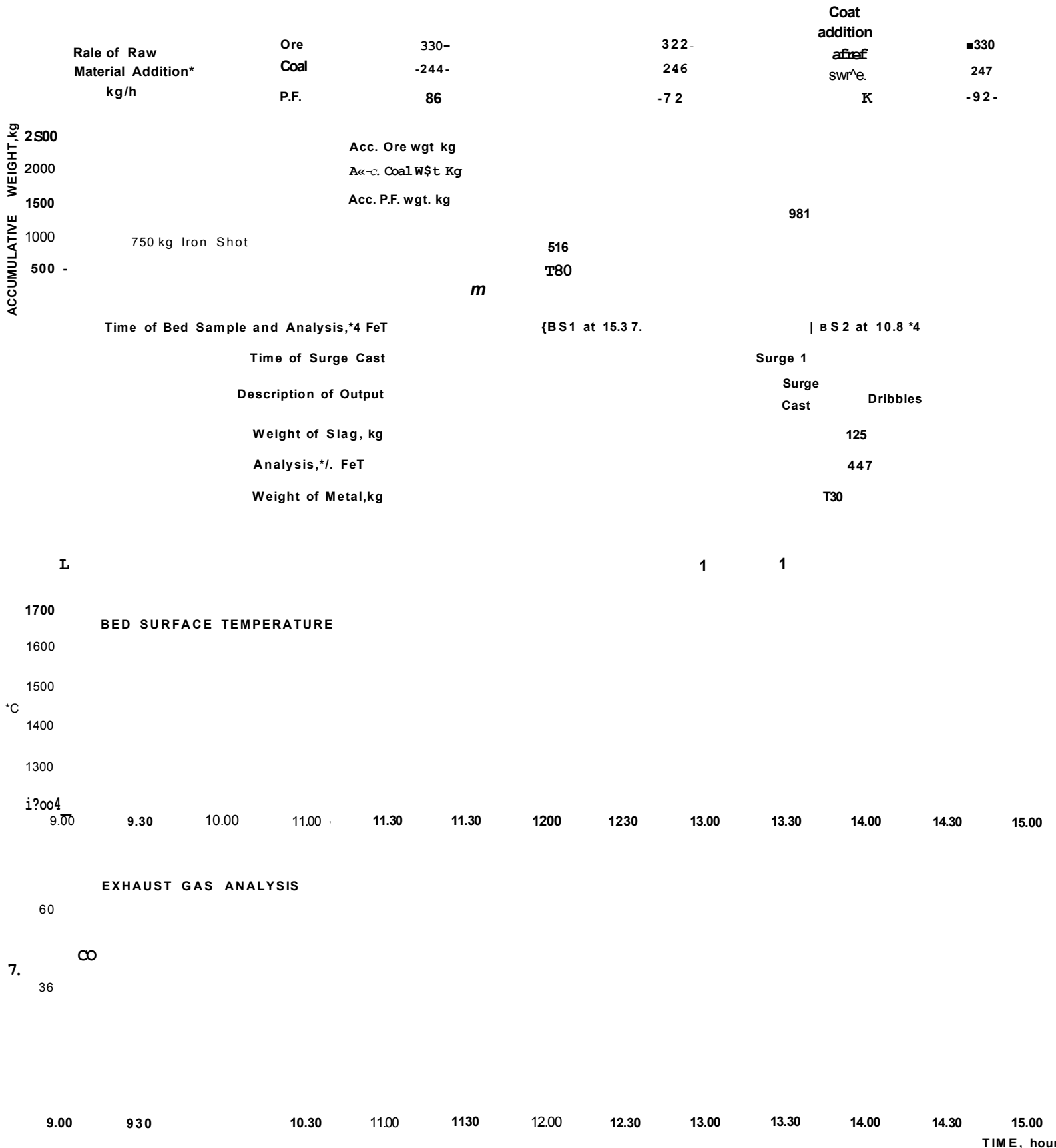   TIME, hour

148

TABLE 6.8

EXP. 122

AIM	To reduce iron ore continuously for a period of 10 hours using the same opera
	parameters as in EXPT 119.

INPUT RATE:-	ORE RATE kg/h	COAL RATE kg/h	CaCO$_3$ RATE kg/h	P.F. RATE kg/h	INDICATED OIL RATE g/h
DESIRED RATE	341	249	60	100	15
ACTUAL RATE (AVERAGE)	330	245	60	90	15
TOTAL ADDITION	2 549 kg	2 107 kg	460 kg	784 kg	750 kg 150 kg

OUTPUT OF MATERIAL	DESCRIPTION OF MATERIAL	TIME OF OUTPUT h	WEIGHT CAST kg		C	Si	S	P	
	Bed Sample No 1	12.00		SLAG			0.115		1
	Bed Sample No 2	13.41		SLAG			0.174		1
	Surge Cast 1	13.45/13.50	94	SLAG			0.015		4
			130	METAL	0.014	<0.01	0.13	0.27	
	Dribbles after Surge	13.50/14.00	125	SLAG			0.068		4
			10	METAL					
	Bed Sample No 3	15.34		SLAG			0.095		1
	Surge Cast 2	15.35/15.45	120	SLAG			0.012		1
	Natural Surge	15.45/15.52	106	SLAG			0.014		1
	Remelt	15.52/16.15	75	SLAG			0.015		4
	Bed Sample No 4	17.18		SLAG			0.095		1
	Surge Cast 3	17.20/17.28	62	SLAG			0.028		1
	Natural Surge	17.28/17.35	117	SLAG			0.046		1
	Remelt	17.52/18.07	54	SLAG			0.087		4
	Bed Sample No 5	18.44		SLAG			0.117		2
	Surge Cast 4	18.47/19.00	118	SLAG			0.014		1
	Natural Surge	19.00/19.05	85	SLAG			0.094		1
	Remelt	19.07/19.26	50	SLAG			0.046		3
	Total Bed Collapse	20-10	50	SLAG			0.17		3
			630	METAL	0.009	<0.01	0.25	0.027	
	2nd Bed Collapse	20-40	165	SLAG			0.024		3
			85	METAL	1.61	<0.01	0.23	0.025	
					1.98	<0.01	0.25	0.026	
	Metal in Feed End Chamber from Bed Collapse		950	METAL	0.057	0.12	0.17	0.032	
	Bulk Sample of Metal from 1st Collapse (Exhaust End)				0.008	<0.01	0.17	0.021	
	Metal from Turntable		50	METAL					

YIELD	Wieghed Yield 69%

MATE

	Iron Shot					TOTAL
A51I		181.9		50.17		
Fe T	708.8	L623.7	21.0	2.76	5.0g	2364.3
Fe U	708.8			X	s	708.8
C	21.9		1112.5	467.0	444.8	2046.
Un	2.77					2.77
Si	10. 12					10.12
S	1.27	0.255	15.12		5.25 4.67	26.56
P	5.25	0.765				6.01
CaO		25.49	11.64	246.5	3.31	236.9
UgO		5.09	1.82	0.92	0.85	8.68
A1 &		12.74	44.56	1.84	14.04	73.18
SiO^		165.7	88.23	10.12	23.83 ,	287.9

INPUT
  Iron \JLnLts ftom (i)
  (li)
  (iii)
OUTPUT
  Assshot Temotin:
  Matalti-C iron "w
  Iron Assoc. witU
  ITOV\ U'Aaccou.r\te

|	44.1	129.5	55.9	10.0	22.5	17.0	33.3	19	20	12.7	15.1	18.4	628.2	59.4
Fe		129.5		10.0									628.2	
		0.02											0.06	
Uc														
Si		0.01											0.06	
	0.014	0. 17	0.085		0.014	0.015	0.011	0.017 0.054	0.04	0.016	0.08	0.023	085 1.58	0.039
		0.35											0.17	
CoO		2.8		28.2	25.7		13.44	25.7	23.9	19.7	6.91	6.3		14.4
		3. 07		21.2	21.2	2.5		31.2	31.7	21.1	5.2	8.3		9.8
	16.6		26.2			7.7 13.68	4.30		7.50		6.9	4.4		27.6
SiO			16.2			9.7		24.9	21.0	18.3				27.9

ISO

7   DISCUSSION

7.1   Scope of the Thesis

The work covered by this thesis has involved high temperature kinetic
experiments on the solid carbon reduction of iron bearing slags, room
temperature measurements of mass transfer rates, and the development and
operation of the pilot plant for a revolutionary new ironmaking process.
The development of successful operating procedures for the pilot plant
has entailed the testing and modification of a mathematical model
subsequently used to test the effects of different proposed operating
practice, as well as an extensive range of experiments carried out on the
pilot plant itself. These separate facets of the thesis are discussed
separately below and are followed by some speculation on the possible
future of this ironmaking process.

7.2   The Mechanism of the Carbon Reduction of Iron Bearing Slags

The reaction between iron bearing slags and solid carbon, as represented
by the equation:-

$$(FeO)_{slag} + C_{solid} \rightarrow Fe_{liquid} + CO_{gas} \qquad \dots\dots\dots (7.1)$$
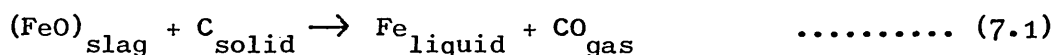
involves four phases. Simultaneous contact between three or more phases
can only be achieved along a line, and any reaction occurring by this
mechanism would be expected to be slow. Mass transport and chemical
processes may both play a part in controlling the rate of reaction,
because of the complicated nature of the reacting system, it is to be
expected that the measured rates of reaction will be strongly dependent
on the experimental conditions. The reaction is also strongly endothermic
and heat transfer into the reacting species could be important in main-
taining the reaction. However, the high temperature kinetic experiments

reported in this thesis were carried out in carbon crucibles within an induction furnace so the supply of reaction heat should not be a rate limiting factor. Also the iron product was allowed to accumulate during the course of the experiment which may have had some influence on the results. For example, Philbrook and Kirkbride[1] and Tarby and Philbrook[2] working with low iron oxide concentrations in their slags showed that the reaction rate with carbon saturated iron was higher than with graphite, thus emphasising the complication introduced when the iron product is allowed to remain.

An observation made on opening the crucibles after each of the crucible experiments in this work was that, in addition to large globules of iron at the bottom of the crucible, there were small spherical globules of iron on the slag surface and within the solidified slag, and more significantly and consistently there were many small iron droplets covering the inner surface of the carbon crucible. These were sufficient to have produced a continuous thin iron film over the crucible wall during the high temperature experiments.

There are two possible explanations for the iron globules situated in the slag and attached to the walls. The iron may have been produced by the reduction of the iron oxide in the slag or the globules may have originated in the bulk metal. In either case they were carried upwards in the slag either attached to, or as a thin film around, bubbles of carbon monoxide generated in or near to the metal phase. The distribution of the small iron globules, particularly as a thin film on the inner surface of the crucible walls, was a reproduceable characteristic of the experiments, and clearly any proposed mechanism proposed for the reaction must account for it.

In addition to the kinetic data for use in the mathematical model of C.I.P., it was hoped that the crucible experiments would yield an understanding of the mechanism of the reduction that would lead to a more accurate model simulation. If it is assumed that only two phase contact is necessary to describe adequately the reaction mechanism where there is an ample area for interaction, then there are six areas of two phase contact for the four phases shown in equation 7.1, namely the slag-carbon, slag-metal, slag-gas, carbon-metal, carbon-gas and metal-gas interfaces. An examination of the chemical reactions that are occurring at some of these interfaces, as well as the transport of reactants to them, in relation to the results of this experimental study and those carried out by other workers, may provide an understanding of the more important processes determining the overall reaction rate.

If we assume that the nucleation of liquid iron occurs easily at the slag-carbon interface, the direct reduction of liquid iron ore by solid carbon at that interface can be represented by the following equations:-

$$O^{2-} + \boxed{C} = C(O) + 2e^- \qquad \ldots\ldots\ldots\ldots (7.2)$$

and

$$Fe^{2+} + 2e^- = Fe \qquad \ldots\ldots\ldots\ldots (7.3)$$

where $\boxed{C}$ = a free site on the carbon surface for oxygen absorbtion

$C(O)$ = an oxygen atom adsorbed onto the carbon surface

Chemical reaction can continue until the carbon surface has no free sites available, i.e. it is saturated with oxygen, and to proceed further the adsorbed oxygen must react on the surface of the carbon to produce adsorbed carbon monoxide molecules. Free sites can then be

153

liberated by desorption of these carbon monoxide molecules either con-
currently with the nucleation of carbon monoxide gas, or, if a gas
phase is already present, merely by the surface diffusion of the carbon
monoxide molecules. It is possible that the desorption step could be a
rate limiting step, as found by Blyholder and Eyring[29] during their work
on the gasification of carbon by oxygen and carbon dioxide, or that the
rate could be limited by the nucleation of the carbon monoxide gas phase.
However, if the overall reaction $FeO + C = Fe + CO$ is considered to
take place with $a_C = a_{FeO} = 1$, the equilibrium pressure of the CO is
3×10^3 atm and pores as small as $60 \, \text{Å}$ could act as nucleating sites if
filled with gas and if the liquid slag has a contact angle of 140° and
a surface tension of 570×10^{-3} N/m as quoted in reference (30). Thus
it appears unlikely that it is the nucleation of the carbon monoxide gas
that is rate limiting.

Once nucleated, the carbon monoxide bubbles could grow by surface
diffusion of the carbon monoxide molecules, freeing further adsorption
sites. Any one bubble would continue to grow until large enough
to detach itself from the surface although the rate of growth might
decrease as the diffusion paths lengthen. The carbon surface freed
when the bubble detaches itself would be immediately washed with slag
so that the reaction in that area could recommence, thus giving rise to
a pulsating reaction system.

As an alternative to this system, it could be considered that small
bubbles could be detached from their initial growth points to sweep
across the carbon surface, collecting further carbon monoxide molecules
as they move. Such movement has been observed in laboratory experiments

using a mercury/perspex model, in which bubble movement was observed, not only up the vertical walls under the action of buoyancy forces, but also horizontally across the bottom of the vessel. Circumstantial evidence has also been obtained in other laboratory kinetic experiments for a mechanism involving the movement of very small bubbles. Davies et alia[8] could not observe bubbles when iron bearing slags were reacted with the coal crucibles that contained them, and concluded that the bubbles of carbon monoxide gas that they felt must be formed were too small to be observed under the difficult high temperature experimental conditions. Similarly, Shavrin[7] immersed a carbon rod into slags containing 10% FeO but could not observe bubbles escaping from the system even though carbon monoxide was formed by reaction. In a second experiment, they coated the upper immersed section of the rod with a layer of refractory cement. In this case, vigorous bubbling was observed and the graphite rod was found to be severely attacked immediately below the refractory layer. This is the point at which carbon monoxide bubbles would detach after moving up the lower section of the carbon rod. Such detachment would result in the vigorous bubbling that they observed in this second experiment, and to reaction rates sufficiently enhanced at the point of detachment by the pulsating mechanism suggested previously to give rise to the severe attack that they found. Shavrin concluded, therefore, that the reaction taking place along the carbon rod itself involved the movement of small carbon monoxide bubbles which had to detach themselves from the rod upon meeting the refractory layer.

Actual reaction areas were virtually impossible to assess in the work described in this thesis, but measurements made by Davies et alia[8] for an FeO - SiO_2 slag reacting in a carbon crucible at the lower temperature

of 1 500 °C gave a reaction rate, and therefore a CO desorption rate, of 9.5 $cm^3.s^{-1} cm^{-2}$ per unit area of the contact interface between the slag and the crucible. This compares with the maximum gasification rate of a graphite surface measured by Blyholder and Eyring[29] to be 3.7 $cm^3.s^{-1} cm^{-2}$ at 1 500 °C. Thus the desorption rate measured in the experiments of Davies et alia would be achieved if the true area of the reaction interface were no more than 2.5 times the apparent area. Since, at a pressure of 1 atm, a slag with a surface tension of 500 x 10^{-3} N/m and a contact angle of 140° would fill all surface cavities greater than 15 microns in diameter, this ratio between true and apparent reaction areas could be easily achieved. Thus the desorption of CO would appear to be an attractive possibility as the rate controlling step, but it is difficult to reconcile such a rate controlling step with the linear dependency that has been found (see section 5.1) with the FeO content of the slag. The electron transfer reaction producing the molten iron product could not either be reconciled with this linear dependency, and in any case would occur extremely quickly once the iron phase had been nucleated. Thus it can be concluded that the chemical processes occurring at the slag-carbon interface are unlikely to be rate controlling.

It is worth considering at this stage the behaviour of the molten iron product. The molten iron may form as a thin film clinging to the gas bubbles or as small droplets at the reaction sites. If the iron formed as a thin film clinging to the gas bubbles it would be carried up in the slag layer with the rising bubbles to collect as fine iron droplets on the upper surface of the slag. Eventually these droplets would coalesce and fall from the upper surface of the slag layer to settle out as an iron layer in the bottom of the crucible. However, such settlement could

never be complete and fine iron droplets would always be found at the upper surface of the slag layer. Although such droplets were sometimes found they were relatively rare. An almost complete covering of iron droplets was, however, always found over the surface of the crucible in contact with the slag, so it was concluded that the iron formed as fine droplets at reaction sites on the crucible surface. The occasional droplets found on the upper slag surface were thought to have been carried there after being caught up in particularly large and vigorous gas bubbles. Since the iron droplets appeared to be formed on the crucible surface, sufficient heterogeneous nucleation sites would exist there for the nucleation of iron to be easily accomplished so that this step could not be considered as the rate controlling step either.

It is possible that the behaviour of the gas could give rise to the rate controlling step. Indeed, X-ray studies[30] of the reaction between spheres of carbon and iron containing slags in which they had been immersed suggested that the spheres were shrouded in an apparently continuous gas film. Davies et alia[8] considered the possibility that the counter diffusion of CO and CO_2 across this film could be the rate controlling step, the reaction $FeO + CO \longrightarrow Fe + CO_2$ taking place at the slag gas interface, and the reaction $CO_2 + C \longrightarrow 2CO$ at the carbon gas interface. Obviously 1 molecule of CO_2 would be produced by this mechanism for each atom of iron, so that the molar rate at which iron is produced would be equal to the molar transport rate of CO_2. This latter rate would be given by Fick's first law:-

$$\overset{11}{\dot{n}}_{CO_2} = - C \, D_{CO/CO_2} \, \frac{dX_{CO_2}}{dx} + X_{CO_2} \cdot \left(\overset{11}{\dot{n}}_{CO} + \overset{11}{\dot{n}}_{CO_2} \right) \quad \cdots\cdots\cdots\cdots \quad (7.4)$$

which can be rearranged to give:-

$$\left(1 + X_{CO_2}\right) \dot{n}^{11}_{CO_2} = - C \, D_{CO/CO_2} \frac{dX_{CO_2}}{dx} \qquad \dots\dots\dots (7.5)$$

since stoichiometric considerations at the carbon surface show:-

$$\dot{n}^{11}_{CO} = 2 \, \dot{n}^{11}_{CO_2} \qquad \dots\dots\dots (7.6)$$

However, the partial pressure, and hence the mole fraction, of CO_2 would
be extremely low in any gas film that could form at the carbon surface.
Certainly the mole fraction of CO_2 in equilibrium with the carbon surface
would be $\ll 1$, and even that in equilibrium with the slag is unlikely to
be greater than 0.1. Under these circumstances, the bracketed term on
the left hand side of equation 7.5 is little different from unity, and the
equation can be integrated across the thickness of the gas film to give:-

$$\dot{n}^{11}_{CO_2} = C \, \frac{D_{CO/CO_2}}{\delta} \cdot \left\{ X^S_{CO_2} - X^C_{CO_2} \right\} \qquad \dots\dots\dots (7.7)$$

Since D_{CO/CO_2} varies as $\theta^{1.8}$, and C is given by the gas laws as:-

$$C = \frac{n}{V} = \frac{P}{R\theta} \qquad \dots\dots\dots (7.8)$$

equation (7.7) can be rearranged in the form:-

$$\dot{n}^{11}_{Fe} = \dot{n}^{11}_{CO_2} = b \, \theta^{0.8} \, X^S_{CO_2} \qquad \dots\dots\dots (7.9)$$

where b becomes an empirical constant that must be determined from the
reaction rate experimentally determined at one temperature. The results
obtained by Davies et alia[8] at 1 500 °C have been used in this way to

158

predict reaction rates at higher temperatures, these rates being shown as line 1 in Figure 43. Also shown on this diagram are the results obtained by Davies et alia at lower temperatures (line 2) and the results obtained in this work at higher temperatures (line 3).

The Figure shows that the rates predicted by equation (7.9) fall below the results obtained in this work and, even more significant, show a negative temperature coefficient at variance with both sets of experimental results. This negative coefficient arises because the CO_2 mole fraction in the gas phase in equilibrium with the slag in equation (7.9) decreases more rapidly with absolute temperature than the 0.8 power. These discrepancies between equation (7.9) and the experimental results lead to the conclusion that any mechanism involving gaseous transport across a continuous film at the reacting carbon surface cannot adequately describe the reaction mechanism.

It is possible that the reaction is controlled by the transport of Fe^{2+} and O^{2-} through the slag phase to the reaction interface, in which case the rate of the reaction would be influenced by stirring in the slag, either induced by the motion of the gas bubbles, or artificially by, for example, the rotation of the carbon surface. In either case, the reaction rate could be represented by an equation of the form:-

$$\dot{n}^{11}_{Fe} = \measuredangle \, c_{SL} \left[X_{FeO} \right]_b \qquad\qquad \dots\dots\dots (7.10)$$

in which $\measuredangle$ represents a mass transfer coefficient dependent upon the stirring intensity. If it is the escaping gas bubbles that contribute principally to the stirring mechanism, the value of this mass transfer coefficient would be expected to increase with the rate of bubble

159

FIGURE 43
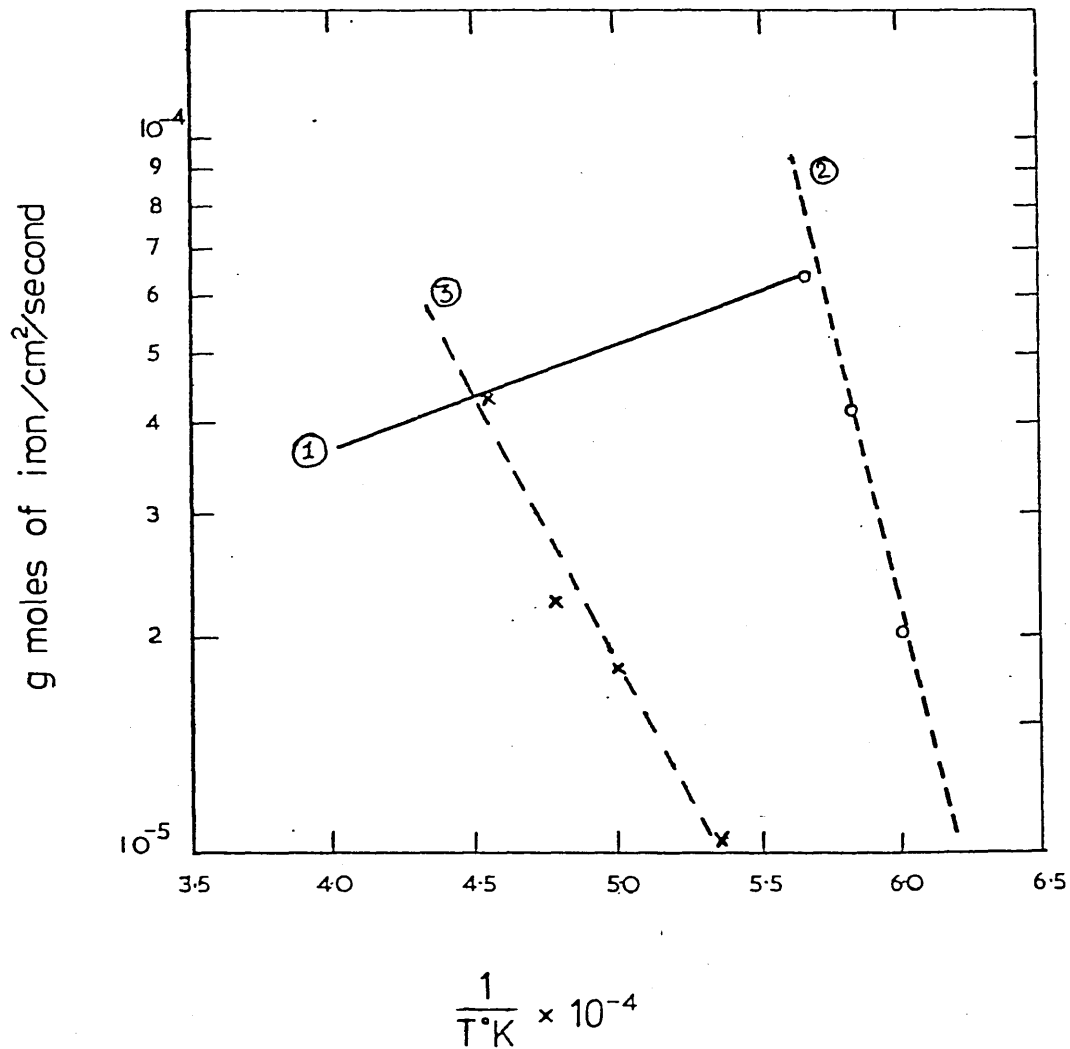
RATE OF REDUCTION TO IRON FOR REACTION
OF CARBON WITH AN Fe BEARING SLAG
VERSUS 1/TEMPERATURE

Line (1) represents rates predicted by equation 7.9.

Line (2) represents experimental rates from Davies et
alia[8] at high iron concentrations in the slag.

Line (3) represents experimental rates from the
crucible experiments.

production and hence with the rate of reaction, and thus to increase
with the FeO concentration in the slag. Hence the reaction rate would
show an order higher than unity towards the FeO concentration in the
slag. This type of behaviour has been reported at stationary carbon
surfaces by Shavrin[7] in borate slags containing 5 to 15% FeO, by Shurygin
et al[31] in calcium aluminosilicate slags containing 2 to 9% FeO and by
Fay Fun[32] in CaO - FeO - SiO_2 slags containing 1.5 to 40% FeO, although
Fay Fun report a decrease in order as the FeO content increased towards
the higher values.

If, on the other hand, mechanical stirring of the slag, produced, for
example, by rotating the carbon surface, were the major contributor to
the stirring of the slag, one would expect the order of the reaction to
be linear with respect to the FeO content of the slag, and the reaction
rate to increase with the rate of stirring. Yershov and Popova[5], working
with a rotating graphite sample, found such behaviour in slags where the
FeO content varied between 10 and 20%, whereas they found the reaction
rate to be independent of rotational speed at slag contents in the range
40 to 60%. They termed the former regime a 'diffusion regime', and the
latter regime a 'kinetic regime'. Sugata[6] also found that the rate of
rotation of the reacting graphite surface affected the reaction rate at
low FeO slag contents.

The crucible experiments reported in this thesis has also suggested that
the reaction rate varies linearly with the FeO content in the slag, but
no attempt could be made to investigate the effect of rotation.

It is difficult to reconcile the various facts known about the kinetics
of this reaction with any single mechanism. However, a mechanism that

separates in space the two reactions represented by equations (7.2) and (7.3) could go some way to explaining many of the observations. Equation (7.2) represents an anodic reaction whereas equation (7.3) is cathodic in form. It is quite possible that these two reactions could take place at separate sites on the carbon surface, electrons being transferred through the carbon itself from anodic regions to cathodic regions. Such a mechanism would certainly require all the metallic iron to be formed on the carbon surface and would thus explain the extensive cover of fine iron drops over the inner surface of the carbon crucible that was always found in this work, these iron droplets forming at cathodic regions on the wall of the crucible. The carbon monoxide gas would obviously form at the anodic sites where the concentration of oxygen atoms adsorbed onto the carbon surface is at its highest. There would be no normal reason for any large separation between the anodic and cathodic sites, so that the reacting surface of the carbon could be regarded as being covered with fine growing droplets of iron interspaced between growing CO bubbles. Under the relatively poor resolution provided by an X-ray system such a reaction surface could easily appear to be surrounded by a halo of gas, indeed by an almost continuous gas film, as has been reported by Alexander and Hazeldean[30].

The recognition of separate anodic and cathodic areas could also explain the variations in the influence that stirring has on the rate of the reaction that seem to be produced by differences in the FeO content in the slag. Obviously a balance would have to exist between the relative sizes of the anodic and cathodic areas and this balance would be disturbed as the reaction rate was increased - because the gaseous product formed at the cathodic areas occupies a relatively large volume and will also

tend to blanket the reaction surface. When the FeO content in the slag layer is low, the rate of production of CO can be controlled by the transport of O^{2-} ions to the anodic regions where small bubbles of carbon monoxide would form offering very little blanketing effect to the reaction surface. Under these conditions, the rate of reaction would be linearly dependent upon the FeO content in the slag, and also dependent on the intensity of the stirring mechanism. Depending on the relative importance of stirring induced by the bubbles by mechanical means, such as rotation or natural thermal convection, the final overall dependency on the FeO content would be first order or greater, as has been found in a number of the separate investigations discussed above.

At higher FeO contents the greater rates at which O^{2-} could be transported to the anodic regions could result in the growth of larger and larger CO bubbles which could have such a strongly blanketing effect that they would impede the reaction. Under these conditions, the reaction rate would be determined by the rate at which the gas bubbles could escape from the reaction surface, and would thus be independent of stirring conditions in the slag, as was reported by Yershov and Popova (see above) for slags containing 40 to 60% FeO. This blanketing effect at the higher FeO contents would also give rise to variations in the slope of plots in which the logarithm of the fractional extent of reaction is plotted against reaction time (see equation 5.11) and Figure 4. Figure 4 shows that this type of behaviour was found in this work for slags which initially contained 60% FeO and, indeed, it was not until a considerable amount of reaction had occurred that the slope of the plots for these more concentrated slags became equal to the slopes determined throughout the experimental time for the slags initially containing 30% FeO.

Thus a mechanism involving separate anodic and cathodic sites together with a blanketing of the reaction surface at high slag FeO contents is quite compatible with the observation made in this work at temperatures up to 1 800 ^{o}C. It is also compatible with the interesting observation made by Shavrin[7] when he coated, with refractory cement, the upper portion of a carbon rod immersed in an FeO containing slag. Reference has already been made to this experiment and to the fact that very heavy attack was found to occur on the carbon rod immediately below the refractory layer. If, as is likely at the temperatures involved in the investigation, the refractory cement had sufficient electrical conductivity to serve as a cathodic area for the discharge of Fe^{2-} ions, the surface of the carbon rod directly exposed to the slag immediately below the coated section would act as an intense anodic area for the large cathodic area above it. Consequently, very heavy and intense attack would occur at this point, as was reported by Shavrin.

Another important feature of the mechanism proposed is that the blanketing effect of the carbon monoxide gas would become more severe, not only as the FeO content in the slag increased but also as the temperature increased. Indeed it would be expected that very high rates of reaction taking place at high temperatures could give rise to the formation of a foam in the slag which could completely blanket the carbon surface. The existence of such foams has been reported by Shavrin, and was found in the crucible experiments at temperatures in the region of 1 800 ^{o}C. In both cases, of course, the existence of the foam rendered any meaningful kinetic measurements impossible. The onset of foaming in the slag at higher temperatures would, of course, completely change the kinetics of the reaction. One would expect that any temperature coefficient established for the rate of the reaction at lower temperatures would cease

164

to apply once foaming became prevalent, and that it would be the behaviour of the foam that would determine the rate of the reaction. Since the maintenance of the foam depends upon the continuation of the gas producing reaction that the foam is itself impeding, the foam would tend to stabilise a constant reaction rate. Any increase in the reaction rate would increase the volume of gas entrapped in the foam and hence its blanketing effect on the reaction surface. The result would be a decrease in the reaction rate and hence a constant rate would tend to be established.

The existence of these foaming conditions at temperatures in excess of 1 800 ^{o}C will be referred to later. For the now, however, it can be concluded that a reaction mechanism involving separate anodic and cathodic areas with gas blanketing limiting the reaction rate under the more reactive conditions explains the observed reaction behaviour more satisfactorily than any other mechanism that has been proposed.

7.3   Convective Heat and Mass Transfer in the Reactor

The coal burning inside the reactor produced a highly luminous flame so that radiative heat transfer was far and away the most important mechanism for heating the rotating bed. Convective heat transfer thus had very little influence on the operating performance of the reactor, as discussed in section 4.1 dealing with the mathematical model. Convective processes were important, however, since it was convective mass transfer that controlled the transfer of oxidising gas to the coke bed, and the removal of gaseous reduction products from the bed.

The convection process in the reactor is extremely complex since flow conditions in the gas phase are determined both by the joint impulse

165

provided by the burner and oxygen jet and by the shearing produced by the rotation of the reactor itself. Although an empirical approach to the complexity of this problem had been adopted in the mathematical model, separate mass transfer experiments on a model of the reactor were conducted to provide independent data for comparison. These experiments have been described and analysed in section 5.2 where the following equation was developed for the mass (and heat) transfer j-factors in the reactor:-

$$J_D \left(= J_H\right) = 20.3 \left(1 + 0.11 \, Re_r^{0.2}\right) Re_p^{-\frac{2}{3}} \qquad \ldots\ldots\ldots\ldots (7.11)$$

In using this equation to estimate mass transfer coefficients in the reactor, it has to be realised that steady velocity profiles cannot become established in the short length of the reactor. Indeed, since virtually all the longitudinal momentum is provided by the burner and secondary oxygen jets, whose combined cross sectional areas are certainly not more than 5% of the cross sectional area of the reactor, gas flow down the reactor will involve considerable axial recirculatory flows. These flows were replicated in the model mass transfer studies since the air used as the mass transfer fluid entered the model through a model burner jet. The size of this jet was determined using the Thring and Newby[11] geometric similarity criterion as modified by Bacon[10] for air flow experiments (see sections 2 and 5.2.2). Once this modification has been made, it is the total momentum flow along the reactor which describes the nature of the axial flow, the Reynolds number in the burner jet itself having been modified.

Reynolds number can be considered to be a measure of the ratio between

momentum flow and frictional force:-

$$Re = \frac{u \rho d}{\mu} = \frac{u^2 \rho (d^2)}{u \frac{\mu}{d} (d^2)} \qquad \qquad \dots\dots\dots\dots (7.12)$$

so that the appropriate Reynolds number to describe the axial flow

field in the C.I.P. reactor is one calculated assuming the total momentum

flow to be uniformly distributed across the reactor. In the model

experiments, this Reynolds number can be calculated by assuming that

the air entering the model burner is immediately uniformly distributed

across the tube of model reactor. In the C.I.P. reactor itself, however,

only the burner fluid and the secondary oxygen carry momentum into the

reactor. Here, therefore, axial flow Reynolds numbers are to be cal-

culated assuming that it is only the mass flows of these fluids that

are to be used in calculating values of Re_p.

Throughout the experiments on the C.I.P. reactor, the flows of oil and

oxygen were assumed constant at 20 gal/h and 200 m_N^3/h respectively,

whereas the flow of the secondary oxygen varied between 140 to 200 m_N^3/h.

The viscosity of the gases within the reactor was calculated from stan-

dard references on gas viscosities summarised in reference (33), assuming

the reactor gases to be a 1 : 1 : 1 : : CO_2 : H_2O : O_2 mixture at

2 000 $^{\circ}$C, this gas composition having been chosen from stoichiometric

considerations. These mass flows and gas viscosities gave axial flow

Reynolds numbers in the range 4 000 to 5 000. No problem was posed by

the calculation of Re_r for the C.I.P. reactor. The standard operating

speeds of the reactor varied between 160 to 180 rpm and these speeds

were used together with densities and viscosities of the gas mixture

specified above to calculate that the rotation Reynolds number varied

in the range $6400 < Re_r < 7200$. Substitution of these values into equation (7.11) gave j-factors varying between 0.11 and 0.13. The average mass velocity of the gases in the reactor as well as their density and Schmidt number are required to calculate the mass transfer coefficients from these j-factors using equation (5.14):-

$$j_D = \frac{h_D}{U} \, (Sc)^{\frac{2}{3}} \qquad\qquad \dots\dots\dots (7.13)$$

Once again, since it is the average momentum flow that determines the velocity patterns in the gas that fix the value of the mass transfer coefficient, the mass velocity, U, appearing in equation (7.13) is that obtained by averaging the burner and secondary jet flows over the cross section of the reactor. As before the density and the property values from which the Schmidt number was calculated, were obtained from standard texts[33] for the gas mixture specified above.

Mass transfer coefficients calculated in this way varied in the range $0.48 \text{ m.s}^{-1} < h_D < 0.51 \text{ m.s}^{-1}$.

As explained in sections 4 and 5.2.3, the mathematical model calculated mass transfer coefficients from the pipe flow equation, equation (4.3), which gave values for the Nusselt number, and then calculated mass transfer coefficient values using standard correlations for the variation of diffusion coefficient with temperature. It was difficult to ascertain the actual mass transfer coefficient values used in the mathematical model since the computer print-out included neither the mass transfer coefficients used, nor the Reynolds numbers that it assumed to apply within the reactor. However, as explained in section 6.6.1, the values generated were too low, and realistic predictions of

the reactor behaviour were only attained when the mass transfer

coefficients generated by the model was multiplied by a factor in the

range from 5 to 10.

It is, then, only possible to estimate the mass transfer coefficient

values that gave satisfactory predictions of the reactor's behaviour.

The model calculated Reynolds numbers using all the mass flow of gas

generated within the reactor, some four times the mass flow used to

calculate Re_P above, which would give a Reynolds number round about

16000. The model also generated extremely high gas temperatures - in

the region of 2 900 K which would give CO/CO_2 diffusion coefficient

values of about $8.6 \times 10^{-4} \, m^2 s^{-1}$. Thus the 'pipe flow equation' would

give mass transfer coefficient values of about $0.05 \, m.s^{-1}$, so that the

application of the multiplying factor that was found to be necessary

on applying the mathematical model would have produced mass transfer

coefficient values fairly close to the values predicted from the j-

factors determined from the model experiments.

7.4   The Use of Factorial Experiments to Improve the

        Mathematical Model

Before the work described in this thesis was begun, the validity of

the mathematical model had been accepted without question. It had been

seen as the tool from which to predict the plant operating conditions

that would result in maximum yield but had failed in this role. Only on

one run had the process produced any iron, and even then the small yield

obtained could not be related to the predictions of the mathematical model.

In effect, the factorial experiments reversed this original approach.

Instead of using the mathematical model to predict the plant operating

conditions that would result in a given level of plant performance, the model was used to predict the plant performance given the operating conditions and these predictions were then tested by comparison with the plant performance actually achieved, the purpose being to test and improve the mathematical model.

At first sight, this might have appeared an over ambitious aim. The mathematical model depended on a great deal of assumptions and contained many parameters whose values had to be assumed from scant evidence. The process itself was extremely complex, this, of course, being the principle reason for the complexity of the mathematical model. Thus it might have appeared that mere comparison between the performance of the plant and the predictions of the mathematical model would be too crude a tool to allow the testing of individual assumptions made in constructing the model or of the individual values assumed for particular parameters.

In the event, the factorial experiments proved an effective means of improving the mathematical model. Apart from the fact that iron was eventually produced continuously under conditions that had been predicted by the improved model, this work has provided two independent assessments of the effectiveness with which the factorial experiments allowed the testing and improvement of individual assumptions made in the model.

In order for the mathematical model to make predictions that agreed sensibly with the results of the factorial experiments, it was found necessary to assume that the rate of the reaction between the solid carbon and the FeO containing slags followed the Arrhenius relationship

up to 1 800 $^{\circ}$C, but that any further increase in reaction rate was abruptly terminated. This is fairly unusual behaviour but does tie in with observations made in the crucible reaction rate experiments described in section 5.1. These experiments could not be carried out at temperatures above 1 800 $^{\circ}$C because the crucibles became filled with a reacting foam which then overflowed from the crucibles into the experimental furnace, rendering continuation of the experiments imposs-ible. The foam was obviously produced by the CO gas liberated by the reaction, in a way analogous to the foam produced in the LD steelmaking process. In that later process, the rate of reaction is constant during the foaming period and this has been attributed to the impedance offered by the gas bubbles to the passage of oxygen ions through the slag to sights where they can react with carbon[35]. It would seem even more likely that a similar impedance would be offered by CO bubbles in the C.I.P. process to the transport of oxygen ions through the slag to carbon surfaces at which reduction was taking place. Once the slag started to foam, this impedance would certainly stop any further increase in the reaction rate since any increase in reaction rate would cause an increase in the gas fraction in the foam and a resulting increase in the impedance offered to the passage on oxygen ions. This increased impedance would result in a fall in the rate of reaction so that the presence of the foam would result in a 'negative feed-back mechanism' that would tend to maintain the reaction rate constant, more or less independent of temperature. The fact that this type of behaviour had to be assumed in the mathematical model before it produced predictions that agreed sensibly with the plant performance is in keeping with the observations of foam formation made in the crucible experiments. More significant is the fact that these

observations showed foam formation to become significant at 1 800 $^{\circ}$C - the self same temperature independently chosen as the result of the factorial experiments as the temperature in the mathematical model at which the reaction rate ceased to increase further with temperature. Thus the factorial experiments can be seen to have been sufficiently sensitive to test this particular individual assumption made in constructing the model. As further evidence it is worth recording that visual observations made under the difficult conditions of plant operation hinted at the formation of foaming slag in those runs that resulted in high iron yields.

Another parameter that was found to be critical in the testing of the mathematical model was the mass transfer coefficient from the gas phase in the reactor to the surface of the carbon bed. The evaluation of this parameter from the results of the model test involving the evaporation of naphthalene has been discussed in the previous section. There it was shown that the value of the mass transfer coefficient determined by extrapolation from these room temperature tests was about 0.5 m.s^{-1}. This value, however, was not used in the mathematical model since a fundamentally different approach to mass transfer had been built into the model from the outset - using the pipe flow equation to predict the mass transfer coefficient. In order to fit the predictions of the mathematical model with observed plant behaviour, it had been found necessary to multiply the pipe flow coefficient generated by the model by an arbitrary weighting factor, a value somewhere between 5 and 10 being found to be the optimum. As explained in the previous section, these values would provide the mathematical model with a mass transfer coefficient somewhere in the range 0.25 m.s$^{-1} < k < 0.5$ m.s^{-1}.

Once again, the similarity between the value found from the factorial experiments to be the most satisfactory value to use in the mathematical model and the value calculated from the completely independent room temperature mass transfer experiments, indicated that the factorial experiments provided an effective technique for testing and improving this individual assumption made in constructing the mathematical model.

These two particular examples showed that testing the mathematical model against the results of the factorial experiments proved to be an effective way of elucidating the values of individual parameters used in describing the actual process. The overall effectiveness of the factorial approach was, of course, shown by the fact that it led to continuous operation of the plant and to the continuous production of iron, as will be described in the next two sections.

7.5   The Planning of the Continuous Experiments

The continuous experiments and the results obtained from them are described in sections 6.7 and 6.8 respectively. In this section, the choice of the conditions for these continuous experiments is discussed together with the relationship between this choice and the previous experimental and theoretical results.

The aim was to choose a set of operating conditions that would not hinder continuous operation either due, on the one hand, to freezing of the bed, nor, on the other, to conditions so oxidising that they would preclude the formation of iron. Furthermore, the operating conditions had to be such that the manufacture of iron at high yield could be maintained over the total period of the 'continuous' experiment.

Examination of the results of the factorial experiments and of the

predictions made from the mathematical model, improved in the light

of the factorial experiments, had suggested that the process was highly

sensitive to changes in input rates of coal and oxygen, and relatively

insensitive to changes in the input rates of oil and pulverised fuel.

However, each input was examined in turn, in the light of the factorial

experiments and using the mathematical model, in order to elucidate its

optimum value for plant performance.

Thus it was found that coal inputs greater than 300 kg/h produced a

thick coal bed which impeded heat transfer so that the slag layer

became liable to freeze and low yields would certainly be obtained.

On the other hand, coal inputs less than 220 kg/h resulted in con-

ditions sufficiently oxidising for no iron to be produced. These two

extremes suggested that the optimum conditions would coincide with a

coal input rate of 260 kg/h but a final decision was not made until

the optimum oxygen input conditions had been considered.

Oxygen input levels in excess of 400 m_N^3/h always resulted in very

high gas temperatures and oxidation of the bed. Oxygen levels below

350 m_N^3/h, on the other hand, always resulted in conditions where the

bed temperatures were so low that solid rings of slag and iron were

likely to build up on the inside of the latter half of the furnace.

Once again, the mean of these two values was not necessarily the

optimum because of interactions between the oxygen and coal input rates.

The input rates of oil and pulverised fuel had been shown to have

relatively little effect on the performance of the plant. In fact,

the oil input rate had almost no effect whatsoever, so the mean rate

174

used in the factorial experiments was chosen as the input rate in the continuous experiments. The input rate of the pulverised fuel, on the other hand, had a greater effect in that rates below 45 kg/h seemed to reduce heat transfer rates from the gas phase to the bed sufficiently for solid rings to form within the furnace, whereas the process performed adequately at almost any rate above this value.

However, it was the oxygen and coal input rates that had the greatest influence on the performance of the plant so several combinations of these rates were tried in the mathematical model in order to find the optimum combination. In the event, this combination did not involve the mean values of the two input rates, but a coal input rate of 237 kg/h was chosen together with an oxygen input rate of 360 m_N^3/h. These conditions coincided almost precisely with a set of conditions used in one of the factorial experiments, where a good yield had been obtained but at the expense of a slightly low bed temperature. In order to counteract this low temperature, then, it was decided to carry out the continuous experiments at these coal and oxygen input rates but to increase the pulverised fuel input rate to 75 kg/h and to adjust the balance between the primary and secondary oxygen flows, 15% more oxygen being sent down the secondary oxygen lance.

Examination of the results of the factorial experiments had also shown that the use of variable speed stirring significantly improved the yield of the process, other conditions being kept constant. Thus the decision was made to carry out the continuous experiments under variable speed stirring in spite of the engineering difficulties entailed.

The first two continuous experiments were conducted under the conditions determined in this way except that control difficulties did not allow the pulverised fuel rate to be reduced below 100 kg/h. Bed temperatures achieved in the two experiments proved adequate, but the iron yields were not as good as had been hoped. It was therefore decided to increase the coal feed rate to 250 kg/h to increase the yield. It was felt that this could be done without cooling the bed too much because the additional pulverised fuel should be sufficient to maintain bed temperatures sufficiently high to avoid the build up of solid rings. The results of the continuous experiments described in section 6.8 showed these expectations to be borne out.

7.6   The C.I.P. Process

7.6.1   Performance in the Continuous Experiments

C.I.P. - the Centrifugal Ironmaking Process - had been designed to operate continuously. The three continuous experiments, conducted under the conditions discussed in the previous section, did, in fact, represent the first test of the plant's ability to operate for long periods of time and thus represented the first real test of the plant's design. Although some of the design aspects tested in this way had been determined prior to the start of the work covered by this thesis, it is pertinent to use this opportunity to review the operation of the plant and of its ancillary equipment under continuous conditions. This review will be carried out in three sections dealing with the ancillary engineering equipment, the design of the reactor itself, and the functioning of the ironmaking process within the reactor.

7.6.1.(a) Ancillary Engineering Equipment

The ancillary engineering equipment performed in a fairly satisfactory

manner. Concern before the continuous experiments were started that the rotating gear would be unable to stand up to the continuous accelerations and decelerations involved in variable speed stirring proved unfounded. Similarly, the twin mechanisms for the continuous monitoring and feeding of solid materials to the furnace had not been operated in tandem before, and the entire solids handling equipment had not been required to handle such large total quantities of material. Fears that this equipment might fail under long term operation were also shown to be unfounded. On the other hand, the continuous experiments showed that the water cooling circuits to the various water cooled probes and cooling jackets could become blocked as fine scale particles built up in the circulating system. However, each probe or cooling jacket had been provided with a double filter system allowing one filter to be removed for cleaning whilst the other filter remained in operation. This arrangement allowed the filters to be cleaned at adequate intervals so that water cooling could be maintained.

The gas analysis probe and the suction gas pyrometer became rapidly blocked from the finely divided ash dust in the furnace atmosphere. Whereas it was normally found possible to clear the gas analysis probe by reversing the gas flow along it, or by 'rodding out' in extreme cases, the suction pyrometer became blocked so rapidly that gas temperatures could never be measured. The performance of the gas analysis probe can be seen in the results section, section 6.8, where gaps exist in the continuous gas analysis record.

The continuous experiments, inadvertently, provided a test for the emergency shut down procedure, and for safety features that had been

incorporated into the original design. The test was occasioned when the feed end dam failed during run 122 so that molten material started to cast backwards into the feed end chamber. The emergency button which maintained rotation but caused all probes to be withdrawn and all feeds to be arrested and replaced by purge nitrogen or air was satisfactorily activated and the furnace brought to a standstill under manual control. The emergency hearth constructed into the feed end chamber proved adequate to hold the molten material that drained from the furnace, and the air and nitrogen purges proved adequate to ensure that dangerous levels of carbon monoxide did not build up on the operating platform.

7.6.1.(b) The Design of the Reactor

One of the basic design features of the C.I.P. reactor was that its refractory lining should be protected from slag attack by the layer of molten iron maintained against the lining by the centripetal pressure developed by rotation. Examination of the lining after the continuous experiments showed that this protection mechanism had worked in a highly effective manner. The only damage to the lining that could be observed was some minor spalling resulting from the emergency shut down procedure that had to be applied at the end of run 122.

The refractory dam at the casting end fared nothing like so well, unfortunately. After all experiments, the dam was so eroded that further operation of the reactor had become highly problematical, this erosion being due to slag attack since the molten iron layer could not be used to protect the dam in the same way that it protected the rest of the refractory lining. A further problem had been noted with the cast end dam, although this did not become manifest during the continuous experiments. The cast end dam could not be secured by a steel

retaining ring at the outer end of the reactor, as could the feed end dam, because the operating temperature in the casting chamber was too high. Thus retention of the cast end dam against the expansion forces generated as the remaining refractory lining heated up depended entirely on the quality of the keying achieved when the cast end dam was built, or rebuilt. A new proposed design that will surmount both these problems will be discussed in section 7.6.3.

The general design of the casting chamber did not prove satisfactory. Molten material could be cast from the reactor itself with relative ease, but a substantial proportion tended to solidify within the casting chamber, frequently in a finely divided state against the walls and roof of the chamber. This material would then reoxidise because the atmosphere within the casting chamber was considerably more oxidising than that at the end of the reactor, this reoxidation naturally reducing the yield of the process.

The continuous experiments naturally offered the first process test of the surge casting technique that had been developed in model studies (see section 6.3.5). In the event, the technique proved an initial disappointment since it tended to demolish the entire carbon bed, cast slag out of the furnace in preference to iron, and to drag unreacted slag from the feeder end of the furnace. However, the continuous experiments in themselves offered limited scope to gain operating experience of the technique and it is likely that further experience will allow improvements to be made in the control that can be exercised during surge casting.

7.6.1.(c)   Performance of the C.I.P. Process

The continuous experiments indicated that the C.I.P. process was capable of steady operation and, although the supply of raw materials had limited the experimental time to a maximum of ten hours, the process itself showed all the characteristics of being able to achieve true continuous operation. Since the experiments did not suffer from the build up of solid rings or from overoxidation, it appeared that the operating conditions chosen from the factorial experiments and the mathematical model came close to those under which the process could be operated as an efficient continuous iron producer.

Although the conditions under which the continuous experiments were carried out were chosen to produce high yields of iron, the large quantities of iron actually produced did allow some examination to be made of its quality. Carbon and sulphur levels were therefore determined in the iron that was discharged from the casting chamber during a casting surge or was obtained from the final bed collapse at the end of one of the experiments. Experiments 118 and 119 were carried out under more or less identical input conditions and the surge cast and end cast iron obtained contained carbon contents varying between 0.56% and 0.87%. This appearance of regular operation was not, however, borne out by experiment 122 which showed very much lower carbon concentrations, varying in the range 0.01 to 0.057%. Although this was the experiment in which the feed end dam collapsed, it also differed from the previous experiments in that the proportion of oxygen fed along the secondary lance was increased by about 15%. Since this would result in the establishment of more oxidising conditions towards the discharge end of the furnace, it is possible that this change in

operating conditions has resulted in the very much lower carbon levels. That such a relatively small change in operating conditions could result in a significant change in carbon levels in the iron is in keeping with the narrowness of the band of operating conditions within which the process can operate satisfactorily.

Sulphur levels in the iron, on the other hand, were found to be much more consistent, varying between 0.13% to 0.25% and were thought to be more or less entirely determined by the sulphur content in the coal used in the process.

FeO contents in the slag discharged from the furnace during the casting surges and the end collapses tended to be fairly high, giving total iron contents in the range 15% to 30%. On the other hand, the FeO contents of the slag removed by sampling from the discharge end of the bed tended to be significantly lower, in the range from 5% to 20%. This is in keeping with the observation made in a previous section that the surge casts tended to drag out unreacted slag from the charge end of the furnace, and does indicate that a graduation of FeO contents in the slag could be set up within the process reactor.

MgO levels in the slag during experiments 118 and 119 remained fairly steady at 10% indicating regular wear of the cast end dam. This wear has been mentioned in the previous section where it was reported that the cast end dam had become severely eroded by the time these experiments were completed thus providing the source for the MgO in the slag. That this is the most likely explanation for the high MgO contents in the slags can be ascertained from experiment 122 in which the feed end dam collapsed due to slag attack and in which the slag contained 20% MgO.

The composition of the furnace gases remained fairly steady throughout the continuous experiments, apart from the periods in which blockage of the gas analysis probe precluded the obtaining of gas samples. Nitrogen levels in the furnace gases were about 20%. Such high levels could only be explained if the water seal at the feed end of the vessel was not quite complete, thus allowing the leakage of air into the reactor.

7.6.2   Guidelines for Operating Practice Established in this Work

As a result of the experiments that have been carried out in this work, a number of guidelines can be established for the successful operation of C.I.P. plant of the size of the pilot scale vessel.

The maximum rate at which the vessel can be warmed up prior to an experiment is 50 $^{\circ}$C/h, and the maximum cooling rate after an experiment is 60 $^{\circ}$C/h both these warming up and cooling down periods to be carried out with a vessel rotation speed of 135 rpm - the lowest possible speed at which an effective water seal can be maintained.

The depth of the bed of molten iron maintained inside the reactor is a critical parameter and this is more or less completely determined by the height of the cast end dam. A dam height greater than 75 mm results in a layer of molten iron that is not gravitationally stable at the casting speeds used in these experiments. If the dam height should be less than 50 mm, the capacity of the reactor to retain molten iron becomes so small that the discharge of molten iron would have to be carried out almost continuously.

The feed rates used in the continuous experiments, and specified in section 6.7, were found to be close to the optimum, but the spread of

the solid materials feed within the furnace is also extremely important. Separate trajectories are needed for the ore and for the coal/limestone mixture. For the ore, the ideal spread is from 0.25 m to 1.5 m, and for the coal/limestone mix it is from 0.25 m to 1.8 m. Flat trajectories are required for both materials in order to avoid carry over resulting from the solids being caught in the main gas stream through the furnace.

In order to get adequate reaction rates it is necessary to use cyclic speed stirring to improve mixing between the phases involved. The optimum conditions for stirring were found to be achieved when the speed was cycled between 185 rpm and 160 rpm at minute intervals. The maximum acceleration and deceleration rates that could be achieved on the pilot plant were 1 rpm/s due to tyre slip.

Although surge casting has been found to be a little disappointing, it is still the best method of removing material from the furnace during continuous operation, although the furnace will not have produced sufficient molten material for a cast to be made until after at least two hours of continuous feeding. The most effective surge casting technique involved starting with the furnace at its maximum rotation speed of 180 rpm and then reducing the speed to 135 rpm before holding it at that speed for five seconds and then immediately returning to 180 rpm. The coal lost in the surge cast must then be immediately replaced by injecting a 50 kg batch of coal. The casting chamber must, however, be maintained at at least 1000 $^{\circ}$C and kept as hot as possible in order to minimise the build up of solid material on its walls and to minimise the subsequent reoxidation that can occur.

In order to maintain efficient operation it is vitally important to obtain regular samples from the bed. The ideal sampling procedure would entail taking the initial sample one hour after commencing feed and then to sample every twenty minutes.

7.6.3 Future Development Work

The pilot plant has operated over many hours of experimental time, enabling a great deal of plant experience to be obtained. During this period a number of plant modifications and redesigns have been made, as described in section 6.1.2. Although the majority of the pilot plant operates in a satisfactory manner, there are a number of important areas where further development work is required.

The refractories in the barrel of the reactor have been subject to many heating and cooling cycles and have held liquid melt for several hundred hours. Apart from some refractory loss due to thermal spalling, the refractory bricks have suffered only the minimum of wear. It can therefore be stated that the concept of protecting the refractory in the barrel of the reactor by centrifuging the iron layer to the inner refractory walls and maintaining a protective barrier to the corrosive iron bearing slag, has proved successful. However, this cannot be said of the refractory in the cast end dam which has suffered from excessive slag attack during the experiments, in some instances causing their premature termination. Also, as stated in section 7.6.1.(b), the cast end dam was subjected to expansion forces, generated as the remaining refractory heated up. The cast end dam, unlike the feed end dam, could not be secured by a steel retaining ring because of the high operating temperature within the casting chamber, thus retention of the cast end

dam relied entirely on the quality of the keying achieved during its construction. In several instances, but not during this work, the cast end dam collapsed during the warming up phase of the experiments. In experiments where the cast end dam remained intact, examination after the experiments indicated that slag attack had so eroded the dam that further experimentation after ten hours continuous operation was highly problematical. Obviously this constraint on the maximum duration of an experiment must be overcome if the full potential of the process is to be examined. It will therefore be necessary to replace the present tar impregnated magnesite brick cast end dam with one which is more resistant to slag attack and is not likely to fail prematurely due to thermal expansion of the remaining barrel bricks.

These two problems may be solved if water cooling pipes were situated inside the cast end dam. The concept would be to pass sufficient cooling water through the pipes to freeze a layer of slag onto the end dam whilst the vessel was spinning. The frozen slag layer would then take up the contour of the dam, and then act as the working lining. The design would have to be such that the flow of water could be care-fully controlled to freeze a slag layer of sufficient thickness to provide the necessary protection, yet not too thick to reduce the diameter of the furnace at the cast end dam. Any serious reduction of the cast end diameter would affect the casting system, and the pressure distribution within the reactor. The cooling water could be pumped through the pipes by attaching a mechanical or electrically driven pump to the outer shell of the reactor. Alternatively, the rotation of the vessel could be used to syphon the cooling water through the pipes. One possible design would be to embed the cooling pipes inside a metal

dam, which is rigidly fixed at the cast end, thus overcoming the problem of movement due to thermal expansion of the barrel bricks. It is possible that a dam constructed from copper or steel could be used, with factors such as ease of construction, methods of installation, position of the cooling pipes and thermal stress problems to be carefully examined.

Further development of the casting techniques will have to be carried out before a controlled casting system is obtained. The problems of the speed surge casting system has already been given in section 7.6.1. (b), whilst this technique successfully casts material from the reactor, the control over the quantity of material cast depends largely on the skill of the operator to manipulate the furnace speed as instability of the rotating layers occurs. The rod casting technique described in section 6.3.6 has provided controlled casting on the model scale, but has not yet been fully examined on the pilot plant.

The development of the bed sampling system provided a method for monitoring the bath conditions between each surge cast. However, the samples extracted from the reactor can only give spot checks and cannot be easily adapted for continuous measurement. On the other hand, the exhaust gases are sampled on a continuous basis, and by injection of an inert tracer gas, such as argon, at a known flow rate, then the gas analysis should be capable of providing a method of monitoring process performance on a continuous basis. For example, deoxidation efficiencies of the bath and carbon balances could be determined.

The development of the process on the pilot plant should continue in tandem with further refining and fine tuning of the mathematical model.

Further studies on the mechanism of heat transfer from the gas core into the rotating bed, particularly during cyclic speed stirring; and the effect of gas core composition, such as variations in the $CO : CO_2$ ratio, on the process efficiency should be carried out.

The production of metal to a given specification has not been attempted and comparatively little is known about the capabilities of the process to achieve this objective. Further experimentation is required to establish what the likely slag and metal composition will be under standard operating conditions, then determine the changes in operating procedure necessary to meet set specifications.

The metal and slag are cast together from the furnace and effective methods of separation must be investigated. At present the liquid slag and metal are collected in specially designed refractory boxes, allowed to settle under gravity, then, after solidifying, they are physically separated. However, more advanced separation techniques such as electromagnetic elevators could be used to separate the liquid slag and metal, provided sufficient quantities of material are involved.

All experimentation to date has been carried out at a fairly low iron ore rate of 340 kg/h, since it was considered important to understand the process behaviour at this fixed iron ore rate under different operating conditions. From an economic viewpoint it is important that the throughput rate is increased, whilst still maintaining high iron yields. This will require some plant development as already discussed at the beginning of this section, and the process understanding gained during this work should be used as a basis from which high rate experiments can be planned and executed.

7.6.4   Scale-Up Problems for Commercial Operation

The future of Centrifugal Ironmaking as a route to liquid steel depends
on the solution of two interdependent problems; one chemical and the
other engineering.   There are several cases where a good process has
failed commercially because of engineering problems.   For example, the
DORED process failed at the prototype commercial scale because of
refractory problems, and the Kaldo furnace eventually failed because
of excessive refractory wear and high maintenance costs.   It is thus
logical and necessary in the case of complex processes, such as C.I.P.,
that both aspects, chemical and engineering are studied in parallel.
A delay in either of these routes could cause a lengthy delay in
progressing from the pilot stage to the commercial scale.

The projected output from a commercial scale C.I.P. unit is 1000 tonnes
per day of hot metal.   This being the minimum production rate which
could be sensibly used in a larger steelworks.   Based on expected
production rates the size of a commercial reactor would be approximately
22 m in length, and 3 m internal diameter.   Current experience has
indicated that a barrel lining of magnesite brick, 40 to 50 cm in
thickness, should give a campaign life of at least two years.   With
this refractory thickness the reactor would weigh around 400 tonnes
and would operate at a speed of between 85 and 100 rpm.

There are several major design problems surrounding such a plant.   The
support systems for conventional rotary vessels utilises tyres mounted
on the vessel, running on rollers carried by bearings.   For a full scale
C.I.P. reactor the bearing size required would be so large that a multi-
roller system would be necessary.   Such a system would, however, be so

complicated to set up and maintain that an alternative system must be sought to avoid the alignment problems already experienced on the pilot scale. If possible, the alternative solution should avoid the wear problem associated with rolling contact which became a significant cause of plant vibration on the pilot scale and which must afflict any similar plant after a certain number of cycles have been reached.

The raw materials feed into a large rotating plant also presents some problems. The feed material must be injected into the reactor in such a way that a predetermined length of the reacting bed can be covered. Since the furnace geometry is that of a long horizontal tube, and since up to half its length may have to be covered by the feed, the material must be accurately injected along a very flat trajectory. It is doubtful whether proprietary equipment will exist to accommodate the feeding requirements and that a development of the feed equipment currently in use on the pilot scale may be the best solution.

In addition to the above there are numerous other engineering problems to be answered. For example, what alternative drive systems are available; what is the optimum method of shell manufacture to minimise inaccuracies which would result in out-of-balance problems? Another important aspect is concerned with the energy utilisation within a commercial unit. That is how to handle the large volumes of very hot gases discharged from the reactor. There are several possible uses, including preheating and pre-reduction of the feedstock, direct quenching then using the potential heat available in the gas as a source of fuel, or for steam raising.

A design study to identify the engineering problems and possible solutions to these problems is required. A further aim of this design study would be to provide a cost assessment for commercial scale operation. Thus the foundations would be set for a detailed design of an intermediate stage plant, producing, say, 5 tonnes per hour of hot metal, to test out some of the new concepts required for commercial scale operation, and provide valuable process experience to complement that already gained from the pilot stage work.

8   CONCLUSIONS

1.   The mathematical model describing the Centrifugal Ironmaking

Process was improved by broadening its predictive capability

from one which was used solely to predict the input conditions

to achieve a high iron yield, to one which, given the input

conditions, could predict the way the process would respond

to changes in the operating conditions. This was achieved by

suitably adjusting a number of key parameters within the math-

ematical model from their original base values. The value of

the convective mass transfer coefficient, derived from the

standard pipe flow equation, was increased by applying a multi-

plying factor in the range 5 to 10; the carbon - iron oxide

reaction rate cut-off temperature was lowered to 1 800 ^{o}C; and

the value of the thermal conductivity for the unstirred coke

layer on the bed surface was increased to 0.42 W/m.K.

2.   From the naphthalene mass transfer experiments an equation was

developed for the mass (and heat) transfer j-factors in the

reactor, such that, $J_D (= J_H) = 20.3 (1 + 0.11 Re_r^{0.2}) Re_p^{-\frac{2}{3}}$. This

equation takes into account both the rotational and pipe flow

Reynolds number. Using this equation mass transfer coefficients

calculated for the reactor fell in the range $0.48 \text{ m.s}^{-1} < h_D$

$< 0.51 \text{ m.s}^{-1}$. The value of the mass transfer coefficient derived

from the standard pipe flow equation, where the effect of rotation

is not allowed for, was estimated to be 0.05 m.s^{-1} i.e. some ten

times lower than that determined from the naphthalene model

studies.

3.   A technique was established for studying the kinetics of
     reaction between solid carbon and liquid iron bearing slags
     for temperatures up to 2 135 K, using a carbon crucible as
     both the container for the liquid slag and the reductant.
     However, no accurate reaction surface area measurements could
     be measured, principally because during the course of experiment
     there was a diminution of slag weight with time, the iron
     product was allowed to accumulate inside the crucible (as fine
     iron droplets covering the walls of the container), also
     foaming of the slag inside the crucible occurred particularly
     at the higher temperatures. Each experiment was characterised
     by an induction period, after which the experimental results
     could be expressed in terms of first order kinetics. However,
     slags with a starting composition of 60% Fe_2O_3 by mass gave,
     in some cases, two values for the reaction rate constant K^1,
     within the same experiment, whilst slags having a starting
     composition of 30% by mass gave only one value. An Arrhenious
     plot gave two populations of points, the slopes of these lines
     giving apparent activation energies of 31 Kcal $mole^{-1}$ and
     36 Kcal $mole^{-1}$.

4.   A mechanism is proposed for the reduction of liquid iron bearing
     slags by solid carbon involving separate anodic and cathodic
     sites. The reaction O^{2-} + $\boxed{C}$ = C(O) + $2e^-$ represents
     an anodic reaction, whereas Fe^{2+} + $2e^-$ = Fe is cathodic.
     It is proposed that these two reactions take place at separate
     sites on the carbon surface, electrons being transferred
     through the carbon itself from anodic regions to cathodic
     regions. When the iron oxide content in the slag is low, the

192

rate of production of CO can be controlled by the transport of O^{2-} ions to the anodic sites, where small bubbles of CO would form offering very little blanketing effect to the reaction surface. Under these conditions the rate of reaction would be linearly dependent upon the iron oxide content in the slag. With increased iron oxide in the slag, or with an increase in the temperature, the increased rates at which O^{2-} ions can be transported would result in the growth of large CO bubbles which would have such a strong blanketing effect that they would impede the reaction. These large bubbles could create a foam within the slag and the continued existence of the foam would result in a balance between gas generation and chemical reaction such that a constant reaction rate would be established.

5.   Only fifteen of the planned sixteen independent experiments were carried out in the factorial series of experiments. The variation in the input parameters used enabled the pilot plant to operate over a wide range of process conditions ranging from fluid, highly oxidising beds, through to operation with a semi-molten bed. This resulted in a wide range in the process yields, varying from 0% to 96%. The variation in plant output provided the basis for a systematic approach to the examination and modification to the parameters used in the mathematical model until it was able to predict, with some accuracy, the ways in which the reactor would respond to the different operating conditions.

6.   The results of the factorial experiments and the predictions made from the improved mathematical model showed that the

193

process was highly sensitive to changes in the input rates of coal and oxygen, and relatively insensitive to changes in the input rates of oil and pulverised fuel. Coal input rates greater than 300 kg/h produced a thick coke layer which impeded heat transfer into the slag layer, resulting in a frozen bed. Coal inputs less than 220 kg/h resulted in a sparse coal layer and oxidising conditions. Oxygen inputs in excess of 400 m_N^3/h always resulted in very high temperatures and oxidation of the bed. Oxygen levels below 350 m_N^3/h resulted in conditions where the bed temperature was so low that localised freezing occurred. Interaction between the coal and the oxygen meant that the mean values of the two extremes in the input rates were not the optimum, but a coal input rate of 240 kg/h together with an oxygen input of 385 m_N^3/h. Also, it was beneficial in all instances if the coal and slag layers were mixed together by stirring.

7. Three continuous ironmaking experiments were carried out lasting for 10 h, 3.5 h and 9.5 h respectively. For the first two experiments, the input rates corresponded to the optimum values determined by studying the results from the factorial experiments and the predictions made by the improved mathematical model. The weighed iron yields from these experiments were 49% and 80% respectively. For the third continuous experiment the coal input rate was increased to 249 kg/h and the weighed iron yield was 70%. The iron content of the slags discharged from the reactor during casting were in the range 15 to 30% Fe^T, whilst the iron content of the slags sampled from inside the reactor were in the range 5 to 20% Fe^T.

8. A casting technique was developed which allowed a portion of
    the bed to be tapped at regular intervals by lowering the drum
    speed from its normal operating level by 45 rpm, holding at
    this lower speed for ~10 seconds, then raising the speed back
    to its original value. At the feed rates used it was found
    that the optimum interval between casts was about one hour,
    when approximately 200 kg of liquid product could be tapped.
    Unfortunately, this technique not only discharged slag and metal
    from the cast end of the furnace but also dragged out unreacted
    material from the feed end of the furnace, lowering the process
    efficiency. Casting in this manner also destroyed the coal
    layer in the reactor and it was necessary to replenish this
    coal layer with an additional 50 kg batch of coal after each
    surge cast.

9. The concept of protecting the refractory lining from slag
    attack by the layer of molten iron maintained against the
    lining, worked extremely well. Examination of the refractory
    after the continuous experiments showed that the only damage
    was some minor spalling. The end dams, particularly the cast
    end dam, suffered from slag attack and the cast end dam was
    so eroded after a continuous experiment that continuous
    operation much beyond 10 hours would be impossible to achieve
    with the tar impregnated brick dam used in this work.

10. The majority of the equipment on the pilot plant worked
    satisfactorily during the continuous experiments and, except
    for the uncertainty of the cast end dam, the pilot plant is

capable of running continuously for longer times. Apart
from the end dam, the greatest potential impediment to
further extension of continuous operation is the design of
the casting chamber. Material collects in the hearth of
the casting chamber after each surge cast and is subject to
oxidation, lowering the process yield. If left to accumulate
this material could also seal the tap hole, making the reactor
inoperable.

REFERENCES

1.   Philbrook, W.O. and Kirkbride, L.D.

        J. Metals, 1956, 206, 351.

2.   Tarby, S.K. and Philbrook, W.O.

        Trans. Met. Soc., A.I.M.E., 1967, 239, 1005.

3.   Krainer, H., Beer, H.P. and Brandl, H.

        Techn. Mitt. Krupp, Forsch-Ber, 1966, 24, 139.

4.   Kondakov, V.V., Ryzhonkov, D.I. and Golinkov, D.M.

        IZV. Vyssh. Uchelsen Chem. Met., 1969, 4, 19.

5.   Yershov, G.S. and Popova, E.A.

        IZV. Akad. Nauk. SSSR. Metally i Tophiro. 1964, 1, 32.

6.   Sugata, M., Sugiyama, T. and Kondo, S.

        Trans. I.S.I. Japan, 1974, 14, 88.

7.   Shavrin, S.V. and Zachorov, I.N.

        Fiz. Khim Rasplov Shlakov, 1970, 55.

8.   Davies, M.W., Hazeldean, G.S.F. and Smith, P.N.

        Physical Chemistry of Process Metallurgy.

        The Richardson Conference

        The Institute of Mining and Metallurgy, 1974, p.95.

9.   Gray, F.A. and Robertson, A.D.

        J. Inst. of Fuel, Oct. 1956, p.428.

10.   Bacon, N.P.

        Joint Symposium on Scaling-Up.

        Institute of Chem. Engr., 1957, p.599.

11.   Thring, M.W. and Newby, M.P.

        Proceedings of the 4th International Symposium on

        Combustion.

        Baltimore, 1953, p.789.

12.   Robertson, A.D.

        J. Inst. of Fuel, Nov. 1965, p.481.

13.   Davies, R.H., Lucas, D.M., Moppet, B.E. and Gabworthy, R.A.

        J. Inst. of Fuel, Aug/Sept. 1971.

14.   Galsworthy, R.A.

        The Gas Council Midlands Research Station

        External Report No. 134, Nov. 1969.

15.   Chilton, T.H. and Colburn, A.P.

        Ind. Eng. Chem. 1934, Vol. 26, p.1183-1187.

16.   Lucas, D.M. and Davies, R.M.

        4th International Heat Transfer Conference,

        Versailles, Sept. 1970.

17.   Harvey, P.H., Nandapurkar, S.S. and Holland, F.A.

        The Canadian Journal of Chemical Engineering,

        Vol. 49, April 1971, p.207.

18.   Eketorp, S.

        Steel Times, May 1967, p.587.

19.   Janke, W. and Garbe, H.

        Sponge Iron by the SL/RN Process.

        2nd Inter-regional Symposium on the Iron and Steel

        Industry of the UNIDO, Moscow 19th Sept. - 9th Oct. 1968.

20.   Josefsson, A. and Johansson, F.

        Kaldo Process - A Comparison of Pilot Plant Experiments

        with Full Scale Operation.

        Iron and Steel Institute - Special Report 96.

21.   Josefsson, A., Bengtsson, E. and Almqvist, K.

        Direct Reduction of Iron Ore by the Stora Method.

        A.I.M.E. Ironmaking Proc. 1964, 23, p.275.

22.   Sgodin, B.

        Metallurgical Research Plant, Lulea, Sweden.

        Private Communication.

23.   Ramaciotti, A.

        Rotored - A New Direct Reduction Process.

        Metallurgiu Italiana, Vol. 67, 1975, No. 12, p.692.

24.   Elliot, J.F. and Glaiser, M.

        Thermochemistry for Steelmaking.

        The American Iron and Steel Institute,

        Addison-Wesley Publishing Co., 1960.

25.   Voice, E.W. and Hawkes, D.A.

        Continuous Iron or Steelmaking Process.

        Patent Application No. 50247/68.

26.   Rose, J.W. and Cooper, J.R.

        Technical Data on Fuel, 1977.

        The British National Committee World Power Conference.

27.   Smith, P.N. and Gare, T.

        Internal BSC Report No. CH/16/70.

28.   Sherwood, T.K. and Bryant, H.S.

        Canadian Journal Chem. Eng. 35, 51-57, (1975).

29.   Blyholder, G. and Eyring, H.

        Kinetics of Graphite Oxidation.

        J. Phys. Chem. 1957, 61, (5), 682-658.

30.   Alexander, J. and Hazeldean, G.S.F.

        Carbon Boil on the Refractory Surface.

        Internal BSC Report No. CH/36/71.

31.   Shurygin, P.M., Boronenkov, V.N., Kryuk, B.I. and Revelstoov, V.V.

        IZV. Vyssh. Uchebn. Zaved. Chem. Met., 1965, 8, 23.

32.   Fay Fun,

        Met. Trans., 1970, 1, 2537.

33.   Treadgold, C.J.

        A Physical Property Prediction Programme for Gas Mixtures.

        Internal BSC Report, Teesside Laboratories,

        Report No. PO/TN/11/78.

34.   Acheson, R. and Hills, A.W.D.

        Physical Chemistry of Process Metallurgy.

        The Richardson Conference,

        The Institution of Mining and Metallurgy, 1974, p. 153.

35.   Field, M.A., Gill, D.W., Morgan, B.B. and Hawksley, P.G.W.

        Combustion of Pulverised Coal.

        The British Coal Utilisation Research Association, 1967.

36.   Larson, H. and Chipman, J.

        Oxygen Activity in Iron Oxide Slags.

        A.I.M.E. Trans. Vol. 197, (1953).

37.   Richardson, F.D.

        Rates of Slag/Metal Reactions and Steelmaking Processes.

        Iron and Coal, (1961), p.1105.

38.   Turkdogan, E.T. and Pearson, J.

        Activities of Constituents of Iron and Steelmaking Slags.

        J. Iron and Steel Institute, March 1953, p.217.

APPENDIX 1

HEAT TRANSFER BY RADIATION FROM THE GAS CORE TO THE BED

In the mathematical model, the reactor is considered to be a combustion

chamber in which the energy from the flame is radiated to the container

walls, in this case the rotating bed. The oil burner located centrally

at the feed end of the reactor combusts a petroleum fuel with oxygen,

the combustion products being carbon dioxide and water vapour. Pulverised

fuel is also injected into the gas core which combusts to carbon dioxide,

but in addition to this the heated carbon particles increase the value

of the emissivity of the gas core. The emissivity of the gas core can be

related to the size and shape of the pulverised fuel cloud and to the

absorption coefficient, $\bar{k}$. It is customary[35] to adopt an equation of

the form:- ε_g = 1- exp $(- f.\bar{k}.l.)$ which gives a sufficiently good

approximation to the variation of cloud emissivity with size. Thus the

heat transferred by radiation per unit area, $\dot{q}_r^{11}$

$$\dot{q}_r^{11} = \frac{1}{\dfrac{1}{\varepsilon_g} + \dfrac{1}{\varepsilon_B} - 1} \, \sigma \, (T_g^4 - T_B^4)$$

APPENDIX 2

PULVERISED FUEL COMBUSTION

Before formulating equations to describe the combustion of pulverised

fuel in the mathematical model, the published results from a number of

experiments were reviewed in order to find an expression for the rate

of reaction of carbon in terms of oxygen concentration at the surface

and the surface temperature. Thus the rate of carbon removal per unit

external geometric surface area, $q_{p.f.}$, was defined as[35]:-

$$q_{p.f.} = K_s \cdot X_{O_2} \quad mol \ C/cm^2/s \qquad \dots\dots\dots\dots (A2.1)$$

where K_s is the surface reaction rate coefficient =

$726 \cdot e \left(\frac{-35700}{R.T.} \right)$ and X_{O_2} is the partial pressure of

oxygen at the reaction surface.

In a mixture of two gases, A and B, the diffusive flux of component

A across a surface in the fluid is given by[35]:-

$$n_{AB}^{\cdot 11} = - \frac{D_{AB}}{R.Tg} \cdot \frac{dP_A}{dy} \qquad \dots\dots\dots\dots (A2.2)$$

This flux is measured not with respect to a stationary frame of reference

but with respect to a surface across which there is no net molar flux of

the two gases. In a combustion system there are usually many gases

present, but equation (A2.2) strictly applies to a mixture of two gases

and the diffusion coefficient is the binary diffusion coefficient, a

property of the two gases. However, equation (A2.2) can be applied by

defining a suitable pseudo binary diffusion coefficient for each gas

relative to the rest of the gas mixture, this coefficient depending on

the concentrations of all the gases present.

The mathematical model assumes that all the volatiles are driven off immediately and thus play no part in the combustion of the pulverised fuel. Since the pulverised fuel particle is thereby assumed to contain only carbon, the net flux across any surface surrounding the particle of species containing hydrogen and oxygen is zero, i.e. for hydrogen:-

$$\frac{1}{RT} \left(D_{H_2} \left(\frac{\partial P_{H_2}}{y} \right) + D_{H_2O} \left(\frac{\partial P_{H_2O}}{y} \right) \right) = 0 \qquad \dots\dots\dots (A2.3)$$

Integrating from the bulk gas to the surface of the particle, across a boundary layer of thickness δ, gives:-

$$\frac{D_{H_2}}{\delta} \left(P_{H_2} - X_{H_2} \right) + \frac{D_{H_2O}}{\delta} \left(P_{H_2O} - X_{H_2O} \right) = 0 \qquad \dots\dots (A2.4)$$

$$\text{Now} \quad \frac{Di}{\delta} = \left[Ki \right]_c \qquad\qquad \dots\dots\dots (A2.5)$$

where $\left[Ki \right]_c$ is the mass transfer coefficient of species i to the carbon particles.

Therefore equation (A2.4) can be written:-

$$\left[K_{H_2} \right]_c \left(P_{H_2} - X_{H_2} \right) + \left[K_{H_2O} \right]_c \left(P_{H_2O} - X_{H_2O} \right) = 0 \quad \dots (A2.6)$$

Similarly for the net flux of the oxygen containing species:-

$$2 \left[K_{O_2} \right]_c \left(P_{O_2} - X_{O_2} \right) + 2 \left[K_{CO_2} \right]_c \left(PCO_2 - X_{CO_2} \right)$$
$$+ \left[K_{CO} \right]_c \left(P_{CO} - X_{CO} \right) + \left[K_{H_2O} \right]_c \left(P_{H_2O} - X_{H_2O} \right) = 0 \quad \dots (A2.7)$$

where P represents the partial pressure in the bulk gas and X represents the partial pressure at the interface.

Now the net flux of carbon across any spherical surface of radius y surrounding a particle is equal to the rate of carbon loss from the particle surface:-

$$\frac{4\pi y^2}{R.T.} \quad \frac{\partial}{\partial y} \quad \left(D_{CO} P_{CO} + D_{CO_2} P_{CO_2}\right) = 4\pi r^2 X_{O_2} K_s \quad \cdots \quad (A2.8)$$

Again, integrating from the bulk gas to the surface of the particle, across a thin boundary layer of thickness δ, gives:-

$$\left[K_{CO}\right]_c \left(X_{CO} - P_{CO}\right) + \left[K_{CO_2}\right]_c \left(X_{CO_2} - P_{CO_2}\right) = r.X_{O_2}.K_s.R.T. \quad (A2.9)$$

At the interface, the sum of the partial pressures of the gases are equal to the total pressure:-

$$X_{CO} + X_{CO_2} + X_{H_2} + X_{H_2O} + X_{O_2} = P_T \quad \cdots \cdots \cdots (A2.10)$$

Also at the interface, the surface concentration of oxygen X_{O_2}, is assumed to be in equilibrium with CO, CO_2 and H_2, H_2O concentrations at the interface, the concentration being related to the equilibrium reaction constants for the reactions involved.

The mathematical model incorporates a solution to these equations and thus derives the pulverised fuel combustion rate for a particle of any specified radius.

APPENDIX 3

OXIDATION OF THE SLAG LAYER

The transfer mechanism assumed in the mathematical model to carry the oxidising species to the coal particle surface can also apply to the slag surface if this is uncovered by coal. It is therefore possible to transfer oxidising species from the gas core and into the slag layer.

Assuming that equilibrium exists at the gas - slag interface, the following relationship can be written between the partial pressure of oxygen at the interface and the ferrous to ferric iron ratio:-

$$\frac{Fe^{3+}}{Fe^{2+}} = \emptyset \left(X_{O_2} \right) \qquad \ldots\ldots\ldots \text{(A3.1)}$$

where X_{O_2} is the partial pressure of oxygen at the gas - slag interface, and $\emptyset$ is a pseudo-equilibrium constant taken from the results of experimental work[36] carried out at 1550 °C. For model purposes it is assumed to be independent over the temperature range the slags experience in the C.I.P. reactor, but dependent on the slag composition, such that:-

$$\emptyset = \left\{ \frac{(CaO)}{(SiO_2)} \right\}^{\frac{1}{2}} \left[1.173 + 0.125 \log \left(X_{O_2} \right) \right]^2 \qquad \ldots\ldots\ldots \text{(A3.2)}$$

Now, if it is further assumed that the net flux of carbon from the gas core to the slag is zero (neglecting any carbon monoxide from carbon dissolved in iron), the transfer of oxygen is a function of the mass transfer coefficient, and the partial pressures in the bulk gas and at the interface. Thus the molar flux of atomic oxygen reaching the gas - slag interface per unit area per unit time is given by:-

$$\dot{n}_O^{11} = k_{CO}\left(P_{CO} - X_{CO}\right) + 2\,k_{CO_2}\left(P_{CO_2} - X_{CO_2}\right)$$

$$+ 2\,k_{O_2}\left(P_{O_2} - X_{O_2}\right) + k_{h_2O}\left(P_{H_2O} - X_{H_2O}\right) \qquad \dots\dots\dots\dots \text{(A3.3)}$$

where k_s is the convective mass transfer coefficient for the species s, and P_s is the partial pressure for species s in the bulk gas.

The transfer of oxygen in the slag is controlled by the mass transfer coefficient, k_{slag}, describing the movement of oxygen ions. The magnitude of k_{slag} will depend, amongst other things, on the temperature of the slag and the degree of stirring, and is an unknown value in this system. Estimates[37] can be made from Open Hearth practice, however the value used in the model can be adjusted so that mathematical model results are in line with plant operating data. The value chosen decreases with decreasing temperature thus preventing the model predicting high slag oxidation rates at low temperatures.

The net flux of iron to the gas – slag interface is zero, and the net flux of oxygen ions into the slag is given by:-

$$\dot{n}_O^{11} = k_{slag}\left(FeO_{gas-slag} - FeO_{bulk\ slag}\right) + 3\,k_{slag}\left(Fe_2O_{3\,gas-slag}\right.$$

$$\left. - Fe_2O_{3\,bulk\ slag}\right) \qquad \dots\dots\dots\dots \text{(A3.4)}$$

The model solves these equations and so predicts the quantity of oxygen crossing the gas – slag interface, and a positive value for $\dot{n}_O$ implies oxygen transfer into the slag. This transfer is clearly undesirable since it provides a source of oxygen into the slag layer, which ultimately could reoxidise iron already produced.

207

APPENDIX 4

METAL OXIDATION

At the slag - metal interface the concentration of dissolved oxygen in the liquid iron is assumed in the mathematical model to be in equilibrium with the liquid iron oxide in the slag. For any temperature, the concentration of oxygen in the metal for equilibrium with any slag where the activity of ferrous oxide is known can be determined from the relationship[38] :-

$$\log \left[\% \; O\right]_{(interface)} = \left\{\frac{\log \left[aO\right]}{\log \left[fO\right]}\right\}_{(interface)} =$$

$$\frac{\left(\log \; aFeO_{(interface)}\right) \left(\frac{-6320}{T} + 2.734\right)}{\log \left[fO\right]} \qquad \ldots\ldots\ldots (A4.1)$$

where $\left[fO\right]$ is the activity of coefficient of oxygen in the metal.

At the slag - metal interface there is a relationship between the oxygen concentration at that interface and the ferrous to ferric iron ratio, such that:-

$$\frac{Fe^{3+}}{Fe^{2+}} = \emptyset^1 \left[O\right]_{slag-metal \; interface} \qquad \ldots\ldots\ldots (A4.2)$$

where $\emptyset^1$ is a pseudo-equilibrium constant related to that given in Appendix 3, equation A3.2; where the partial pressure of oxygen at the gas - slag interface is replaced by the concentration of oxygen at the slag - metal interface.

Since there is no accumulation of oxygen at the slag - metal interface, then:-

$$k_{slag} \left(FeO_{bulk} - FeO_{slag-metal}\right) + 3 \; k_{slag} \left(Fe_2O_{3_{bulk}} - Fe_2O_{3_{slag-metal}}\right)$$

$$+ \; k_{metal} \left(\left[O\right]_{bulk} - \left[O\right]_{slag-metal}\right) = 0 \qquad \ldots\ldots\ldots (A4.3)$$

The concentration of oxygen in the bulk metal is assumed to be in equilibrium with the carbon concentration in the bulk metal. The value of the mass transfer coefficient in the metal, like the value in the slag layer k_{slag} discussed in Appendix 3, is unknown and will depend on the temperature of the iron layer and on the degree of stirring. Again the value of k_{metal} can be adjusted to correspond with experimental data obtained from the pilot plant.

The concentrations at the slag – metal interface may then be determined, and hence the quantity of oxygen entering the metal, $k_{metal} \left([O]_{slag-metal} - [O]_{bulk} \right)$, may be found.

The iron oxidised is equal to the net flow of iron into the slag layer i.e.

$$\dot{n}_{Fe}^{11} = k_{slag} \left(FeO_{slag-metal} - FeO_{bulk} \right) + 2 \, k_{slag} \left(Fe_2O_{3\,slag-metal} - Fe_2O_{3\,bulk} \right) \qquad \ldots\ldots\ldots\ldots (A4.4)$$

A positive value for $\dot{n}_{Fe}^{11}$ means that iron is being oxidised from the metal layer and entering the slag layer. This, of course, represents a lowering of the process yield and is clearly undesirable.

APPENDIX 5

ANALYSIS OF RAW MATERIALS USED DURING C.I.P. EXPERIMENTS

Iron Ore (Lac Janine Concentration)

	%
Fe_T	63.7
SiO_2	6.5
Al_2O_3	0.5
CaO	1.0
MgO	0.2
P	0.03
S	0.01
Moisture	Nil

Coal (Linby), %

Proximate Analysis %		Ultimate Analysis %	
Fixed Carbon	49.29	Carbon	69.66
Volatile Matter	35.45	Hydrogen	4.45
Ash	8.06	Nitrogen	1.59
Moisture	7.2	Sulphur	0.67
		Oxygen	7.55
		Moisture	7.2
		Mineral Matter	8.88

Ash Analysis %		Gross C.V. 32422 kJ/kg
Fe_T	14.8	
SiO_2	41.3	
CaO	9.5	
Al_2O_3	21.0	
MgO	0.4	

Pulverised Fuel, %

Proximate Analysis %		Ultimate Analysis %	
Fixed Carbon	59.56	Carbon	77.36
Volatile Matter	31.04	Hydrogen	4.77
Ash	6.40	Nitrogen	1.71
Moisture	3.00	Sulphur	0.72
		Oxygen	5.40
		Moisture	3.00
		Mineral Matter	7.04

Ash Analysis %		
Fe_T	10.1	Gross C.V. 33494 kJ/kg
SiO_2	47.5	
Al_2O_3	28.0	
CaO	6.6	
MgO	1.7	

Limestone,   %

CaO	53.6
SiO_2	2.2
Fe_T	0.6
MgO	0.2
Al_2O_3	0.4

Gas Oil,   %

Carbon	85.7	Gross C.V. 45357 kJ/kg
Hydrogen	13.4	
Sulphur	0.9	

Oxygen Gas,   %

Oxygen	99.7

APPENDIX 6

PHOTOGRAPHS TAKEN DURING THE FACTORIAL EXPERIMENTS

Photographs were taken from the feed end of the reactor through a high speed shutter arrangement (exposure time of 1/6000th of a second), located on the outside of the static feed end hood during some of the factorial experiments. Before each photograph the feeds were turned off, and 30 seconds were allowed for the fume to clear before the photograph was taken. Unless stated, each photograph was taken after about one hour from the start of feeding. The probe that can be seen on the left hand side of the photograph is the water cooling jacket of one of the feeder probes. The photographs illustrate the operating conditions established in the experiments and observations of these photographs go some way to explain some of the results.

These observations are presented below:-

Experiment 88 (Figure A6.1)

Frozen rings of material were observed inside the reactor on two occasions during this experiment. The photograph shows the first of these and was taken after one hour of furnace operation. The frozen ring is estimated to be approximately 80 cm from the feed end dam.

Experiment 94 (Figure A6.2)

This photograph, again taken after one hour's furnace operation, shows coal coverage over the first part of the furnace with either a coal shortage, or 'sunk' coal, in the latter part of the furnace. The photograph shows a slight build up of material again approximately 80 cm from the feed end dam.

Experiment 95 (Figure A6.3)

The photograph shows that there is very little coal coverage inside the reactor. A small quantity of coal is apparent very close to the feed end dam.

Experiment 96 (Figure A6.4)

This photograph was taken after one and a half hours of furnace operation and shows low temperature in the first part of the reactor with build up of frozen material. The temperature of the bed appears to be higher in the latter half of the furnace with no signs of frozen material.

Experiment 97 (Figure A6.5)

This photograph shows a relatively cold furnace with frozen material and excess coal visible over the first 60 cm of the furnace. The bed temperature did not recover during the experiment, which was prematurely terminated because of the low bed temperatures.

Experiment 98 (Figures A6.6 to A6.9)

During the course of this experiment it was suspected that a failure of the cast end dam had occurred. Photographs were therefore taken at 1 hour 8 minutes, 1 hour 58 minutes, 2 hours 8 minutes and 2 hours 26 minutes from the start of feeding. These photographs show the effect of this dam failure with the coal being 'stretched out' along the length of the reactor as the slag velocity increases with an increase in leakage through the cast end dam.

Experiment 99 (Figure A6.10)

The photograph shows a reactive bed but with no signs of coal on the bed surface. There also appears to be small explosions of smoke coming from individual sites along the bed surface.

Experiment 100 (Figure A6.11)

The indicated bed temperature monitored during this experiment was recording low bed temperatures, which were not borne out by the photograph which shows a relatively high bed temperature, a foaming bed, and reactive conditions. After these experiments were concluded the temperature measuring instrument was found to be at fault.

Experiment 102 (Figure A6.12)

This photograph shows a stable, relatively unreactive bed with a slight build up of frozen material at approximately 80 cm from the feed end dam. Three such rings of frozen material were observed during this experiment but in each instance they were easily melted out.

C.I.P. Furnace (Figure A6.13)

This shows a newly bricked, empty reactor. The same field of view is visible in this photograph compared to those taken when the experiment was in progress. The cast end dam is just visible in the top right hand corner of the photograph, with a small fraction of the feed end dam visible in the bottom left hand corner.

FIGURE Afc.l   EXPERIMENT 88

FIGURE A 6.2.   EXPERIMENT 84

FIGURE Afc.3   EXPERIMENT

FIGURE A 6.4-   SXPER1M ENT 'J

FI SURE Afc.S   EXPERIMENT 47

F I G U R E   A 6. 6   EXPERIMENT   4 8

AFTER   68 NlNS. or feemnc

FIGURE Afc.7   EXPERIMENT

AFTER   I   ʒⅯNS. OF FEEAmc

FIGURE   A   8   EXPERIMENT   3 8

AFTER   U « HIN5 or FEEDING

FI SURE A *b.* 3   EXPERIMENT

AFTgg   I4-k MINS. OF *fEtblNQ*

FISURE A fc. 11   EXPERIMENT 1oo

FIGURE A k. II   EXPERIMENT 1o2.

FIGURE AE./3   EMPTY   REACTOR